Proceedings of the 21st International Ship and Offshore Structures Congress (ISSC 2022) – Xiaozhi Wang and Neil Pegg (Eds.)

Volume 2

COMMITTEE V.2
EXPERIMENTAL METHODS

COMMITTEE MANDATE

Concern for advances in structural model testing and full-scale experimentation and in-service monitoring and their role in the design, construction, inspection and maintenance of ship and offshore structures. This shall include new developments in: best practice and uncertainty analysis; experimental techniques; full field imaging and sensor systems; big data applications for ship and offshore structures; and correlation between model, full-scale and numerical datasets.

AUTHORS/COMMITTEE MEMBERS

Chairman: Soren Ehlers
Nagi Abdussamie
Kim Branner
ShiXiao Fu
Martijn Hoogeland
Kari Kolari
Paul Lara
Constantine Michailides
Hideaki Murayama
Cesare Rizzo
Jung Kwan Seo
Patrick Kaeding

KEYWORDS

Experimental Methods, Scaling Laws, DIC (Digital Image Correlation), Hydrodynamic of Flexible Structures, Wave-in-deck, Hybride model testing, Vibrations, Fatigue testing, Large scale impact testing, Corrosion testing, Full-scale iced load measurements, Health monitoring model, Digital twin model

CONTENTS

1. INTRODUCTION

Design methods and rule requirements have to be benchmarked with experimental or service history data. The Goal Based Standards (GBS) approach by IMO, see e.g., IMO Res. 296(87), 454(100) or MSC.1/Circ.1394, require benchmarking of standards by *measuring the performance of methodologies, assessments, criteria and requirements by using indicators that can be compared with an accepted standard or with experimental and/or service history data, performance levels or outcomes known to be reliable*. This approach calls for a systemic use of experimental results and monitoring of data from ships during construction, in-service and possibly from the end of the life cycle. Thus, the elaboration of experimental outcomes and the handover of information into engineering and management practice need to be further addressed and standardized to fully exploit their potential.

Further, the continues growth of complexity in ship and offshore structures potentially designed outside the range of empirical references calls for reliable means of validation. While computer simulations are continuously improving at the same time, their improvement to a large extent depends on a physical understanding of the underlying phenomena to be captured. Therefore, experimental investigations are essential in driving further developments and innovations through their accurate feedback when performed correctly and meaningful. The latter is however challenging, especially with increased complexity of the phenomena to be investigated. Therefore, this report summarizes the expertise of the contributing authors with respect to their corresponding research fields. The report seeks to give a general overview of the specific experiments dealt with therein, presents the latest publications, possible obstacles to be addressed and closes with future recommendations for further developments and integration of the experiments into engineering practice and scientific developments.

The report at first covers a section on scaling laws relevant to any experiment followed by specific testing concerning: digital image correlation (DIC), hydrodynamics of flexible structures, wave-in-deck, hybrid models, friction, vibrations, fatigue at low temperatures, corrosion, large scale impact, large scale wind turbine blades, full-scale ice loads, health monitoring and digital twin models. Further, a benchmark study on free vibrations of a cantilever beam is carried out to demonstrate the vast possibilities to carry out such seemingly simple experiment followed by a discussion of the results achieved. The report is concluded with a summary and an outline of further research and development recommendations

2. SCALING LAWS

2.1 Introduction

In this chapter a review of scaling laws is provided. Scaled down models are widely used for experimental investigations of large and land-based, aerospace, ships and offshore structures complex structural systems due to limitation in the capacities of testing facilities and moreover the experimentation on scaled models is for economic, convenient and time saving. The scaling concept has been utilized in many engineering applications and helps engineers and scientists to replicate the behavior of the prototypes. This general and past experiences procedure is known as scaling, replica scaling, modelling or similitude and is governed by certain principles. This review is focused on general scaling modelling methods and model ice properties and its application to ships and offshore structures aspects such as hydrodynamic, ship collision, offshore structures and wind turbine structures.

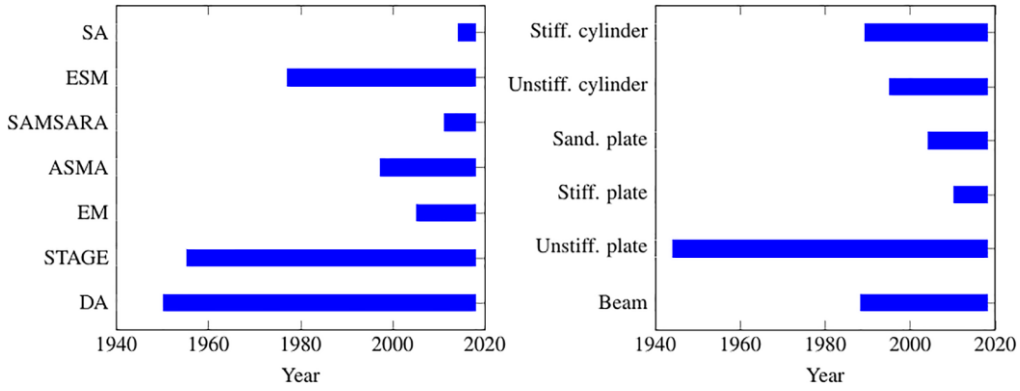

Figure 1: Historic overview of scaling laws and application cases (Casaburo et al., 2019)

Recently, Casaburo et al. (2019) reported a comprehensive review about similitude methods (Figure.1). The overview of similitude methods is reported as per dimensional analysis (DA), similitude applied to governing equations (STAGE), energy method (EM), asymptotical scaled modal analysis (ASMA), similitude and asymptotic models for structural-acoustic research applications (SAMSARA), empirical similarity method (ESM), and sensitivity analysis (SA) as shown in Figure 1 together with the corresponding application cases, respectively, structures. According to this historical review, the model presented by Sterrett (2009) and the relativized application (Sterrett, 2006; 2014; 2015a; 2015b) of his model are suggested as useful.

2.2 Scale modelling methods

2.2.1 Dimensional analysis

Dimensional analysis is a technique that enables the identification of the fundamental quantities that describe a physical phenomenon or system, and it has been utilized effectively in engineering modelling. The complexity and extent of an experiment are commonly simplified using dimensional analysis. Dimensional analysis or, as Coutinho et al. (2018) refer to, the traditional similarity method, is based on the definition of a set of dimensionless parameters that govern the phenomenon of interest. It relies on the concept of dimensional homogeneity, i.e., an equation which describes a physical phenomenon with consistent dimensions (Casaburo et al., 2019).

These concepts are gathered in Buckingham's Π theorem. A wider modelling interpretation and applications of dimensional analysis are given in Tan (2011) and Kunes (2012), while Zohuri (2012) provides first a perspective on classic dimensional analysis and, then, deepens the topic in Zohuri (2017), going beyond Buckingham's Π theorem and approaching self-similar solutions. This analysis has been widely applied to structural components including beams (Oshiro et al., 2011; Ramu et al., 2010; Mazzariol et al., 2013; Zai et al., 2015) and plates (Hu, 2000; McKown et al., 2008; Christoforou et al., 2009; Xu et al., 2016; Yang et al., 2013; Mazzariol et al., 2014).

However, for some applications the dimensional analysis does not directly involve the Buckingham's Π theorem. Here, the scaling laws are determined by defining just one scale factor, which expresses the prototype/model-ratio of parameters as a power law. Dimensional analysis, as a classical similitude analysis method, because of the uncertainty of the basic vector of solutions, is a trial-and-error approach and can require significant calculation efforts. Additionally, not all Π terms have a physical meaning and, in general, the equations characteristic of the phenomena under observation can only be formulated in an incomplete form. Therefore, the procedure of dimensional analysis may not be implemented easily into an algorithm.

2.2.2 Applied to governing equations

Similitude theory applied to governing equations is applied directly to the field equations of the system, including boundary and initial conditions, which characterize the system in terms

of its variables and parameters (Kunes, 2012). Because similar models are governed by an equivalent set of field equations and conditions, similitude conditions may be derived by defining the scale factors and comparing the equations of both prototype and model. The derived similitude conditions relate geometric, structural, excitation (force amplitude, force phase, excitation frequency, etc.), and material properties of the system to its response such as beams (Rezaeepazhand and Wisnom, 2009; Yazdi and Rezaeepazhand, 2013; Asl et al., 2016; Shokrieh and Askari, 2013; Asl et al., 2017a; Balawi et al., 2015), plates/shell (Simitses et al., 2000; Zhu et al., 2014; Zhu et al., 2017; Rezaeepazhand and Yazdi, 2011; Yazdi, 2013; Singhatanadgid and Na Songkhla, 2008; Luo et al., 2013; 2014), and cylinders (Torkamani et al., 2008; Torkamani et al., 2009; Luo et al., 2014; Ungbhakorn and Singhatanadgid, 2009).

An advantage of such method is that it allows to derive a set of conditions more specifically than those obtained through dimensional analysis, because they are equation driven, which means that the relationships are forced by the governing equation. This implies that the physical meaning and the procedure is more structured with respect to the one used in dimensional analysis, but it may lack a standard action sequence. Thus, also this method cannot be implemented in an algorithm (Casaburo et al., 2019). Furthermore, the range of applications is limited to those systems with at least a set of governing equations and the derivation of similitude conditions still requires a certain calculation effort.

2.2.3 Energy Methods

Energy methods have been proposed instead of the governing equation method. One exploits the principle of conservation of energy and is introduced by Kasivitamnuay and Singhatanadgid (2005). The energy method is based on the principle of conservation of energy, which states that if there is no energy loss (in terms of heat and chemical reactions), the strain energy stored in the structure is equal to the sum of kinetic energy and the work made by external forces. The energy equation given by this principle includes the structural domain, the applied loads, and the boundary conditions. The system is considered as a whole and there is no need to determine explicit and implicit scale factors separately. For deriving the similitude conditions, all the considered energies are scaled simultaneously, so that a scaled energy equation is able to be obtained.

Recently, the application of the energy method to the problem of structural similarity has been studied by Kasivitamnuay and Singhatanadgid (2017). The original sets of complete similarity conditions and scaling laws for the displacement were obtained for linear and nonlinear elastic beams under simultaneous application of various load types. The complete similarity condition was achieved using a geometrically similar model or distorted model. The latter satisfied an additional condition.

This method is more straightforward than the applied governing equation method, because it provides the scaling factors for structural behaviour even when the structure is made of several components, while keeping the same level of generality and obtaining the same conditions. However, a certain calculation effort is required, especially for complex systems.

2.2.4 Empirical Similarity Method

For rapid prototyping, dimensional analysis is commonly used, even though challenges exist related to the difference in material properties between the prototype and model, the sensitivity to distortions, too restrictive use of information, and dependence of cost and time on geometrical complexity. For these reasons, Cho and Wood (1997) proposed the empirical similarity method. Advances in the empirical similitude technique are presented in terms of sources of coupling between material properties and geometric shape that produce distortions in the current empirical similitude technique (Cho et al., 2005).

This is based on the testing of a specimen pair: one specimen with simple geometric features fabricated through rapid prototyping and the other fabricated through the actual production

process. By measuring the state vectors of this pair and the scaled structure obtained through rapid prototyping, a state transformation is derived. In such transformation, the usual scale factors are replaced by weighting factors. The empirical transformation matrix can be considered as an advantage, but the fact that additional specimen pairs are required leads to additional manufacturing and testing.

2.3 Application to ships and offshore structures

2.3.1 Hydrodynamic

Since many areas of fluid dynamics are still complicated making accurate analysis mathematically very difficult, a lot of effort has been devoted to develop accurate similarity methods for fluid dynamics, hydraulics, aerodynamics, and naval hydrodynamics. In fact, the oldest methods of scale model experiments are found in the field of naval architecture. Due to the limitations in the capabilities of hydrodynamic and structural testing facilities along with the cost of experimentations, scaled models are widely used for experimental investigations. The modelling accuracy depends upon the model material properties, fabrication accuracy and loading techniques. In order to achieve similitude between the model and the real structure, the geometric, hydrodynamic (Froude, Strouhal and Reynolds) and structural (Cauchy) similitudes must be satisfied. However, the Reynolds number in a Froude model is smaller by more than an order of magnitude. The distortion of Reynolds number in the model requires certain corrective measures in the model tests and scaled data. Concerns about Reynolds Number scale effects on drag coefficients and on the Strouhal Number, and difficulties in manufacturing small scale riser models with the appropriate structural properties, will sometimes lead to the conclusion that it is best not to attempt to model, i.e., vortex shedding on these components.

In certain circumstances, surface tension effects may start to become important in very small-scale model tests where they are not significant at full scale. This is one factor, for example, which ultimately limits the scale ratio that can be used when testing models for very deep-water conditions.

Effects of water and air compressibility are not normally considered in offshore engineering, except when designing ships' propellers and thrusters. Propeller and thruster design are specialist issues, that are normally considered only by manufacturers and specialist testing laboratories. Air compressibility is nonetheless a factor limiting the maximum speed (hence the maximum Reynolds Number) that can be used in wind tunnel tests. Air entrapment and compressibility may also affect the very short-duration acoustic shock pulse sometimes seen in wave slamming or green water impact experiments. This pulse is usually of too short a duration to have any structural significance for the design.

The interaction between a wave and solid wall can be split into three Elementary Loading Processes (ELP), these processes involve the direct impact between wave and wall (ELP1), the building jet (ELP2) and the expansion of entrapped or escaping gas (ELP3). Due to the different characteristics of each ELP they all require different Froude values in order to properly scale them. The global impact force resulting on the face of the structure is a result of these three ELP's which subsequently provides a significant issue when scaling the total force acting on the structure (Scharnke, 2019).

For many decades' model-testing tanks, or water basins, have been used for designing ship and offshore structures through Froude and Taylor models in regular and irregular seas. However, frictional and wave making resistance, propeller performance, ship manoeuvrability in smooth and rough water, cavitation, ship bending vibrations due to wave impact and slamming, sea keeping, and many other performances would be impossible to predict without model experiments. For example, when dealing with offshore structures, habitability is a factor not to underestimate. These structures are subjected to loads that are easy to model as long as still water is considered. However, complex phenomena such as wave loads and drifting forces may also

need to be considered. Oceanic environment is also characterized by wind, waves, currents and, in particular applications, ice flows, continuous winter sea ice, and icebergs.

Vassalos (1998) reviewed information of similitude, dimensional analysis and the use of governing equations for model experiments and addresses the modelling of some common ocean engineering tests.

One interesting problem is the scaling of impact/slamming pressure with entrapped air. This phenomenon is not only a challenging issue in offshore engineering practice but also in other applications including coastal engineering and sloshing (Bullock et al., 2001; Cuomo et al., 2009; Karimi et al., 2017). Several researchers have attempted to introduce new scaling methods to scale the impact/slamming pressure from model size to prototype size (Cuomo et al., 2010), yet these methods still required further improvement in various areas. Bullock et al. (2001) performed laboratory wave measurements for drop tests along with field data to investigate the effects of air on the impact pressure of fresh and sea water. The experimental data was scaled and compared with the actual field data using both Froude and Cauchy laws. It was concluded that Froude scaling overestimates the impact pressures by more than 10% whereas Cauchy law underestimates it.

Dias and Ghidaglia (2018) reviewed recent articles on wave slamming in various applications including the fundamental analytical models, scaling methods and experimental techniques. In case of scaling, the authors state that Froude scale is used for geometry although in different applications such as the existence of a gas pocket or building jet, the analytical model for scaling impact pressure must be selected accordingly. Still, it was denoted that slamming is affected by numerous parameters such as geometry, mixture of liquid and gas and surface tension. First, is the issue of validation, since these techniques were developed in a single model scale and they are required to be validated with different model scales. Furthermore, the methods were used for breaking waves on vertical walls in coastal regions, and their suitability for offshore structures applications should also be investigated.

A scale effect study was performed by Scharnke (2019) with the use of focused waves to identify the most important elementary loading process. In this regard, two test campaigns were conducted using 5 near to fully breaking focused waves with 10 repetitions and two different ambient pressures (1000 mbar and 50 mbar). Two model scales of 1:25 and 1:50 of a fixed platform deck at two different air gaps were tested. The horizontal and vertical forces as well as local pressures underneath the deck were captured using 6 DOF global loads, force panels and pressure cells. It was concluded that in the global load measurements, direct impact is the dominant loading process and different scales have effects on the measurements particularly negative vertical impact force.

Streicher et al., (2019) conducted a study looking at the non-repeatability, scale and model effects in laboratory measurement of impact loads induced by an overtopped bore on a dike mounted wall. Model prototypes at scales 1:4.3 and 1:25 were constructed to simulate the overtopping bore impact forces on a dike mounted vertical wall. Streicher et al. (2019) states that a scaled down version of a prototype can be considered if three criteria are met when scaling. These criteria are, geometrical similarity (similar in shape), kinematic similarity (similar in motion) and dynamic similarity (maintaining all force ratios). It was noted that the first two criteria were easily scaled with the third requiring a balance of inertial, gravitational, fluid friction, elastic compression, pressure and surface tension forces. The balance of these is unobtainable within normal scaling laws so it is critical that the dominant loading force is identified so that the correct scaling can be applied. Froude scaling was noted to be a source for unwanted scaling effects if air-water is modelled with emphasis on entrapped air in turbulent flows due to the compressibility of the water between the model, which can be accounted for reliably with Froude scaling. It was also noted that the air to water void ratio was larger in the prototype

compared to small-scale model testing which resulted in impact forces measured in small-scale testing being less dampened due to lower compressibility of the fluid.

The investigation of slamming loads on an offshore structure using analytical, experimental and numerical methods can be a difficult task to complete with restrictions and limitations being present for each method. Analytical methods provide a relatively quick way to gain an estimate on slamming force and impact pressure. Experimental methods which use a scaled model of the proposed structure provide a secondary solution to analysing the effects of wave slamming and the forces and pressures involved. Model testing can result in uncertainties when scaling the structure with forces and pressures scaled conventionally through Froude scaling methods being subject to levels of uncertainties.

2.3.2 Ship collisions

There are many publications on experimental testing of colliding ships (Vredeveldt and Wevers, 1992, Lehmann and Peschmann, 2002; Tabri et al., 2008; Calle et al., 2017; Aguiar et al., 2012). In all of them, the ships are scaled-down, sometimes significantly (1/4, 1/45, 1/35, and 1/100 scaled models). What really jumps out from these works is the difficulty in realizing the experimental tests. In case of a ¼ model, practical steel thicknesses and structural details are possible, but at the smaller scales material behaviour and failure is different. Typically, ductility goes up with decreased thickness and mild steel is not available at thickness below 3 mm. So, a different metal should be chosen. Scaling for buckling, bending, membrane and shear deformation also requires different scaling factors, namely linear or quadratic. So, prior to the test structural elements shall be categorized as predominantly bending or membrane, for adequate scaling the thickness. As far as this committee is aware, there is no systematic series of tests and analyses reported to address this in full, although methodologies are available for executing such a program.

Structural details cannot be scaled properly. Omitting details invalidates the experiment with respect to similarity. The manufacturing difficulties are mentioned also by Ohtsubo et al. (2017) and Calle et al. (2017). For example, welding is limited by restricted accesses. To fabricate all the components would lead to an enormous complexity, disproportionate cost, and long times for assembly. Therefore, simplified geometries are a necessity: only the main plates and stiffeners are typically considered. To reproduce the impacting body, Lehmann and Peschmann (2002) and Tabri et al. (2008) use a rigid bulbous bow as an indenter (instead of making a second, scaled-down ship model).

2.3.3 Offshore structures

Limitations in testing equipment open the way to small-scale testing also for investigations on seismic and penetration response and performances of related offshore fixed structures. Applications to investigate the dynamic response of buildings and physical infrastructure, especially when subject to seismic phenomena. Therefore, in civil and offshore fixed structural engineering was to consider in selecting a suitable set of scaling factors, procedure often complicated due to the great number of possible sets. They show that the whole procedure can be divided into two distinct types depending on whether the scale factor is chosen for mass or time.

An offshore fixed structures build as a frame structure resting on the seabed can be considered similar to land-based structures. A relevant work on the topic has been performed by Kim et al. (2004). Because the scaling laws are derived for the elastic range, the inelastic response of small-scale models exhibits some discrepancies. The authors apply and compare three scaling laws, based on mass, time, or acceleration, according to the importance of gravity; they are derived by means of dimensional analysis. When using the same scale factors for length and force, the comparisons of pseudodynamic tests (Kumar et al., 1997) with the three similitude laws lead to inelastic responses which are practically coincident. Pseudodynamic tests on steel

columns prove that these laws work well also in the inelastic domain. Furthermore, they propose a modified similitude law which considers both a scale factor for length and a stiffness ratio; it can effectively simulate the seismic response of prototype structures. When dealing with the inelastic range, conventional similitude requirements based on geometry may not be suitable. To overcome some problems related to the scale factor reduction, Kim et al. (2009) proposes models with dissimilar materials to those of the prototype.

Most of the experimental modelling of jack-up rigs foundations has been conducted to predict the behaviour of the footing under combined loading conditions, which is important for prediction of the overall system responses (Kong, 2012; Gaudin et al., 2011; Cassidy et al., 2004; Bienen et al., 2009). Two broad types of experimental investigations have been undertaken: single and multiple jack-up footing models at 1 g (normal gravity) (Byrne and Houlsby, 2001; Cassidy and Cheong, 2005; Cheong and Cassidy, 2016), or geotechnical centrifuge-based methods (at higher gravity) (Cassidy, 2007; Bienen et al., 2007). The experimental results of footing tests are derived from laboratory-scale floor models, and are used to validate the footing-model features and calibrate its parameters, with or without loading paths, during installation conditions.

Numerous studies on predicting on-footing stiffness have been conducted under working loads on a scaled model in 1 g (Vlahos, 2004; Vlahos et al., 2008) and in centrifuge-test conditions (Dean et al., 1996; Tsukamoto,1994; Teh and Leung, 2010; Zhang et al., 2013; Zhang, 2018). In addition, a model jack-up unit and actual installation loading path have been introduced in the development of geotechnical centrifuge tests for physical modelling of push-over capacity. Most studies have not considered ship collisions between the rig and an attendant vessel (i.e., horizontal impact loads) during normal operation.

Experimental methodologies with geotechnical centrifuge facilities are best suited to providing correct scaling for the self-weight of structures and replicating in situ soil stress conditions. This is achieved by centrifugally accelerating a small-scale model of a real geotechnical structure to a sufficiently high g level to simulate a prototype stress field in the model. The small-scale model is constructed at a reduced scale of 1:N and accelerated at N × g, where N is the desired g level (Taylor,1995). However, centrifuge facilities are currently unable to replicate impact loads (i.e., horizontal loads, such as ship or iceberg collisions).

2.3.4 Offshore wind turbine structures

In order to pursue commercial development of floating wind turbine technology a validated aero-hydro-servo-elastic numerical model, or fully-coupled simulator, is needed to accurately predict the dynamic system behaviour to efficiently optimize floating platform designs in offshore structures field. For properly model the dynamic behaviour of a floating wind turbine system subjected to aerodynamic and hydrodynamic loading, an appropriate scaling methodology must be used. A major challenge is overcoming the inability to simultaneously maintain Froude and Reynolds numbers for a scaled floating wind turbine experiment (Martin, 2011). In wind tunnel testing Reynolds number scaling is commonly used to establish model parameters in order to properly represent the relationship of viscous and inertial forces for a fluid flow (Çengel and Cimbala, 2006). In wave basin testing Froude number similitude is typically employed to properly scale the gravitational and inertial properties of wave forces, the dominant external forces for a floating vessel or structure (Chakrabarti, 1994).

Due to the special characteristics of laminated composite structures, the design of a scaled-down model of a large composite structure can be challenging. Static and fatigue tests with scaled model on composite beams, rotor blades, and system were performed by Nielsen et al. (2013), Branner and Berring (2014), Asl et al. (2015; 2017a; 2017b; 2018).

Asl et al. (2015; 2017a; 2017b; 2018) investigate composite I-beams analytically, numerically, and experimentally in the framework of model analysis for subcomponent testing; the beams

are equivalent to the spar caps and shear webs of wind turbine blades. Similitude conditions are obtained by means of similitude applied to governing equations. The novelty of these works is in the use of partial similitude. It is possible to obtain a complete similitude with ply-level scaling and keeping the same aspect ratio. When the laminate thickness is supposed to be scaled down below the range in which there is no integer number of laminae left in the stack up, however, ply-level scaling is no more achievable; reducing the lamina thickness is not an available option. Ply-level scaling is applicable only to specific lamination schemes but the possibility of keeping the same lay-up in the scaled models as in the prototype is limited by manufacturing constraints, since only fabrics with specific thicknesses are available in industry.

Thus, a partial similitude is a likely outcome due to manufacturing issues. The manufacturing issues is provided by Branner and Berring (2014). The scaling of the manufacturing defects (dry spots, dry areas, voids in the resin, misalignment of fibers, fiber waviness, wrinkles, delamination between composite layers and debonded areas in the adhesive bonds) and geometric imperfections (surface dimples and misalignment of structural parts) is more challenging and much research is needed in that area. With down-scaled tests it is realistic to build artificial and well-defined defects into these smaller and much less expensive blades. The effect of defect can then be tested in a more controlled way using down-scaled testing. Much research is however needed to study similarities and differences between artificial defects and real manufacturing defects.

2.3.5 Model ice testing

An appropriate way to forecast or validate full-scale ice loads are model ice tests. Such tests are conducted with model ice, which is a surrogate material mimicking the behaviour of sea ice in scale. Model ice has a smaller grain size than sea ice which is adjusted by the production process. Additionally, model ice contains a chemical dopant with a freezing point below 0°C that supports the adjustment of critical ice failure stress as a function of the temperature (e.g., Schwarz 1977, Zufelt and Ettema, 1996 and von Bock und Polach et al., 2019).

For global ice resistance loads especially the model ice behaviour in downward bending is of significance. Earlier research on fine grained model ice doped with ethanol showed that the bending stiffness is significantly lower than it should be according to the scaling similitudes of Froude and Cauchy (von Bock und Polach, 2015). Recent research showed this effect is not limited to a certain model ice type, characterized by gran structure and dopant, but is a unique property of model ice (von Bock und Polach et al., 2019a). This effect is reduced with increasing ice thickness which is presumably due to the increased strength and stiffness of the top-layer due to increased freezing or cooling duration (von Bock und Polach et al., 2019b).

The compressive properties, respectively the compressive strength, are of significance for the loading of vertical structures (e.g., side shells). In full-scale such tests are usually conducted with cylindrical specimens (e.g., Moslet 2007), while those in model scale are usually rectangular. The geometrical difference can hamper the transferability of full-scale results to model-scale results. In model scale the used specimen dimension vary and this geometrical variation has an impact on the measured nominal compressive strength (Suominen et al., 2019). Furthermore, also the boundary conditions, such as the specimen being tested in-situ and vastly grown to the parent ice sheet (von Bock und Polach et al., 2013) or fully extracted (Suominen et al, 2019) appears to have an influence on failure pattern and therewith strength. However, the complexity of the problem and the impact of other influencing parameters is not yet fully understood and requires additional research.

3. APPLICATIONS OF DIC

The application of Digital Image Correlation (DIC) techniques has certainly come into play in many recent experimental evaluations, as the method allows for elucidating the surface strain behaviour of a component evaluated either in the laboratory and in the field. The methods rely

on applied patterns or speckles on a component surface creating a reference image, and then tracking their deformation on subsequent images where the change in strain from the baseline is captured. Two- and three-dimensional approaches can be utilized to not only capture in plane behaviour but also out of plane strains. However, the utilization of this capability comes with many details that need to be carefully applied, not only is the field of view important, but also the camera selection, DIC speckle pattern size, lighting conditions, as well as the calibration pre/during experiment, as well filtering and processing methods to evaluate the extracted data. One resource that outlines extensive good practices was developed by the International Digital Image Correlation Society (www.idics.org) through a technical committee chaired by Jones and Iadicola et al. (2018), where extensive details are provided towards standardizing and developing good practices. It is worth noting that wide availability of digital devices is also modifying the way structural behaviour is represented: in lieu of numbers and tables showing stress, strain and displacement in single points, more and more coloured plots are used not only for e.g., FE analyses but also for experimental data captured by techniques like DIC able to provide variable gradients over a certain surface. Hence, DIC appears to be in line with the application of digital photos and videos technologies in the ship and offshore structure industry, helping and enhancing human efforts in design and condition assessment.

Besides various commercial instrumentations available on the market, see the following, covering almost all currently available ones to the best of the Committee's knowledge:

- DANTEC Q-400 (www.dantecdynamics.com)
- StrainMaster (www.lavision.de)
- Aramis (www.gom.com)
- VideoGauge^{TM} technology (www.imetrum.com)
- VIC 2D / VIC 3D (www.isi-sys.com, www.correlatedsolutions.com)
- sDIC(2D) / sDIC(3D) (www.seika-di.com)

There are a few open-source initiatives under development by several researchers. E.g., Ncorr is an open source 2D digital image correlation MATLAB program (www.ncorr.com), see Blaber et al. (2015) and Harilal and Ramji (2014). Other initiatives started like those of Eberl et al. (2021) or Atkinson and Becker (2020).

Additionally, in the following papers and web pages, open software and systems available in the internet are exemplarily mentioned pointing out that such measurement systems are nowadays leaving research to approach the field, even if it is believed this will need some time to be established:

- Belloni et al. (2019) developing py2DIC software,
- Olufsenet al. (2020) developing DIC software,
- Digital Image Correlation Engine, iDICs (2021) by Sandia National laboratories.

An interesting overview about DIC standards, training, and global networking is also presented by the international Digital Image Correlation society (iDICs, 2021) providing news and continuous updates on this rapidly growing technology. Interested reader is referred to this information source to obtain fresh news.

Various applications of DIC to monitor cracks in fatigue tests have been reported recently for ships and offshore structures. DIC was used to assess the strain field at the crack tip by Carroll et al. (2013) and Malitckii et al. (2019) or to detect fatigue damages on a microscopic scale by Rupil et al. (2011). Kovárík et al. (2016) performed tests on a resonance testing machine without test interruptions using DIC to assess cracks on flat, coated specimens under bending loads.

Friedrich and Ehlers (2019) presented a procedure using DIC for crack monitoring in resonance fatigue testing of welded specimens. The relative sharp notch at the weld and the resulting stress concentration makes them particularly prone to fatigue damages but represents also a complicated surface morphology for DIC measurements. A 3D DIC-system with two cameras is employed, which allows to account for out of plane displacements of the specimen and measure the strain field over the entire width of the tested specimens. The cameras are triggered by the force signal from the testing machine to capture images at the peak of the applied cyclic load, without interrupting the test. The high loading frequency of the resonance testing machine is accommodated by a short exposure time. Images are taken at a fixed interval of load cycles. After completing the fatigue test DIC is evaluated to calculate and plot the strain in the specimen's axial (loading) direction. In the image sequence acquired over the duration of the test, a forming crack will become visible in terms of elevated strains (Figure 2). A macroscopic crack is assumed when strains exceed 1%. From the results it is possible to determine the number of load cycles until initiation of a macroscopic crack and to monitor crack growth over the duration of the test.

The presented procedure offers a straightforward way to study the development of cracks in fatigue tests. It allows detection of technical cracks and monitoring of crack propagation (e.g., to determine crack propagation rates in fatigue tests). The illustrative nature of the results facilitates their interpretation and assessment. The technique is applicable to resonance testing machines with high loading frequencies without interrupting the tests. The measurements are fully automated, so no continuous supervision is needed. It is applicable on welded specimens presenting a relatively complicated geometry in the region of interest. On small-scale specimens, it allows coverage of the whole width of the specimen. Furthermore, the procedure is characterized by a simple setup and basic post processing, making it a practical alternative to existing methods.

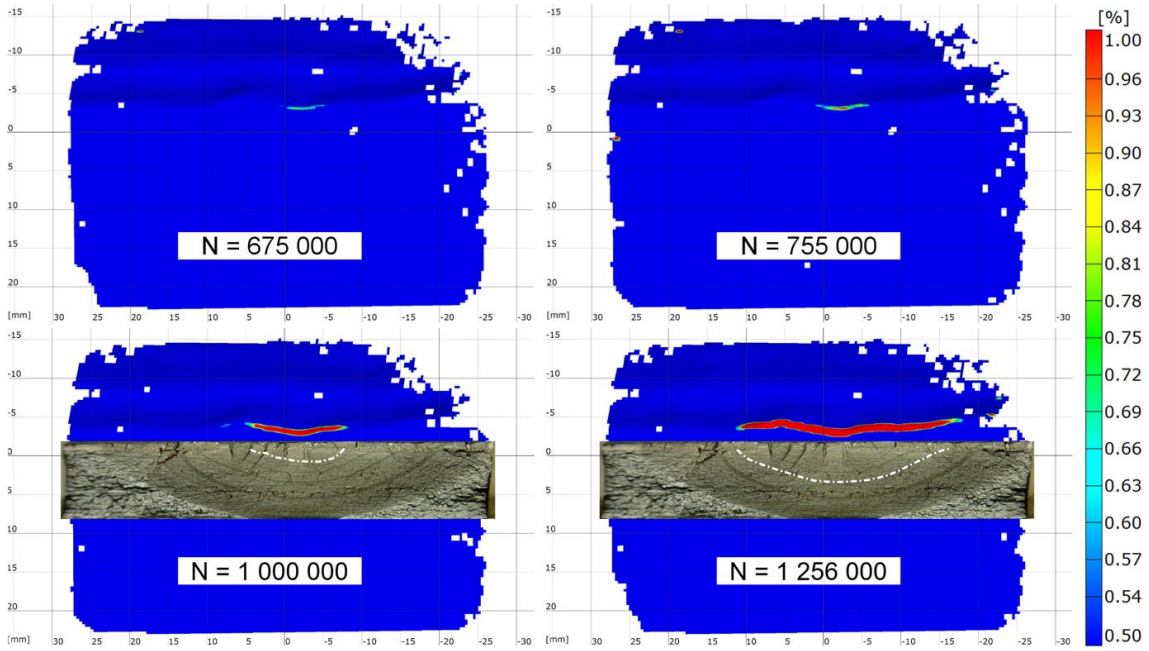

Figure 2: Percent strain in the loading direction (vertical) showing the development of a crack and comparison with beach marks. N = number of load cycles. (Friedrich and Ehlers, 2019)

An interesting application field for DIC is the fluid-structure interaction experimentation, where structural behaviour needs to be assessed without fluid flow disturbances. Banks et al. (2015) discussed their methodology developed for the wind tunnel environment. Other work in DIC has coupled theoretical formulations with DIC data to develop Hybrid-DIC approaches to develop strains around penetration as outlined by Khaja and Samad (2020), and verifying

crack growth rates with electric potential and complementary DIC measurements as outlined by Hosdez et al. (2017), where authors obtained acceptable agreements during experimental evaluations. DIC methods continues to be implemented in many experimental evaluations to elucidate the surface strains field behaviour and compare responses with failure models. When working on larger scales, the micro vs. macro response begins to come into play, for instance work by Du et al. (2019) looked at comparing target tracking of bridge support cables using digital image correlation techniques, where the DIC showed benefit in dealing with complex backgrounds when compared to other target tracking techniques. Along a similar note, Rong Wu et al. (2019) utilized DIC techniques to measure deformations of wind turbine blades in operation and developed a non-contact structural fault detection finding technique. Structural health monitoring is also being aided by DIC, such as the work by Ngeljaratan and Moustafa (2020) where a bridge truss structure was measured in-situ to capture its frequency response and compared to conventional accelerometer data. In cases like this, DIC can help capture global response and begin to highlight detailed areas that could be further investigated, or where a more detailed speckle pattern could be applied to capture localized fracture behaviour.

Worth mentioning is that some DIC applications are included in the benchmark study performed by the Committee and reported in section 15.

4. HYDRODYNAMICS OF FLEXIBLE STRUCTURES

Hydrodynamics of flexible structures, like offshore risers, umbilical and floating tunnels, play an important role in response prediction under waves and currents, especially when vortex-induced vibration (VIV) occurs. A large amount of research has focused on better measuring and predicting the hydrodynamic loads, forming several practical hydrodynamic coefficients databases which have been widely used in VIV prediction tools for industry. These databases are mainly generalized from 2D experiment results on rigid cylinders undergoing vortex-induced vibration or forced motions in purely CF (Gopalkrishnan, 1993) or IL (Aronsen, 2007) direction. Although these databases make great contributions to the field of VIV research, some important aspects of VIV phenomenon of a flexible pipe, such as Reynolds number effects, roughness effects, three-dimensional flow field effects, higher order force components, hydrodynamics for bare-buoyancy pipe and VIV suppression devices etc., have not been sufficiently modelled in the coefficient database obtained from rigid cylinder experiments.

Recently, a novel inverse finite element method has been developed by Song et al. (2016) and Wu et al. (2016). With the application of this method, for the first time, the real hydrodynamic coefficients distribution along a flexible pipe undergoing VIV are presented. The results indicated great differences between the real coefficients on a vibrating 3D flexible pipe and conventional ones got through 2D purely CF or IL forced oscillation tests, as illustrated by Figure 3. This new observation demonstrated us the huge differences between the reality and current practices, and it has been one of the significant progresses in the VIV field in last several years. Fan et al. (2019) further discovered that these differences were mainly because that the 2D forced oscillation tests didn’t consider coupling effects between CF and IL VIVs. If the 2D forced oscillation trajectory of a rigid cylinder is the same as that of a section on a flexible pipe, their hydrodynamic coefficients are basically the same as well. They also concluded that the phase angle between cross-flow and in-line response had a strong influence on the hydrodynamic coefficients for both rigid and flexible cylinders.

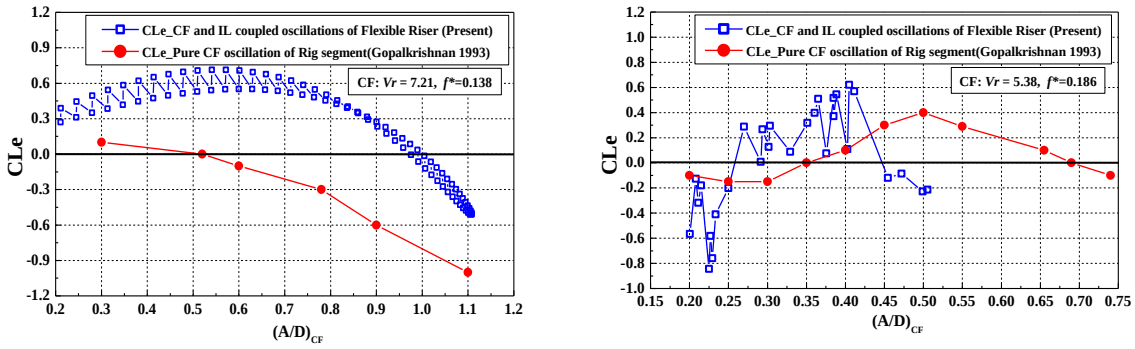

Figure 3: CF excitation coefficients vs. non-dimensionalized response amplitude (Vr =7.21 and Vr =5.38) (Song et al. 2016)

Inspired by the novel method developed by Song et al. (2016) and Wu et al. (2016), many researchers investigated the hydrodynamics on flexible pipes with buoyancy modules or strakes. Fuet al. (2017) and Zhang et al. (2018) discovered great ramps of VIV hydrodynamic coefficients between the bare cylinder and the adjacent buoyancy elements, where the added mass coefficient could reach up to 40 (shown in Figure 4), which has been proved to be within the same level as those observed by forced oscillation tests by Wu et al. (2017). Furthermore, Zhang et al. (2018) discovered that the added mass coefficient will be always continuous along the flexible pipe with staggered buoyancy modules under VIV conditions.

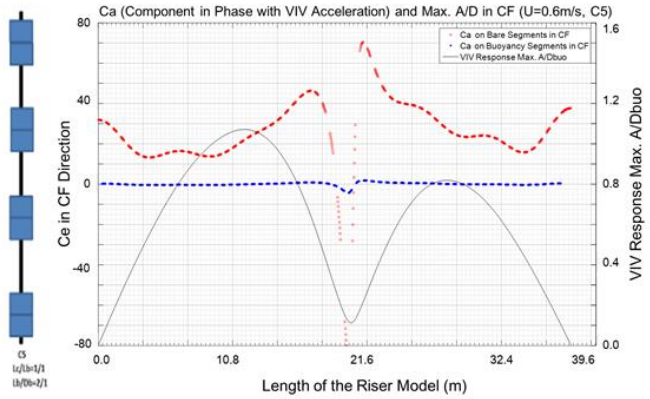

Figure 4: Identified CF added mass coefficients from a staggered buoyancy case C5 U=0.6m/s. (Fu.et al. 2017)

This novel finding provides guidelines for the hydrodynamic coefficient model application in VIV predictions for risers with buoyancy elements, like steel laze wave risers. Ren et al. (2019) investigated influences of helical strakes on the drag coefficient of a long flexible pipe undergoing VIV with the Reynolds number ranging from 1.1E4 to 9.5 E4. Helical strakes with 6 different parameters set of pitches and heights were studied. It is surprisingly found that the helical strakes with pitch of 5D can reduce the mean drag coefficient, whose value deduces from around 1.8 for bare pipe to 1.3, especially under low Re numbers (1.1E4 to 5 E4). While for staked pipe under oscillatory flow with small KC number, there is a significant amplification on drag coefficient which can reach approximately 10 (Ren et al., 2020). This amplification may lead to serious engineering safety problems potentially and must be taken into consideration in a real project.

Liu et al. (2018; 2020) proposed the Forgetting Factor Least Squares (FF-LS) method to identify time-varying hydrodynamics of a flexible riser under multi-frequency and modulated vortex-induced vibrations (VIV). The difference between coefficients under the basic frequency usually used in VIV prediction and those under multi-frequency coupling was firstly proved

and was found to be a result of the coupling effect between the basic frequency and high frequency. Besides, the time-varying feature of hydrodynamic coefficients was found to be the main contributor for the modulated VIV amplitude and frequency. If the time-varying hydrodynamic coefficient is replaced with a time-invariant value in VIV prediction, the amplitude and frequency of predicted VIV responses will be constant instead of changing with time, as given in Figure 5. Zhang et al. (2021) further developed an inversion method with consideration of spatial-temporally varying tension and relative flows. With this method, for the first time, hydrodynamics on a steel catenary riser under vessel heave motions were identified, as presented in Figure 6. And results indicated that variations of tension and flow velocity were strongly correlated with time-varying hydrodynamic coefficients. These new findings provide key inputs to the prediction of vessel motion induced VIVs, making the prediction possible.

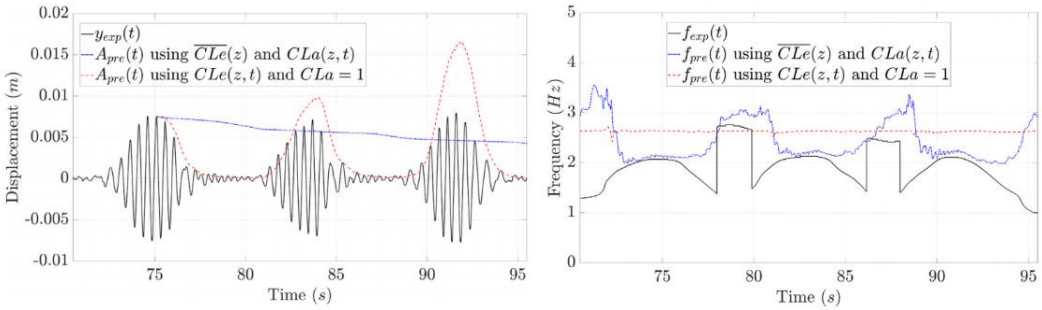

Figure 5: A comparison among the amplitude and instantaneous frequency of experimental VIV with predicted ones (Liu et al. 2020)

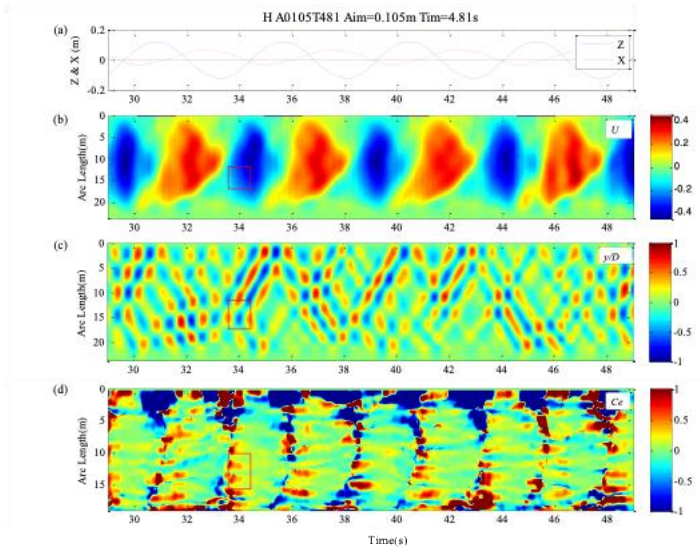

Figure 6: (a) Time history of imposed in-plane vessel motion; (b) in-plane velocity U; (c) non-dimensional displacement y*; (d) excitation coefficient Ce; forgetting factor μ= 0.945; the red frame marked an excitation region of VIVs. (Zhang et al. 2021)

To study the effects of Re numbers and surface roughness on hydrodynamics of VIV, Yin et al. (2018a) performed free and forced oscillation tests on a full-scaled rigid riser under prototype Re number (~ 6E5) with two different surface roughness ratios, which are 5.3E-5 and 1.0E-3. Only CF VIV was considered in the tests. The drag coefficient and excitation coefficient were found to be dependent on both Re number and surface roughness ratio. Distribution of excitation coefficient along non-dimensional frequency and amplitude ratio under prototype Re number (4E5) is totally different from that under low Re number. This finding strongly indicated that Re number effects should be considered in offshore riser/pipeline design. In addition, Yin et al. (2018b) performed model tests with a circular cylinder subjected to forced

motions taken from measurements with a flexible pipe under VIV. The measured IL excitation coefficients were applied in VIVANA to predict the combined IL and CF VIV motions and compare with model test data. Application of the updated IL coefficients improves the prediction of the combined IL and CF VIV responses. Wu et al. (2020) compensated the limitations of the mathematical model and the hydrodynamic parameters used in the existing perdition tools by using adaptive parameters and data clustering method. Results have shown that improvement of both the prediction accuracy and consistency have been achieved. Since the proposed method is semi-empirical, more model test data or onsite test data is needed to increase the robustness of VIV prediction.

To investigate the effect of wake interference on hydrodynamics of a twin-tube submerged floating tunnel (SFT), Deng et al. (2020) conducted a self-oscillation test with rigidly connected twin cylinders, as well as numerical simulations considering wave-induced hydroelastic and flow-induced vibrations. The cross flow (CF) response amplitude and lift force coefficients were observed to be strongly related to the spacing distance and flow velocity, as expected. The lift forces on the two cylinders strongly depend on the reduced velocity, but their rates of change are different. This difference induces an extra torsional moment, which is suggested to be considered in SFT design. Moreover, the influence of free surface reduces the VIV amplitude and its magnification on drag forces when a newly defined nondimensional depth h' ($h' = f_n h/U$, where U, f_n and h denote the flow velocity, natural frequency and submergence, respectively) is smaller than 0.55. From the numerical simulation, the VIV induced vertical motion and the corresponding bending moment, which are much larger than those induced by waves, reach maximum at the middle of SFT due to the unevenly distribution of the supporting pontoons. For the wave-induced hydroelastic features, the 2nd order wave forces substantially increase the lateral motion at the middle part of the SFT by exciting the low frequency eigenmodes. More extra pontoons in the middle could be an efficient way to decrease the hydrodynamic responses.

5. WAVE-IN-DECK EXPERIMENTS

Offshore installations in many global locations including Gulf of Mexico (GoM), Australian North West Shelf (NWS) and the North Sea are exposed to harsh metocean conditions which generate severe wave events. During the period 2004 – 2005, offshore installations located in the GoM were exposed to destructive forces of hurricanes Ivan, Katrina and Rita (Kaiser et al., 2009). An appreciation of the extent of damage generated by these extreme weather events can be gained from (Kaiser et al., 2009) where a total of 118 offshore structures were completely destroyed, and 72 other structures were severely damaged. In many cases, insufficient air gap (the vertical distance between the design wave crest and the lower deck underside of an offshore platform) has been reported to be one of the major reasons for damage sustained by offshore structures. This was evident in December 2015 when an enormous wave hit and damaged the accommodation block of an offshore drilling rig in the North Sea leaving one person dead and two more injured (REUTERS, 2016).

When attempting to ensure the survivability of offshore structures to large wave impacts, attention frequently focuses on extreme wave events, i.e., freak or rogue waves. These waves appear surprisingly as walls of water. Rogue waves are rare and strongly nonlinear waves that occur during extreme weather events that can cause serious damage to ships and offshore structures (Bitner-Gregersen and Gramstad, 2015). Current regulations used in the design of an offshore platform for a specific site (ABS, 2014, API, 2007) require a minimum air gap of 1.5 m between the expected magnitude of a 100-year wave crest (including tide and storm surge) and the underside of the lowest deck of the platform. According to the current design practices for floating structures (ABS, 2014, API, 2010), the survival conditions (1,000-year return period) are commonly used by designers for evaluating minimum required deck clearance (zero air gap). The recommended crest values for the North Sea and the Norwegian Sea have recently

been increased (Scharnke et al., 2014). New platforms will be designed with an air gap sufficient to avoid impacts with a 10-4 annual probability crest, or equivalent to 10,000-year return period. Wave-in-deck forces are one of the most critical loads that affect the structural design of both fixed and floating offshore structures (DNV, 2014).

5.1 Measurement of Wave-in-Deck Loads

Wave-in-deck impact events occur when the dynamic air gap reduces to zero, as a result of either a reduction in the static air gap, i.e., deck clearance or when an extreme wave exceeds the deck clearance. In model testing, the deck clearance adjustment is performed either by moving the deck up and down using a fine-tune mechanism or by changing the water depth of a wave tank. Load cells are used to measure the global forces generated due to the impact of the wave crest against the deck structure. As the structural dynamic response in force measurements may be introduced when a fixed deck model, the deck acceleration components can be monitored using an accelerometer mounted on the deck plates. The localised slamming pressures can be measured using piezoresistive pressure transducers. The pressure transducers should have a high resonance frequency, making them suitable for the measurement of slamming pressures. Furthermore, the tip of each transducer should be mounted flush with the underside of the deck to avoid any disturbance on the pressure readings. According to DNV-RP-C205 (DNV, 2014), a minimum sampling frequency of 20 kHz should be used for data acquisition system in order to capture the short-duration slamming pressures. Free oscillation tests in dry and wet conditions should be conducted to find the natural frequencies of the complete test rig in relevant degrees of freedom.

Fixed Deck Model	Fixed Multicolumn Model	Floating Model
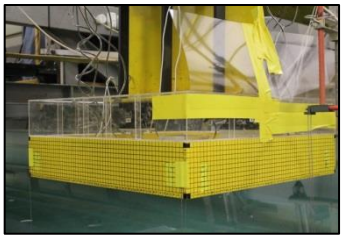	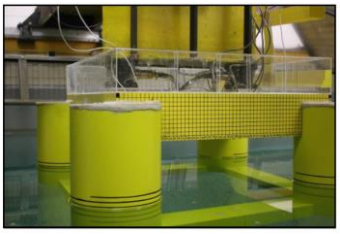	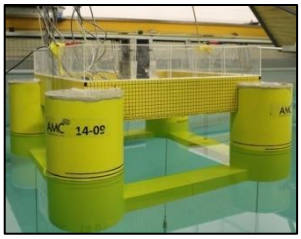
Measurements: ▪ Wave elevations ▪ Global wave-in-deck forces ▪ Localised slamming pressures ▪ Deck accelerations	**Measurements:** ▪ Wave elevations ▪ Global wave impact forces ▪ Localised slamming pressures ▪ Deck accelerations	**Measurements:** ▪ Wave elevations ▪ Tendon/mooring tensions ▪ Localised slamming pressures ▪ Surge motion

Figure 7: Test models and measured parameters for wave-in-deck experiments.

5.2 Fixed Offshore Structures

The simplest way to investigate wave-in-deck impact problems is a simplified rigid model where the deck structure is idealised as a flat plate or as a box-shape (Abdussamie et al., 2014a, Abdussamie et al., 2014b, Abdussamie et al., 2017a, Baarholm, 2009, Bhat, 1994, Scharnke and Hennig, 2015). Current design practices (API, 2007, DNV, 2014, ISO, 2007) recommend several theoretical approaches such as the global/silhouette approach (API, 2007) and a detailed component approach, e.g. the momentum method (Kaplan et al., 1995), to evaluate the wave-in-deck loads acting on fixed offshore platforms. However, such engineering approaches rely on potential flow theory. This theory simplifies the analysis by assuming an incompressible fluid with a free surface to derive global loads from the change of fluid momentum during the wave impact, using wave kinematics of a non-disturbed wave field. The effects of diffraction and entrapped air are therefore neglected, both effects that can strongly influence the platform behaviour and loads.

Scharnke et al. (2014) reported that the load model recommended by the American Petroleum Institute (API) (API, 2007, DNV, 2014) underestimates the measured horizontal wave-in-deck loads on a fixed deck of jacket platform in both regular and irregular wave tests. Even though the API loading model used wave kinematics obtained by Stokes fifth order wave theory, the underestimation of the loads was severe, particularly in irregular waves (Scharnke et al., 2014). The momentum method was also found to underestimate the magnitude of the wave-in-deck forces on a fixed horizontal deck subjected to unidirectional regular waves (Abdussamie et al., 2014a, Abdussamie et al., 2014c).

A more complex investigation of the phenomenon should include the effect of columns on the magnitude and distributions of the deck loads. Scharnke and Hennig (2015) investigated the effect of substructures on the magnitude of wave-in-deck loads by attaching a fixed box-type deck structure to a square column. The authors concluded that the column presence significantly increases the magnitude of global vertical forces and local pressures.

A recent coupled numerical and experimental work has been done at the Australian Maritime College by Mohajernasab (2021) on the scaling effect and air entrapment during wave-in-deck. The scaling study considered wave-in-deck forces and pressure on different scales of box-shaped models without air pockets. The objectives of this study were to improve the methodology of scaling wave-in-deck forces and pressure. The experimental study conducted using three different scales of a prototype and all the parameters including wave time histories, water depth and air gap were scaled using Froude scaling method to establish a solid investigation into the effects of scaling. The selected experimental models were manufactured according to Table 1 and shown in Figure 8. Each model was divided into five and four equal lengths in x and y directions and at each intersection, a pressure transducer was mounted, hence, a total number of 12 points (in 4 rows and 3 columns) were defined on models where pressure was captured. A six degree of freedom load cell was mounted in the centre of each model.

Table 1: Models specification that were used for the experimental tests and the target full scale model.

Scale	Length/Width [mm]	Height [mm]	Water Depth [mm]	Air Gap 1 [mm]	Air Gap 2 [mm]
1:1	76,000	13,750	70,000	9,000	8,000
1:75	1013	210	800	120	107
1:100	760	135	700	90	80
1:125	608	110	560	72	64

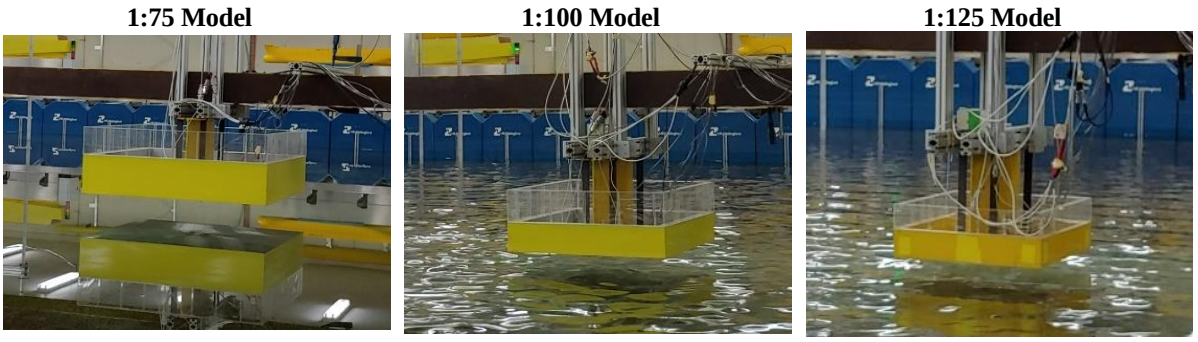

Figure 8: Deck models that were used for the experimental tests.

In the air entrapment study, 3 sizes of air pockets (Table 2 and Figure 9) at 3 different depths created 9 different conditions for air to be entrapped underneath the deck during a slamming event. These pockets were assembled using acrylic sheets on the underside of the 1:75 model scale and placed in the middle of deck (Figure 10). Pockets sizes were selected based on the structural member spacing potentially can be chosen as the distance between main stiffeners on a full-scale deck. During the experiment, pressure values were captured across the diagonals of the pockets as well as the global forces in horizontal and vertical directions. This work is

still ongoing, and its outcomes can answer two main questions in wave-in-deck phenomenon: Firstly, what is the effect of air entrapped on the local and global wave-in-deck slamming loads and secondly, how can model scale testing methodologies be improved to account for the effects generated by the presence of entrapped air?

Table 2: Models specification that were used for the experimental tests and the target full scale model.

Parameter	Model Specs	Full Scale
Length/Width	1013 mm	76.0 m
Height	210 mm	15.7 m
Air Pocket Specs		
Length/Width	203 mm (20% of Deck Length)	15.22 m
	152 mm (15% of Deck Length)	11.40 m
	101 mm (10% of Deck Length)	7.61 m
	40 mm	3.00 m
Depth	30 mm	2.25 m
	20 mm	1.50 m

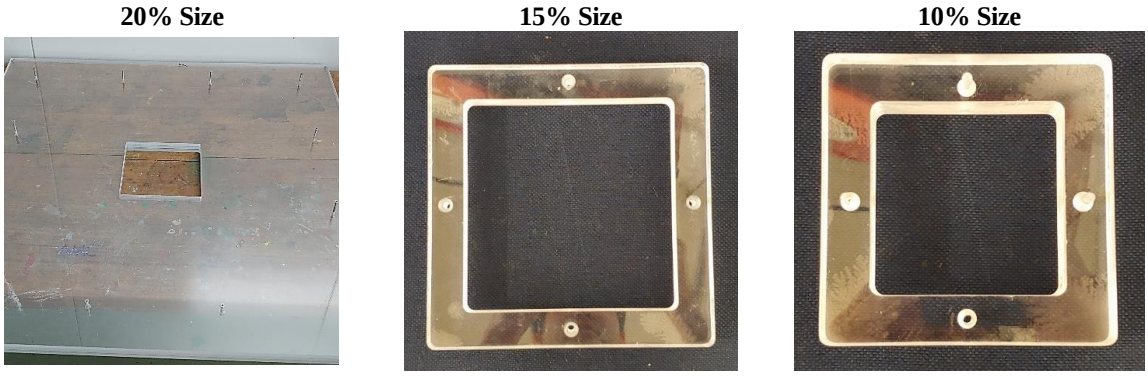

Figure 9: Different air pocket sizes.

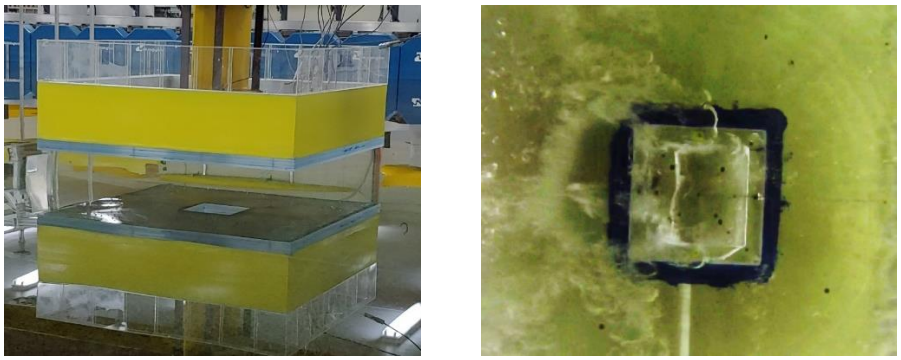

Figure 10: Acrylic sheets used to create air pockets mounted on the underside of the deck and a snapshot of air entrapment during slamming.

5.3 Floating Offshore Structures

The current engineering knowledge required to accurately predict the magnitude and distribution of wave-in-deck loads and the resulting global response of floating structures such as TLPs and semisubmersibles remains limited. This fact is reflected in the very limited number of papers reporting on model tests of typical multi-column floaters currently available in the open literature (Abdussamie et al., 2017b). Johannessen et al. (2006) and Hennig et al. (2011) investigated the dynamic air gap, wave loads and floating platform response under extreme wave conditions. Both investigations reported that a wave-in-deck event can lead to an additional extreme response mechanism and a step change in the extreme loading magnitude. It must be

noted that complete and detailed results of these types of experiments are usually subjected to project confidentiality requirements and are therefore not available in the public domain.

5.4 Repeatability of Wave-in-Deck Slamming Pressure

5.4.1 Slamming Pressure Magnitude Selection

A typical pressure time history of wave-in-deck bears a resemblance to Figure 11 (a) where the pressure rises instantaneously as the impact occurs and reaches its peak. Subsequently, as the water leaves the area, pressure drops and stabilizes to the atmospheric pressure. However, in several circumstances, particularly in regular wave conditions where multiple impacts are happening, the pressure time history does not follow the explained trend and unusual noises emerge in the signal as it depicted in Figure 11 (b). These noises are originated by various sources:

1) A droplet of water from an impact may go inside a pressure transducer and affect the recording signal.
2) Pressure transducers specially when they are used with a high sampling rate collect excessive noises during testing.
3) The disturbance in wave crests after impact occasionally induces extra noises into the recording time history.

These undesirable noises cannot be filtered out using any analogue or digital filter, thus, they were not considered in the selection of peak pressure magnitude and the peak values were selected manually by looking into the pressure time history individually for each impact.

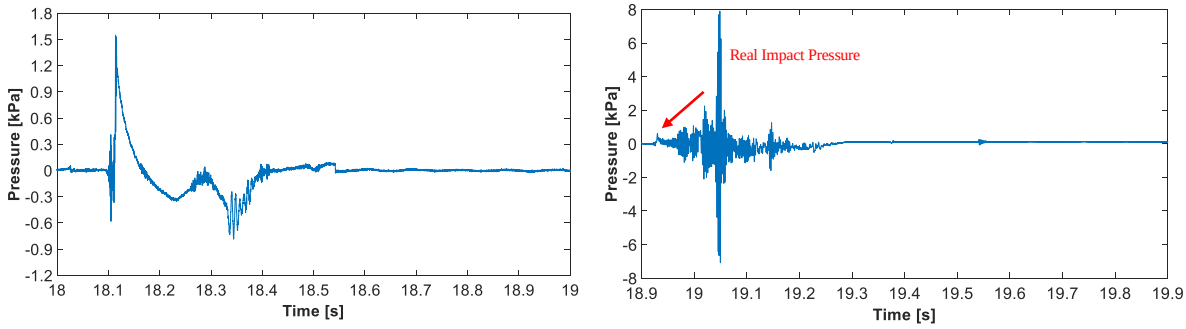

Figure 11: Time histories of (a) a typical impact pressure and (b) an abnormal impact pressure.

Uncertainty analysis of pressure measurements is introduced by demonstrating how vary the impact pressure associated with an extreme wave impact measured in multiple runs. As an example, the pressure distribution along the bottom plate of a fixed deck structure is presented in Figure 12 using boxplots such that the variation among the different runs can be investigated. The maximum and minimum values, the first quartile (the 25th percentile) and third quartile (the 75th percentile), Q1 and Q3, as well as the median pressure values, measured in multiple runs, were combined into a single plot. The vertical centreline between PT#8 and PT#9 denotes the geometric centroid (x = 0) of the bottom plate. The boxplot definition is given in the legend of each graph. The square symbol (▪) represents the mean value of peak pressures measured by a transducer in different runs. Only PT#1, PT#11 and PT#15 detected outliers as depicted by cross marks (+). Using boxplots indicated how the impact pressures vary amongst multiple runs having approximately an identical wave condition. The variation in impact pressures was examined by investigating the uncertainty attributed to the transducer itself, its location (which may be affected by side edges) as well as the deck clearance.

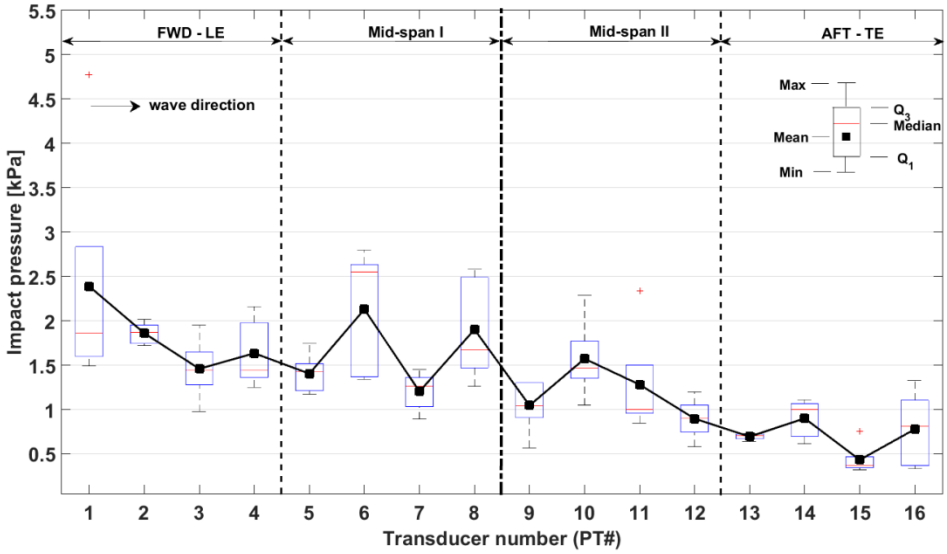

Figure 12: Boxplots showing impact pressures measured by sixteen PTs in multiple runs.

5.5 Numerical Development

Model tests are arguably the best approach for estimating wave-in-deck loads (Scharnke et al., 2014). However, model testing is costly, time-consuming and involves several drawbacks such as scaling effects. It is therefore not surprising that computational fluid dynamics (CFD) based methods used for calculating wave-induced loads on offshore structures have received an increasing amount of attention in recent years. Commonly used commercial codes such as STAR-CCM+ and ANSYS FLUENT are available for modelling and solving wave-in-deck impact problems using the volume of fluid (VOF) method to capture free-surface hydrodynamic flows (CD-Adapco, 2012, Fluent, 2009).

There is a large body of work on CFD investigations of wave impact loads on fixed deck structures (Abdussamie et al., 2014b, Birknes-Berg and Johannessen, 2015, Iwanowski et al., 2014, Ren and Wang, 2004). However, very little work on fixed with columns and floating structures has been reported to date. Iwanowski et al. (2009) and Lee et al. (2014) investigated the air gap of a simplified, fixed semisubmersible having a static deck clearance of 18 m (full scale). CFD-based codes including ComFLOW (Iwanowski et al., 2009) and CD-adapco STAR-CCM+ (Lee et al., 2014) were employed at full-scale dimensions to generate regular waves with the aid of the free surface VOF method. The computed wave run-up and wave impact pressures on the platform's columns were compared against model tests (Iwanowski et al., 2009). The authors observed a large variation in peak pressures for different wave events in both experimental and numerical tests which led them to conclude that the peak magnitude of the impact pressure is an extremely localised phenomenon in both time and space.

There have been even fewer numerical investigations on floating TLPs (Buchner and Bunnik, 2007, Rudman and Cleary, 2013, Wu et al., 2014). Buchner and Bunnik (2007) employed an improved VOF (iVOF) method implemented in ComFLOW for solving the dynamic response of the SNORRE-A TLP subjected to extreme regular waves. Rudman and Cleary (2013) employed the Smoothed Particle Hydrodynamics (SPH) technique to simulate the fully non-linear dynamics of a large breaking wave hitting a TLP. These numerical studies were not validated against model tests. Wu et al. (2014) conducted a numerical study using STAR-CCM+ to investigate the air gap of a TLP under irregular extreme waves by applying the same input wave signal used in the model test. Each wave signal required 20 or more iterations in order to achieve a satisfactory match between measurements and numerical results. This implies that their proposed CFD technique is still too time expensive to be used for practical applications (Birknes-Berg and Johannessen, 2015).

Recently, a robust overset grid technique was used by Wu et al. (2014) and Chen et al. (2008) to allow for numerical models with six degrees of freedom (6DOF). Unlike traditional mesh techniques such as dynamic mesh or sliding mesh, the mesh in the overset grid technique does not deform and thereby remeshing is not required. The method can therefore be employed with adequate numerical stability for modelling large amplitude motions such is the case of the surge motion in TLPs. Nevertheless, any new CFD simulation technique can only be trusted by the industry if its results have been thoroughly validated against experimental data first.

In practice, both numerical and experimental studies are required to investigate the effects of air pocket on the wave-in-deck loads (ABS, 2017). However, the open literature suggests that both aforementioned approaches are still not straightforward. Experimentally, due to the presence of the air pocket, a conventional scaling methodology based on existing similitude laws cannot be implemented. Meanwhile, CFD studies must be validated by experimental results and in addition, due to the nature of the problem in hand, the computational cost of these studies is very high. It is suggested that, in order to obtain a real understanding of the problem, both approaches must be interrelated to achieve meaningful results.

5.6 Model Tests versus CFD: Fixed Deck Model

Figure 13 shows the arrangement of pressure transducers (PTs) on the bottom of the deck. The bottom plate of the model was divided into 20 equal sized areas by 7 lines (3 in wave direction and 4 perpendicular to the wave direction). PTs were located on each intersection which resulted in 4 PTs rows and 3 PTs columns for a total of 12 pressure sampling points (numbers as PT#1 to PT#12). A corresponding number of piezoresistive pressure transducers (Endevco 8510C-50) with capacity of 0 to 344 kPa and 320 kHz resonance frequency were utilized to measure the pressure at these locations with the sampling frequency of 20 kHz for data acquisition system.

The impact pressure was also recorded for each condition using 12 PTs. The first impact time histories of PT#2 for all runs of same wave condition and the FFT results are shown in Figure 14. The time histories are only for the first impact. The impact occurs at approximately 8.83 s. In Figure 14 (b) the FFT results are depicted. No modal frequency is observed in this figure and only the frequencies of various wave orders exist. Since no modal frequencies and high frequency noises did not emerge in the FFT results, filtering was not preformed.

The measured slamming pressures have been used to validate a Computational Fluid Dynamics (CFD) model. As an example, the time history of pressure at each pressure point is shown in Figure 15 First and foremost, CFD simulation can predict the local at each point relatively accurate, however, several inconsistencies can be seen throughout the time histories. In Row#1, for instance, CFD overestimates the pressure from the second impact at all three pressure points, while in Row#3 it is vice versa as CFD prediction peak points are lower than experiment. Furthermore, maximum pressure recorded in experiment occurred at PT#7 whereas CFD simulation shows that PT#2 is the highest pressure point among all the 12 points. Nonetheless, magnitude-wise, the mean values for maximum pressure in both approaches are in close agreement.

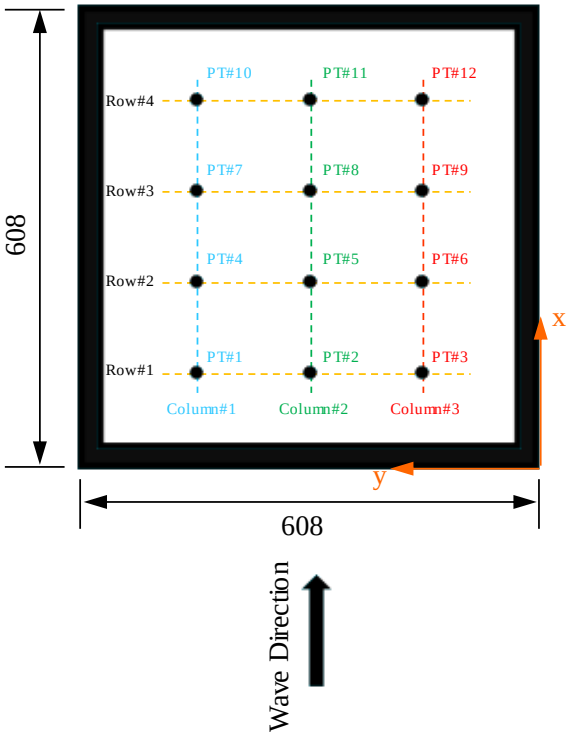

Figure 13: Arrangement of PTs on the underside of the model.

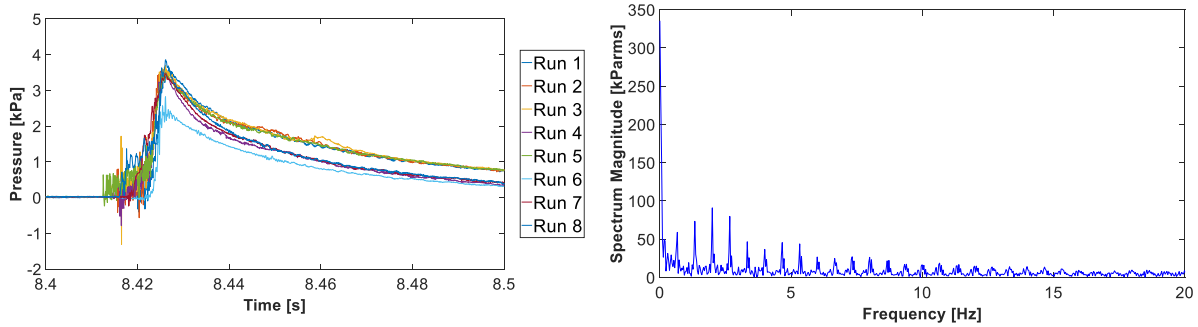

(a) (b)

Figure 14: (a) Time histories of pressure recorded in PT#2 and (b) FFT results of pressure for all runs.

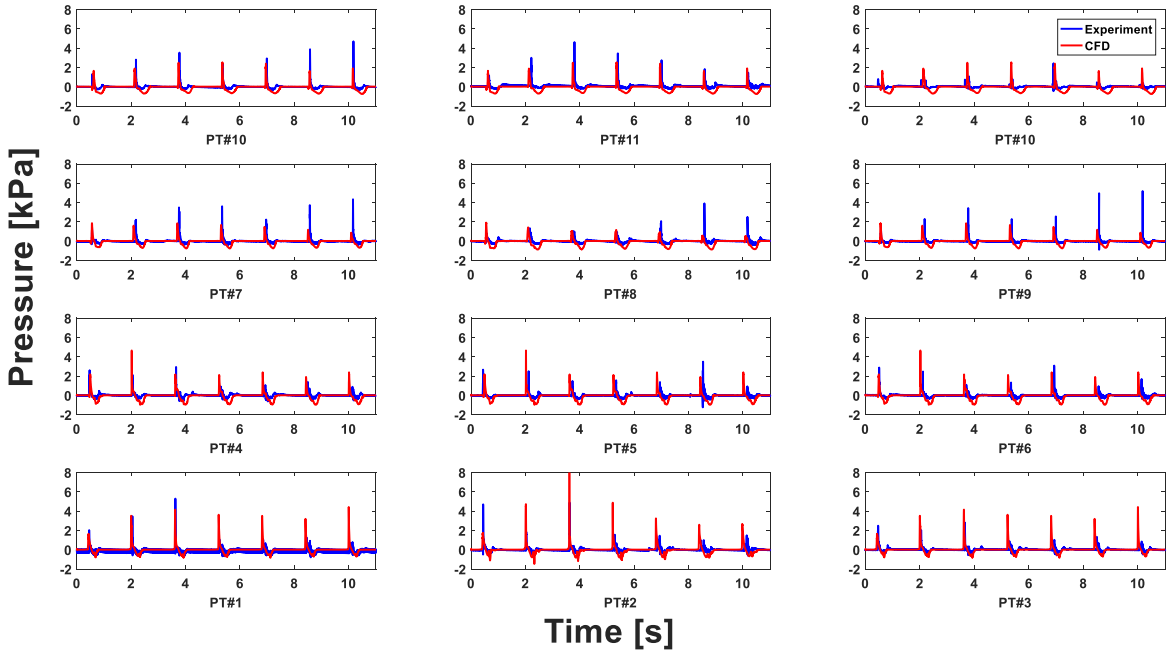

Figure 15: Time history comparison of experimental and numerical pressure at each pressure point.

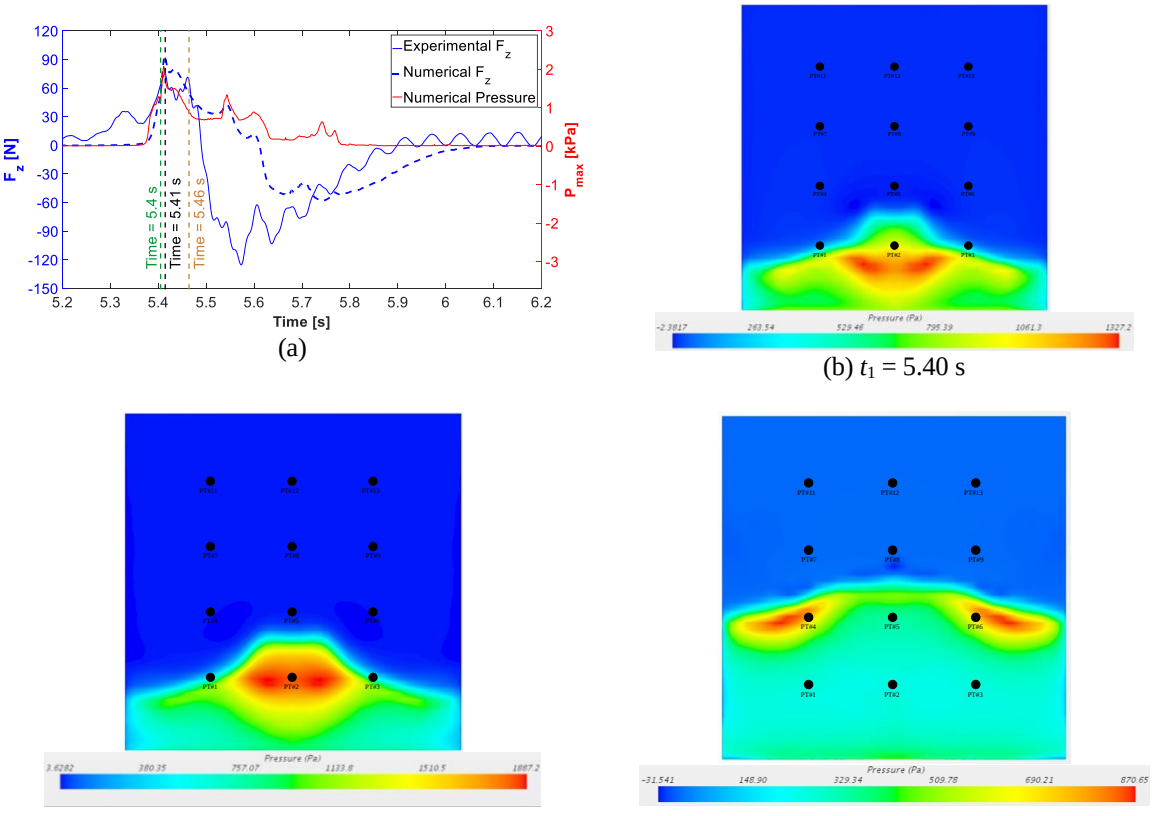

(a)

(b) t_1 = 5.40 s

(c) t_2 = 5.41 s

(d) t_3 = 5.46 s

Figure 16: Time history comparison of experimental and numerical Fx and Fz.

Figure 16 (a) demonstrates the vertical force time history of the fourth impact in both CFD and experiment as well as the maximum pressure time history on the underside of the deck. Three distinct times (t1 = 5.40 s, t2 = 5.41 s and t3 = 5.46 s) in time history and their corresponding pressure distribution have been extracted and shown in Figure 11 (b), (C) and (d). It should be mentioned that t2 is when the maximum Fz occurs and t1 and t3 are when Fz is half of the

maximum vertical force before and after t2. The pressure distribution during the impact is at its maximum near the deck centre line (around PT#2) and it decreases towards the sides until it reaches the highest magnitude at t2. Subsequently, the pressure distribution is inverted as the maximum pressure moves to the sides and occurs around PT#4 and PT#6 and the centre line experiences the lowest pressure. Furthermore, comparing the experimental and numerical vertical force values at these three times, which is respectively, 60.1 N and 47.8 N at t1, 85.4 N and 93.8 N at t2 and 39.1 N and 46.8 N at t3, suggests that although the pressure distribution in experiment and CFD may not follow an exact location-wise trend, the resultant force during the impact is fairly similar.

6. HYBRIDE MODEL TESTING

Hybrid model testing (HMT) combines physical model test and numerical simulations to solve problems that physical model tests alone cannot conveniently or reliably address. In marine model testing, the challenges like ultra-deep water, multi-phase fluids, parameter traversal and so on cannot be avoided. HMT is regarded as the most promising technique to solve these issues. As of today, HMT is still immature, some advanced applications however have been developed.

To test the floating structures in ultra-deep water, the active truncation based on HMT has already been proposed in 1990's (ITTC, 1999). The main idea is modelling the floating structures at a reasonably large scale and the upper part of mooring and riser system in physical space. The lower part of the mooring and riser system connected to seabed is simulated on a computer. The two parts interact at the truncation point through sensors and actuators located on the floor of ocean basin. Cao and Tahchiev (2013) and Sauder et al. (2017, 2018, 2019) investigated the feasibility of this method through simulation studies. However, it has never been fully implemented in practice.

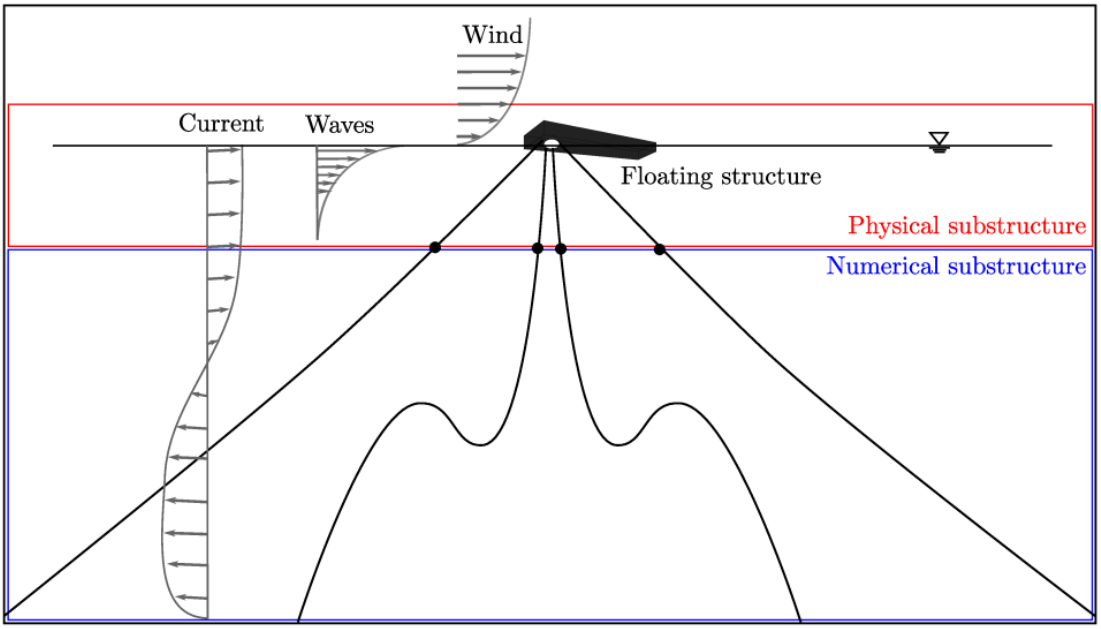

Figure 17: Schematic of active truncation (Sauder et al. 2019)

When performing hydrodynamic model testing of the offshore wind turbine (OWT), issue of multi-phase fluid arises as the major challenge. Since gravity, inertia and viscous loads all have a significant effect on the response, Froude and Reynolds scaling laws should be satisfied at same time in model testing. However, incompatibility between two laws exists in physical model test. Aim at this problem, Sauder et al. (2016) developed HMT of OWT in ocean basin. The physical model of OWT without rotor/nacelle assembly (RNA) placed in the ocean basin

and numerical model of RNA is built in software. Since hydrodynamic loads are physical, aerodynamic loads calculated numerically at full scale should be scaled down according to Froude scaling. In contrast, Bayati et al. (2014, 2017) used HMT to enhance wind tunnel testing of OWT. Hydrodynamic loads are numerical and aerodynamic loads are physical. These important applications provide a good reference for solving incompatibility between scaling laws in multi-phase fluid.

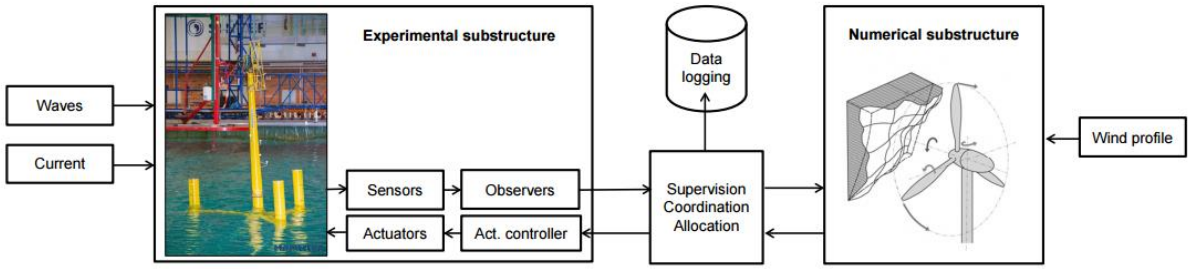

Figure 18: Basic strategy of HMI application to OWT (Sauder et al. 2016)

In fluid-structure interaction (FSI) studies like vortex-induced vibration (VIV), complex physical phenomena are related with some essential parameters of the system, such as mass, spring stiffness, damping and combined parameters. Normally, these parameters are depended on physical system model by the mechanical arrangement. Parameters cannot be conveniently changed and precisely controlled. Recently, Hover et al. (1998) combined the advantages from numerical and experimental methods and developed HMT methods to investigate VIV based on force feed-back. The experimental results using HMT are demonstrated in towing tank studies of uniform and tapered cylinders. In their studies, the sensor measured the fluids force and computer calculated the movement in next time step based on kinetics. The actuator finishes the movement command at the next time. The cycle of measuring fluid forces, computing movement at next time step and executing the object's movement is repeated at a fast rate, producing a simulation of the equivalent purely physical system. Muse et al. (2008) used the similar technique to study the aerodynamic issues. Lee et al. (2011) adopts a position/velocity feedback system in VIV energy extraction studies, though their forces are modelled rather than measured. Mackowski and Williamson (2011) proposed a new approach called cyber-physical fluid dynamics (CPFD) to realize the same target and further extended this method to investigate VIV under nonlinear spring system. HMT allows researchers to impose mass-spring-damping parameters in virtual space and can artificially adjust and precisely control these critical parameters. It is a very helpful and exciting idea to solve the involved problems.

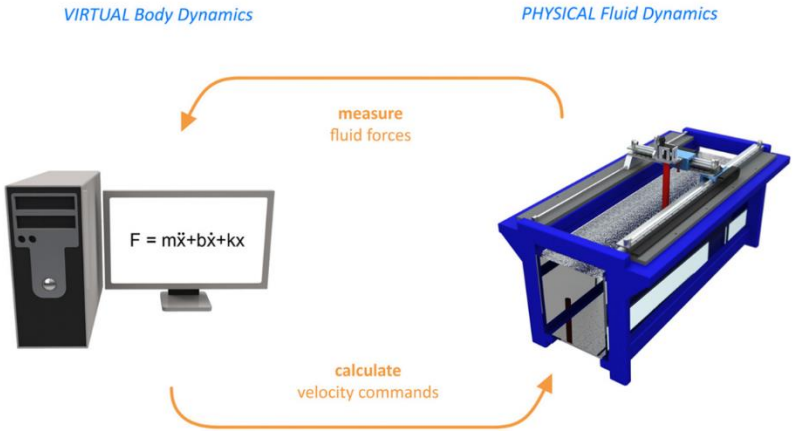

Figure 19: The concept of a hybrid cyber-physical system draws on both computation and experiment (Mackowski and Williamson, 2011)

7. FRICTION TESTS

The world can't move without friction. Nevertheless, quantifying friction is a complex matter. In maritime and offshore operations, two main areas exist where friction is of importance: machineries and mechanical connections, and in cargo/ mechanical handling operations. For the first low wear and low friction are of interest. Lubrication may be a factor, while the ambient conditions may be severe: hot, cold, corrosive environment, abrasion by particles. For cargo/ mechanical handling, friction is needed to keep the load in position.

Typical maritime and offshore applications are shaft glands, cribbing wood, wheels over deck, chain links (e.g. Out-of-Plane Bending) and pipe grippers. For these applications, surface conditions and environmental conditions are important parameters. Small specimens may be used for screening the theoretical friction coefficients and find trends. Any apparatus measuring friction has to be able to (Menezes et al. (2013)):

- Supply relative motion between two specimens
- Apply a measurable normal load
- Measure tangential resistance to motion

There are many methods to test the smaller specimens. The typical method is a Pin-on-Disc method, as detailed in ASTM G99-17 (2017). Normally dynamic friction and wear coefficients can be established. A disk is driven continuously while a pin is normally stationary with a load applied to it. Note that the geometry of the pin can differ from test to test (e.g., non-rotating ball, flat-ended cylinder, etc.). instead of the rotating disc, a reciprocating flat surface can be used. Details are provided in ASTM G133-05. Other, less common, methods include rotating cylinders or rotating balls. Canestrari et al. (2017) listed a large range of methods. At Tribonet.org (http://www.tribonet.org/tribology-testing-standards/) a comprehensive list of ASTM standards (ASTM, 2012) is provided for various kinds of the friction, wear and erosion tests.

Larger or even real size specimens should be used to confirm the actual behaviour. Such measurements will also allow to find the static friction coefficient. A typical set-up suited for flat samples is shown in Figure 2020. The vertical force is the normal force on the surface of interest. The outer material and central material represent the items of interest, e.g., cribbing wood and steel (deck/ cargo). The horizontal force and displacement are recorded to establish at what force slip starts and what force is required to maintain motion. Such set-ups can accommodate ambient conditions such as low or high temperatures and humidity. Numerous repetitions will allow to measure wear by gravimetric or thickness measurements. This arrangement of the set-up has double the friction force and as small differences in the contact area may change the result, repetitions are essential to find reliable values of the friction coefficient for one surface. It is not advised to have one of the surfaces frictionless, as ultimately frictionless is not feasible. Then two different friction coefficients appear, making it harder to find the one of interest.

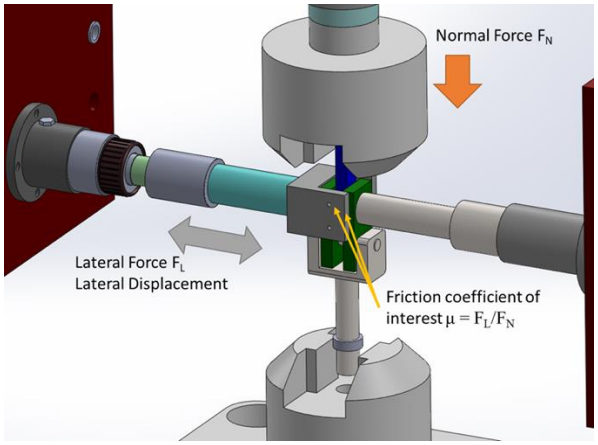

Figure 20: Schematic for friction test with flat samples

Similarly, rotational set-ups can be devised. A typical test scheme for a journal bearing is described in Dragt et al. (2015). This large-scale test set-up allowed for measuring the static and dynamic friction coefficient, and the wear. Also, in such large set-ups, environmental conditions can be varied.

Concluding, friction tests can be split it eh standard, small size specimen standard tests, and the large size, more representative tests. While the standard tests are well covered by standards and guidelines, the larger set-ups are to be tailor made and require goo understanding of the physics as results require interpretation by the experimenter.

8. VIBRATIONS

Increasing ship size, requires more torque and thrust from propulsion systems for normal operations which could result in excessive shaft vibration. The trend to build lighter structures results also in more vibration modes, and also with natural frequencies in the range of the excitation. Vibration aboard ships can result in discomfort for personnel and passengers, and in more severe cases to major machinery and equipment failure. During operation, marine structures are subjected to various loads, with substantial distortions and nonlinear responses, so it is quite challenging to understand the behaviour (Kandasamy et al., 2016). If the vibration exceeds the maximum allowance, damages could occur, which would threaten the safety of the vessels and crews. Specific for offshore rigs, the deep-water drilling/production riser may experience vortex-induced vibration (VIV) exerted by unsteady currents and waves, which could result in fatigue damage.

8.1 Measurement methodologies

When an issue arises with extreme vibrational response, measurements are the first step to investigate the situation. Mode shape and natural frequency are the most important parameters, besides damping. Taking a hull girder vibration mode as example, there are several levels of detail one can measure. Essential is to predict the vibration modes. Locations for measurement, and excitation need to be at locations with larger response. The minimum sensor suite are the accelerometers placed at the locations outside nodes. The recordings will provide the natural frequency and with sufficient accelerometers over the length, also the mode shape(s) will show. The time series can be used to find damping based on the amplitude decline over each cycle. When the excitation input spectrum is also known, the transfer function can be derived. Input can be recorded by using for example an instrumented hammer or an imbalance in the form of an eccentric motor. The benchmark study executed by the current committee members provide details on how to perform such measurements.

8.2 Recent Developments in Mitigation of Vibration

To reduce vibration effectively, Yucel et al. (2020) designed a new foundation for auxiliary engines which can work as a vibration reducer. In terms of harmonic vibration analyses, the developed foundation acted as a better vibration reducer on the engine room floor by comparing different foundation models. Liao et al. (2018) proposed a wire-type tuned vibration absorber (WTVA) comprising of shape memory alloy (SMA) wires to reduce the induced vibration. Proposed WTVA experiments were carried out using a six-degree-of-freedom platform, and the experimental results suggested maximum efficiency of around 90% in vibration reduction. In case of large wind turbine generators being supported by slender towers the frequency of the passing blades may come close to the natural frequency of the tower, especially during transient conditions such as start and stop. The Tuned Mass Damper, such as applied in Taipei 101 tower, is a well-known solution to absorb excessive vibrations and is also being proposed in wind turbine generators, e.g., Brodersen et al., 2017.

Tian et al. (2019) focused on the vibration response of the ship propulsion and investigated dynamic responses of the shaft established on a scaled shaft test platform. However, the experimental investigation indicated a severer vibration on the shaft under transverse loadings than under vertical loadings due to structural properties. Tian et al. (2018) conducted an experiment on several vibration characteristics of the propulsion with different factors. During the navigation of a large vessel along the China coastline, real-time data were collected using several sensors from ship hull and shaft propulsion system. The experiment concluded that the rotational speed of the shaft had less effect on the whirling vibration. However, the vibration in the stern of shaft was greater than that on the head of the shaft.

8.3 Numerical Developments

Laakso et al. (2019) developed a correction method for equivalent single layer (ESL) elements to improve the accuracy of modal free vibration results of ship deck structures. The method was validated in a case study of ship deck structure against shell mesh results, and the result found to be promising. However, the developed method is limited to only one in-plane stiffened deck plate with constant stiffener spacing, mass and stiffness. Jiao et al. (2015) developed a scaled segmented model and tested in tank to study system hull girder vibrations and wave impact response of a large ship in regular waves. The simulated results proved Hydro-elastic method as a better approach to estimate the wave loads responses of the ship. Li et al. (2019) conducted an experimental measurement of the flexural vibration transmission spectrum for a finite periodic stiffened plate. The flexural vibration wave propagation within specific frequency range is forbidden as it may result in the significant suppression of structural vibration. However, the experiment results show complete and directional flexural wave band gaps of periodic bi-directionally orthogonal stiffened plates. By tuning the geometrical parameters, the flexural wave vibration band gaps can be artificially modulated and optimized. Zou et al. (2020) developed a new bearing force prediction model that consider the complex vibrations of the propulsion-shafting as shafting vibration produce bearing forces. The proposed model is established based on BEM and rotor-dynamics theory. The study suggested that the axial vibration only causes the axial and torsion bearing forces, and does not lead to the lateral or vertical bearing forces. Boo and Park (2019) introduced an efficient vibration analysis technique for ship structures utilising the algebraic dynamic condensation (ADC) method. The ADC method was applied to calculate the vibration properties of 16,000 TEU class container vessel and its performance was compared with the automated multi-level sub-structuring (AMLS) method to demonstrate the effectiveness.

9. FATIGUE TESTING AT LOW TEMPERATURES

Material selection for ships and offshore structures exposed to sub-zero temperatures is traditionally based on Charpy and fracture toughness test results of the base materials and its welded connections (von Bock und Polach et al. 2019b; Braun et al. 2020b). In the last years however, fatigue properties have been the focus of a couple of studies due to the acceleration of fatigue crack growth below the so-called fatigue transition temperature, where ductile crack growth is superimposed by cleavage burst, see (Walters et al. 2016; Zhao et al. 2020a; Sallaba et al. 2022). Moreover, standards like ISO19906 state that attention should be given to the validity of fatigue design curves at sub-zero temperatures. Thus, recent efforts have been made to analyse the fatigue strength in terms of stress-life (S–N) curves (Liao et al. 2019; Braun et al. 2020c; Braun et al. 2020d; Braun et al. 2020e) and to analyse the applicability of state-of-the-art fatigue assessment methods for sub-zero temperatures, see (Milaković et al. 2019; Braun et al. 2020a; Braun et al. 2020b; Braun et al. 2020d; Braun et al. 2021a; Braun et al. 2021b; Braun et al. 2022a; Braun et al. 2022b; Braun and Ehlers 2022; Zhao et al. 2020b).

In order to perform fatigue crack growth tests or S–N tests at sub-zero temperatures a couple of points have to be taken into account. First of all, the testing temperatures required to perform tests at the possible extreme design temperature conditions is usually not sufficient, see Braun

(2021a and 2021b). Most standards require testing to be performed at the lowest anticipated service temperature minus a certain safety margin in the range 10 to 30 K below the design temperature depending on the test and the corresponding standard (Hauge et al. 2015). Such low temperatures can often only be achieved in cooling chambers working with liquified nitrogen or helium—considering extreme conditions of around -60 °C (Kubiczek et al. 2019). Other cooling agents are possible but are often not advisable due to the risk of ice accumulation in cracks during testing if the humidity of air is not low enough. Consequently, a high quality of insulation is needed in order to achieve dry air conditions similar to extreme low temperature weather conditions. Another benefit is the possibility of using optical measurement systems, which won't work on icy surfaces. For fracture surface investigations after the tests a quick conservation of the surfaces is required. Moreover, a low humidity in the test chamber prevents corrosion of the fracture surface during the tests. After injecting evaporated nitrogen, it is required to keep the temperature constant for a certain amount of time to allow for throughout cooling of the test specimen and the specimen clamps. In order to ensure a constant testing temperature, it is recommended to measure the temperature by thermocouples or resistance thermometers like PT-sensors. Thermocouples require a reference temperature measurement e.g., the laboratory temperature which could by flawed by changes during the day-night cycle. Moreover, attention should be paid to the supported temperature range of the used temperature measurement device.

Figure 21: Middle tension specimen equipped for crack growth rate measurement by direct current potential drop method with crack detection gauges and PT100 resistance thermometers

In general, all measurement equipment has to be adjusted for changes of conductivity with temperature. For strain gauges this means that dummy or reference measurements are required to correct the signal for temperature response. In case of fatigue crack growth measurements by direct or alternating current potential drop method changes in calibration curves should be taken into account by appropriate calibration curves or by finite element simulation, see Doremus et al. (2015).

Concluding, fatigue testing at low temperatures demands special attention to the set-up and instrumentation. The testing temperature is normally lower than the application temperature, and liquid nitrogen may be needed to cool down the area of interest to -60 °C. Temperature compensation is required for sensor, either strain gauges or potential drop methods.

10. CORROSION TESTING

Corrosion is a well-known deterioration mechanism, costing industry a lot in terms material loss and associated maintenance and repair. Coating is a logical measure to reduce the corrosion over time. However, this subject is not treated here. Below considerations are given to testing for the corrosion process itself, as well as experimentation regarding corroded specimens.

In short, corrosion is an electrochemical process where two connected materials have a different potential, by which the lower potential material reduces in mass. Corrosion can show as a

uniform corrosion, where large parts lose material, typically steel plates that become thinner over time. There are also plenty of localised corrosion variations, which pose a local risk to the structure as in pin holing, crack initiation, both fatigue and instable crack growth or accelerated growth of fatigue cracks. For the purpose of this paragraph, localised corrosions in all its forms are referred to as pitting. As corrosion is determined by the composition of the material on microlevel, as well as the environmental conditions, every test may turn out to be unique. Also, translation from actual corrosion damage towards the specimens pose severe challenges to the researcher.

Most testing procedures regarding the corrosion process, are tailored for the uniform corrosion process. The previous ISSC report (ISSC 2018) gives an overview of the available methods. Typical standards are the ASTM G31-12a and ASTM G89. For uniform corrosion rate testing, reproducibility is a serious issue and is best treated as comparative testing with a statistical approach. Hence, sufficient specimens, e.g., minimum of ten, need to be exposed to the same conditions on order to obtain confidence in the results. Preferably, the specimens are grouped, in order to find variation within same conditions, and similar conditions. Electrochemical measurements during the corrosion testing provides insight in the corrosion process, to the extent that activity and particular phases of the corrosion layer forming can be distinguished.

For material prone to pitting, standards exist that specify testing methods. The results boil down to identifying the susceptibility to pitting, and often is used for comparative purposes, e.g., ASTM G61-86. As pitting is seen as a threat for integrity due to its accelerated growth and crack initiating behaviour, strength assessments with specimens showing localised corrosion are performed for e.g., fatigue. In such cases, it is important to describe the shape of the pit precisely. Descriptions may be used for very fine mesh modelling, as well as comparing results among individual specimens. Diameter and depth are bare minimum, for better comparison scanning methods are better in which the radius of the potential crack initiation is derived. Subsequent analyses need to be compatible with the resolution of the scanning methods. When scanning has finer resolution than the reference theoretical or experimental background, a theoretical accuracy will result, not bearing actual relevance. When the radius is an important parameter in the qualification, but the measured radius is not part of the background data to create the qualification, there is no evidence to support the findings.

Uniform corrosion results in an irregular pattern in the thickness profile of plates and stiffeners. Such a profile may inflict a buckling mode, similar as the imperfections resulting from the ship building process.

Corrosion effect on structural strength is most reliably investigated through full scale experiments of real corrosion since the size effect and differences of artificial corrosion is uncertain. Nakai et al. (2007) has investigated effect of corrosion on various failure modes and proposed associated formulas for equivalent uniform thickness, while tension through tensile tests is the most commonly investigated failure. Since the corroded surface is not smooth according to testing standards, it is merely the apparent material properties that are tested. The cross-sectional area is applied when calculating stress for yield or ultimate tensile stress, and the definition and measuring of this for the corroded specimen varies making comparisons between studies difficult as illustrated by Fernandez and Berrocal (2019). Power spectral density can be applied to describe corroded surface elevation on one side or the remaining thickness itself (Yamamoto et al. 1992, Rahbar-Ranji 2012, Melchers et al. 2010 and Gathimba et al. 2019). However, it is important to apply a threshold for lower frequencies, for example set to the correlation length of corrosion, so that it is corrosion characteristics that is described rather than bending and warping of the plate (Neumann und Ehlers, 2019).

Linear corrosion prediction models described by corrosion rates are popular and useful for predicting shorter intervals, examples of such models are Melchers' phenomenological model and Paik's simplified model fitted to data of various structural members (Melchers et al., 2010;

Melchers, 2014; Paik et al., 2003). In addition to non-linear prediction models, later models include how the spatial surface distribution changes with time, such as Guo et al. (2008), Paik and Kim (2012) and Garbatov et al. (2005; 2019), Garbatov and Guedes Soares (2010).

Reports from Norwegian Petroleum Safety Authority's focus on ageing highlights how the bath-tub curve should be utilized to predict onset of wear-out and plan maintenance through calculation of the form of the hazard curve (Ersdal et al. 2011, Galbraith and Sharp 2007). Hazard function may be calculated from data of time to failure such as found by Garbatov et al. (2005), or predicted by defining a degrading limit state function as done by Barone and Frangopol (2014) and by Moan and Ayala-Uraga (2008).

Corrosion effect on structural strength is most reliably investigated through full scale experiments of real corrosion since the size effect and differences of artificial corrosion is uncertain. Nakai et al. (2007) has investigated effect of corrosion on various failure modes and proposed associated formulas for equivalent uniform thickness, while tension through tensile tests is the most commonly investigated failure [12]. Since the corroded surface is not smooth according to testing standards, it is merely the apparent material properties that are tested. The cross-sectional area is applied when calculating stress for yield or ultimate tensile stress, and the definition and measuring of this for the corroded specimen varies making comparisons between studies difficult as illustrated by Fernandez and Berrocal (2019). This said, numerous experiments find that ultimate tensile strength (UTS) decreases with increasing degradation as discussed in the literature review of Neumann (Neumann et al., 2018, 2019a, 2019b, 2019c; Neumann and Ehlers, 2019, Neumann, 2019), where also a prediction for corroded UTS taking size into consideration is presented (Neumann et al. 2019). Recent development has shown a surprising development proposing that apparent yield strength of corroded members may not be reduced at all for degradation in tolerance range of offshore structures (~<25%). This is evident from Garbatov's tests showing some cleaning methods may increase yield strength. Others also investigates the composition and grain size, suggesting the reason for the observation, but it is also observed on artificial corrosion, attributing the effect to local strain hardening prior to reaching yield point (Garbatov et al. 2019, Li et al. 2019 and Sheng and Xia 2017). Other than reporting a not clearly defined yield point, most researchers find little change in Youngs modulus for corrosion within typical tolerance levels, except for corroded pre-stressed re-bars (Vu et al. 2017). The most dramatic effect observed in corroded tensile tests is the reduction in ductility and fracture, which cannot be described by a uniform reduced equivalent thickness. Various surface characteristics are attempted applied to describe this reduction (Xu et al. 2016, Wang et al. 2017, Sun et al. 2018, Gathimaba and Kitane 2018). This, in addition to the local effect of stress increase from corrosion on fatigue initiation calls for an accurate description of the corrosion surface morphology (Xu and Wang 2015).

Power spectral density can be applied to describe corroded surface elevation on one side or the remaining thickness itself (Yamamoto et al. 1992, Rahbar-Ranji 2012, Melchers et al. 2010 and Gathimba et al. 2019). However, it is important to apply a threshold for lower frequencies, for example set to the correlation length of corrosion, so that it is corrosion characteristics that is described rather than bending and warping of the plate (Abbas and Shafiee 2018). From industry experience there is a need for investigating correlations in UTM readings between different locations in tanks to avoid excess tank openings and readings. Additionally, class often questions the quality of UTM on corrosion since numerous "growing thicknesses" are observed for older structures. Further, a recurrent question from authorities is how widespread general corrosion affects the global stress levels, specifically redistribution and upscaling of stresses due to corrosion.

11. LARGE SCALE IMPACT TESTS

Impact tests are showing the material and structural behaviour under dynamic loading. Having the behaviour of both the material and the structure under consideration, the test and the interpretation becomes complex. In this context, large scale is considered to cover specimens built of elements with practical thickness and dimensions. For steel, that means 4 mm is a minimum thickness, as these materials will have the material properties similar to the large thickness (20mm plus) and exhibit a combination of membrane end bending deformation. Some large-scale structural experimentation is described in the ISSC report of 2018.

Large scale impact experiments are normally expensive and repetitions are not always to be expected. One shall be aware of the limitation of a single test, exhibiting many aspects which are normally treated isolated such as strain rate dependent material behaviour, crack propagation, and local buckling. When the overall objective is clearly devised, first of all a test plan is to prepared, which shall include the selection of specimen with associated boundary conditions, the failure metrics, the test protocol, associated needed numerical correlations, instrumentation requirements, and interpretation of results to achieve the overall objective.

In order to build trust in the results and specify the details of the test, preparation in way of FE analysis and material tests are advised. Actual material properties as well as failure limits are derived from simple material tests, which is used in FE to make predictions. The failure mode as expected to appear in the full-scale test shall be covered by the material test done. A typical example is presented by (Bijleveld et al. (2018)).

Regarding specimen description, the main things to consider are scaling issues, boundary effects, multiple impacts and interaction between impactor and specimen. Deformation/ failure modes may follow different scaling rules, e.g., linear or quadratic. Hence scaling may induce another mode to be dominant, obviously apparent when buckling modes are important manifestations of the deformation. Material properties of small thickness plates are relatively superior to the larger thickness of the same description. While maybe considered to be conservative to use higher yield materials, this is not true for impact. The structure will behave elastically for a larger part of the event, resulting in stiffer behaviour and possibly inducing other failure/ deformation modes. Similarly, the effect of heat affected zones and welds may be different in the scaled conditions. The specimen shall further be large enough to avoid interference with the boundary conditions. When the available energy is not sufficient the break a specimen at once, repetitive testing may be required. This will require special attention during the data analysis, and is acceptable as long as at each single impact clearly more plastic deformation is inflicted than elastic. In reality, the impactor may be an equivalent structure as the impacted one in terms of stiffness and strength, e.g., a bow striking side structure. In experiments, normally the impactor is made stiff in order to reduce the number of parameters. In the analyses, this normally imposes no problems. In terms of energy absorption though, a rigid impact will show a minimum value of energy that will be absorbed in the simulated event.

Failure criteria, or experiment success criteria, should refer to the objective of the test. So, if buckling is to be assessed, that shall also be observed. If cracks initiate and propagate prematurely, the experiment is a failure, or needs repurposing. Regarding the interpretation, one should always be aware of the limitations and the statistical effects that play a role, also in single experiments. For instance, impact location will most probably deviate from the intended location. Hence the resulting forces and energy absorption values are to be considered with a reliability range. Analyses done as part of the preparation, can be used to assess the sensitivity of such deviations.

Last but not least, large scale experiments are rare, and to make full use of such opportunities, enough sensors shall be placed. Force measurement, possible with accelerometers, and strain gauges are a minimum. For the short duration events, accelerometers can be very well used for speed and displacement as well by integrating the acceleration signals, as shown in (Haag 2017).

For larger structures, DIC may be very well suited as it covers the large parts of the structure and may therefore capture also areas originally considered not relevant.

12. LARGE SCALE WIND TURBINE BLADE TESTING

12.1 Current standard procedure for blade testing

The International Electrotechnical Commission (IEC) is a worldwide organization for standardization comprising all national electrotechnical committees (IEC National Committees). Wind turbines are standardized by IEC. According to the current IEC 61400 standard series for wind turbines coupon tests of materials and full-scale tests of the blade are required in order to certify wind turbine blades.

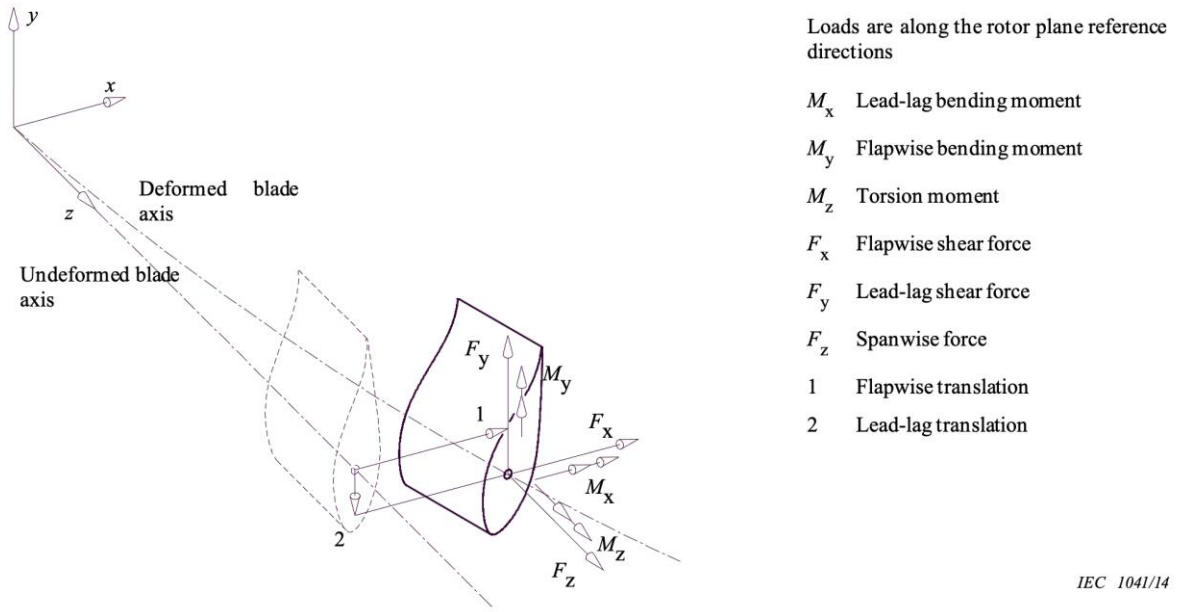

Figure 22: Rotor flapwise, lead-lag coordinate system

One or two of the first prototypes of the blades are usually tested both dynamically and statically following the requirements in the IEC 61400-23 standard on full-scale testing (IEC 61400-23, 2014). Full-scale blade tests are performed in order to verify that the blade type has the load carrying capability and service life provided for in the design. The test program for a blade type shall according to the standard be composed of at least the following tests and in this order (IEC 61400-23, 2014):

- mass, centre of gravity and natural frequencies;
- static tests (two flapwise and two lead-lagwise directions);
- fatigue load tests (flapwise and lead-lagwise);
- post fatigue static tests.

The standard requires that the entire test sequence is performed on one blade, unless it can be shown that combination of flap and lead-lag loading is not critical for the blade. If so, the flap and lead-lag sequence of testing may be performed on two separate blades (IEC 61400-23, 2014).

Fatigue tests must normally be done at natural frequencies of the blade by including exciter and tuning masses, to obtain the design loads along the blade. Forced loading may be used for very small blades, but for bigger blades the amount of energy used by a forced excitation will simply be too large, making testing at natural frequencies the only possibility.

12.2 Industry challenges with current standard and outlook on future trends

The cost of a large blade itself is high and the time needed for the dynamic test can be several months for large blades, which also make cost due to waiting time for market introduction significant (Mishnaevsky et al. 2017). Therefore, is full-scale testing very costly. In table 3 is shown the expected test time as a function of blade length. The natural frequencies for future long blades are estimated based on those known for the DTU 10 MW reference wind turbine (Bak et al. 2013) with 86.4 m blades. The test times takes into account that tuning masses are added to match target loads and that tests regularly are stopped for inspections. As it can be seen test time for a 150 m blade is expected in exceed one year when also static tests are included. Currently the longest blade is the 107 m made by LM Wind Power for the GE Haliade-X 12 MW. Wind turbine sizes are still expected to increase with no indication when it will level out. The industry is therefore concerning with the long time-to-marked for future large turbine blades and are interested in ways to shorten the test time. It is a question at which size and when will it stop to make sense to test these long blades according to current standard.

Table 3: Expected fatigue test time as a function of blade length

Blade	Natural freq.		Test time
length	flap	edge	days
86,4	0,61	0,93	167
100,0	0,5	0,75	205
120,0	0,41	0,61	251
150,0	0,32	0,47	323
200,0	0,23	0,33	453

In the wind industry, we are currently looking at different ways to shorten test time. One way is to develop more advanced test methods, which loads the blades in more directions at the same time, and/or accelerate the tests by testing at higher loads and fewer cycles. Another way is to test part of blades. By shorting the blade, the natural frequency of the remaining part will increase. But also replacing full-scale tests by testing short parts of blades as subcomponent tests can be a way forward to decrease time-to-marked.

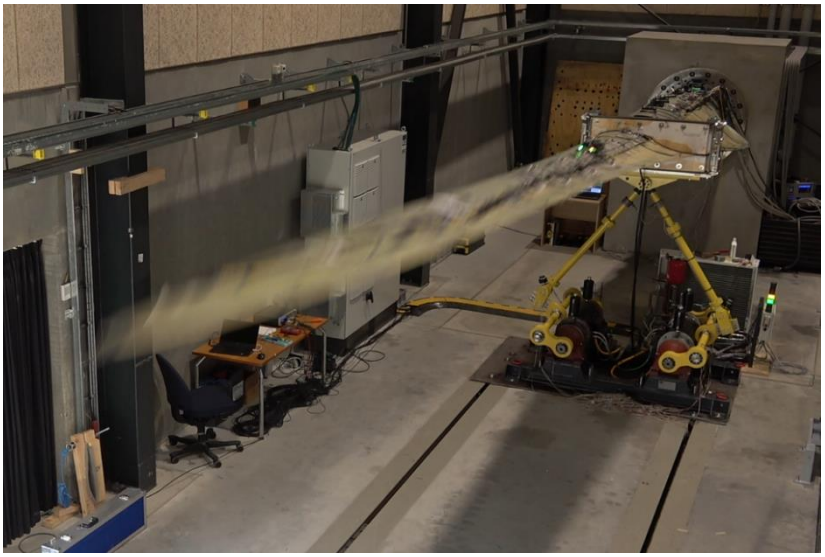

Figure 23: Dual-axis fatigue testing using electric exciter with which both uni- and dual-axial tests can be carried out. Test at DTU Large Scale Facility.

12.3 Development of more advanced test methods (state-of-the-art)

In the project BLATIGUE, an optimized method for multi-axial fatigue testing of wind turbine blades was developed, with which improved fatigue tests compared to current standard fatigue tests were obtained in terms of both accuracy and total test time (Castro et al. 2021a & Castro et al. 2021b). In this approach, the response of the blade is accounted for at the material level

by considering strain-based damage targets. An optimal combination of different test blocks (i.e., flapwise, edgewise, chaotic and phase-locked) can be obtained to reach the damage targets in the entire blade while minimizing the total test time, and satisfying predefined error limits. The combination of test blocks is found using continuous linear optimization. Aeroelastic simulations are carried out to estimate both target and test strain-based damage in the blade.

This method has been applied numerically and demonstrated in full-scale testing to both a small blade (i.e., Olsen Wings 14.3m blade) (Castro et al. 2021a) and a large blade (i.e., SGRE 75m blade), showing that improved fatigue tests compared to current standard tests can be obtained.

As an example, Table 4 shows a comparison between the standard test, different optimized uniaxial and multiaxial tests, and when all are combined, when the method was applied to the Olsen Wings 14.3m blade. As shown in Table 4, a reduction of the total test time of 50% was obtained with the proposed method when all load block types are combined in comparison with the standard test. In addition, the strain-based target damage was reached in all blade regions (i.e., EDR_{min}=1.00), while the maximum total damage from the test in any part of the blade, D_{max}^{test}, remained similar to that of the standard test.

Table 4: Comparison between the standard test and different optimized solutions for the Olsen Wings 14.3m blade. (Castro et al. 2021a)

	$T/Tstd$	EDR_{min}	EDR_{max}	D_{max}^{test}
Standard (no optimized)	1.00	0.02	6.96	0.70
Uniaxial	6.66	1.00	839.96	26.02
Chaotic	0.53	1.00	187.22	0.65
Phase-locked 1 : 2	2.84	1.00	414.47	2.28
All combined	0.50	1.00	170.78	0.69

That the strain-based target damage in reached in all regions of the blade shows that these dual or multi axis test methods has the potential to test blades under more representative loading compared to operational loads.

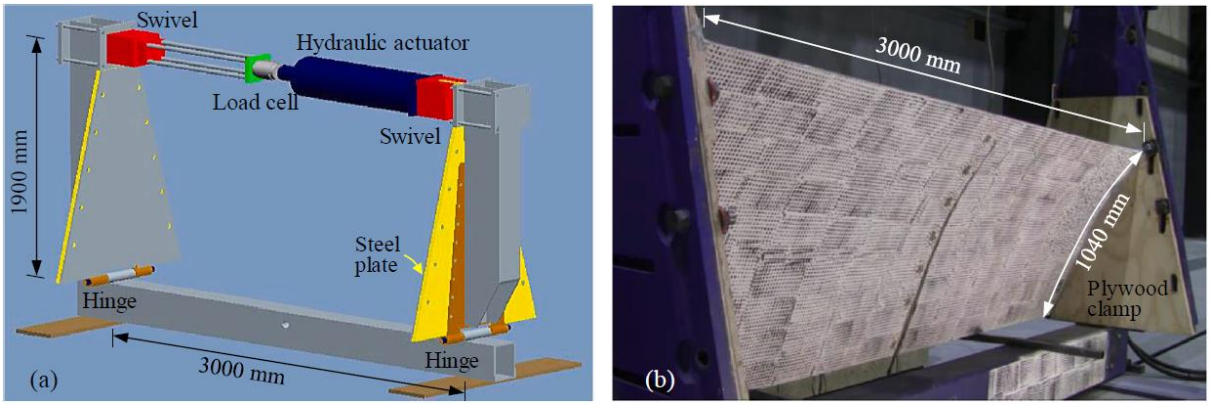

Figure 24: Subcomponent test setup. (a) U-shaped test rig. (b) Trailing edge part of blade inserted in test rig. Test at DTU Large Scale Facility.

*12.4 **Testing parts of blades (state-of-the-art)***

In recent years, subcomponent testing has been increasingly used (Branner et al. 2016 & Chen et al. 2019) to understand the structural behaviour of trailing edge parts of wind turbine blades, which is considered a critical part of these composite blades. The subcomponent testing of critical parts could be an important complement to the full-scale blade tests that are mandatory for certification of wind turbine blades. The trend of using subcomponent testing is also reflected by the 2015 DNV GL rotor blade standard DNVGL-ST-0376 (DNV GL, 2015), which makes it possible to use subcomponent testing as part of blade certification (Pansart, 2015).

There are limitations to testing the full blade, which testing parts of blade may solve. The lack of representativeness in full blade testing is a problem. Testing one or two prototypes does not provide a statistical distribution of the structural performance of the whole population of blades. In particular, the blade used for the certification test is usually one of the first blades from series production, which is still subject to developmental modifications. How the performance of the prototype blade represents later blades from series production is often unclear (Rosemeier et al., 2019). Testing several subcomponents to failure will give a better statistical distribution for estimating the strength of blades as more tests are necessary to obtain statistically meaningful results to increase structural reliability.

The limited coverage of realistic design loading conditions is another problem. Testing of full blades is limited to testing at natural frequencies. The combination of flap, edge and torsion loads seen in reality is not possible to capture fully in full blade tests. Also, transient loads such as impact during transportation and installation are currently not simulated during full-scale test and will also be difficult to implement in the future. Testing with more complex and realistic loading on subcomponents can be a way forward.

Subcomponent tests also offer an opportunity to evaluate structural integrity of composite rotor blades in more details e.g., for critical parts such as trailing edge sections. In Chen et al. 2019a subcomponent testing is used to validate an advanced nonlinear finite element model and to understand progressive failure behaviour of the trailing edge section during its entire failure sequence. The same model is then modified and used in a detailed numerical study (see Chen et al. 2019b) to propose a method to improve the load-carrying capacity of the trailing edge section by structural reinforcement. Using subcomponent testing to validate numerical models and certify the load levels to which the subcomponent can be exposed to without failure. This can be the basis for relying more on numerical modelling of the full blade as long as the load level of the full blade is kept lower those the subcomponents were exposed to.

13. FULL-SCALE ICE LOAD MEASUREMENTS

Ice covered waters are challenge for shipping and other offshore structures. Moving ice floes, driven by wind and sea currents can exert high forces and induce structural vibrations as ice is pushed against offshore structures. The models based on ice-mechanics and ice physics are not yet able to predict ice loads exerted on structures. The main reason for the low predictability of the models is, that ice force is a result of a complicated and continuous fragmentation process of ice failing against a structure (Figure 24). Thus, full scale ice load measurements play a significant role in the design of ships and offshore structures in ice covered waters. Full scale measurements of fixed vertical offshore structure are discussed here.

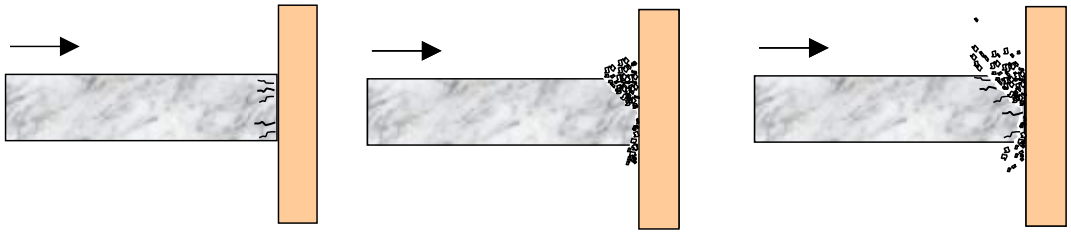

Figure 24: Continuous fragmentation process of ice when ice is compressed against a vertical offshore structure.

Materials like natural ice are heterogeneous and crystalline, containing pores and flaws and other weaknesses. Due to natural heterogeneity, ice exhibits spatial variation in strength. As illustrated in Figure 25, ice pressure against fixed structure is usually varying along the contact zone (non-synchronized failure). When failure is synchronized, pressure is more evenly distributed, and ice-induced structural vibrations may occur.

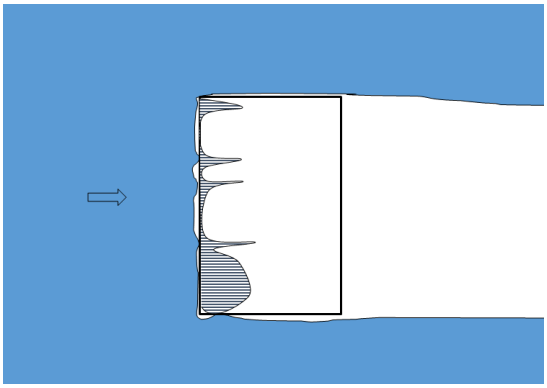

Figure 25: Ice-pressure during non-synchronised failure.

Ice structure interaction tests

To ensure safety and efficiency of structures, both total ice loads and local ice pressures are of interest. Local ice forces are usually measured using load panels (Hellgren et al. 2020), which are installed along the structure close to waterline. Besides the forces, accelerometers and tilt meters are important in measuring the dynamic response of the structure. But, without further information about ice, the forces and accelerations were useless. At least the following data should be recorded besides forces and accelerations:

- Ice thickness
- Ice velocity
- Ice type (ridged, rafted,..)

It is also recommended to install at least one video-camera to record ice actions. For the analysis of the results, structural compliancy and dynamic properties were important to measure. Once the mechanical properties of ice vary in time and space, the following variables should be measured frequently: Compressive strength, tensile strength, porosity and salinity, granular structure and temperature profile.

Testing compressive strength of ice is important and more challenging than often expected. There is a quite significant scatter in the mechanical properties of natural ice as illustrated in Figure 26. In general, the source of the scatter is the heterogeneous nature of ice. Other possible sources of scattered results are: poorly prepared specimens, end conditions, and compliancy of the test frame. As noted by Hawkes and Mellor (1970) and Schulson and Duval (2009) straightness and parallelism of the specimen ends are of importance in compressive testing. But, in field conditions it is quite challenging to achieve the specimen tolerances given by Hawkes and Mellor (1970) or Schulson and Duval (2009). The lateral constraints introduced by the loading platen affect both the strength and failure pattern of the samples (Schulson et al. 1989). To minimize the effect of the lateral constraints, brush platens are recommended (Schulson and Duval, 2009, p. 238). The stiffer the loading frame used in compression tests, the better it is. The objective in the tests is to ensure constant strain rate during testing. If loading frame is compliant, more energy is stored in the frame. When ice gradually fails the stored energy is released inducing non-constant strain rate as shown by Kolari (2016). Jones (1982, 2007) suggested that the rate dependent compressive strength at higher rates may be “due in part to machine stiffness considerations”.

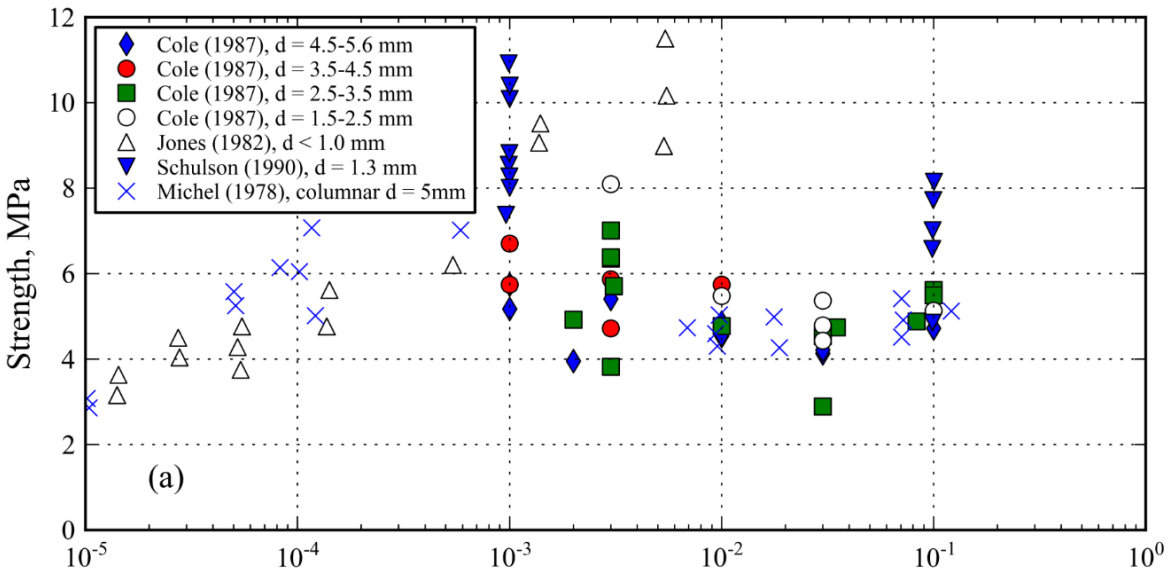

Figure 26: Variation in compressive strength of granular and columnar ice (Kolari 2016).

14. HEALTHMONITORING AND DIGITAL TWIN MODELS

This section outlines different Structural Health Monitoring (SHM) methods for structural assessment of offshore platforms. SHM is essential for marine and offshore structures to reduce the unexpected loss caused by downtime by detecting potential damages and helps provide estimates of remaining useful life. For instance, the offshore jacket platform, a type of bottom-fixed offshore structure, is composed of slender tubular members which can be prone to adverse environments. Therefore, it is practical to follow appropriate and timely damage identification process for extended life cycle. The SHM methods are used for ensuring the safety and reliability of the structure and materials used for constructing offshore platforms. The selection of a proper SHM method must be made in accordance with the material type, experience, known failure modes of the structure and the limitations of the SHM sensors and devices. The data gathered by the SHM techniques are the inputs to the reliability analysis of novel structures, and therefore, they have a significant impact on the accuracy of the failure probability estimation. The proper implementation of such techniques, however, requires dealing with several challenges.

Table 5 summarises the commonly used non-destructive SHM methods for offshore structures including oil and gas rigs/platforms, renewable energy structures and aquaculture units. The methods listed in Table 5 are used for monitoring the deterioration in both material (changes in material properties) and structure (changes to geometric properties).

Table 5: Structural health monitoring methods used for offshore systems.

Purpose	Method/ Principle	Advantages	Limitations	Ref
Monitoring excessive deformations, corrosion, fatigue crack propagation	Acoustic emission	High-resolution (up to microscale), easy to use and cost-effective monitoring	Sensitivity of these methods to the background noise limits their applicability in offshore environments; limited distance between measurement point and damage location.	(Jüngert, 2008, Tziavos *et al.*, 2020, Liu *et al.*, 2018, DeCew *et al.*, 2013)
Strain monitoring	Strain gauge, Fibre Bragg Grating (FBG), Quantum Resistive Sensors (QRS), Fibre optic cables	Easy to install sensors must be placed within the critical parts of a component to obtain data on the micro-level damages	Short service-life of the sensors, sensitivity to misalignment and lack of robustness	(Ziegler *et al.*, 2019, Maes *et al.*, 2016) (Mieloszyk and Ostachowicz, 2017)
detection of cracks and corrosion	Ultrasonic techniques	Non-contact with the capability of being used with drones. Minimal preparation time and fast to obtain results, high penetration depth waves and accurate imaging	sensitivity to misalignment of sensors, expertise, and labour intensity and calibration difficulties in the absence of relevant standards	(Gunn *et al.*, 2019, Brett *et al.*, 2018)
detecting the anomalies, damages, and cracks	Thermal imaging or thermography methods utilise thermochromic coatings and liquid crystal sheets, infrared cameras and thermocouples	Non-contact and can be used with drones in an automated inspection	Sensitivity of the thermal sensors to temperature variations, the minimum detectible defect size and the need for post-processing algorithms. These methods have limited application in the offshore environment.	(Gao *et al.*, 2016, Chatzakos *et al.*, 2010, Newman, 2016)
Modal monitoring and fatigue	Operational Modal Analysis (OMA), Experimental Modal Analysis (EMA), Frequency Domain Decomposition, Natural Frequency shift using: piezoelectromechanical and microelectromechanical systems (MEMS), Accelerometers Velocimeters Accelerometer Linear displacement sensor	Reliable and easy to implement for non-operating (offshore) and onshore platforms	large amount of uncertainty induced by the involved external parameters such as wind and wave loading and scouring effect. Also, in offshore environment it is difficult to measure the wave and wind loads.	(Pacheco *et al.*, 2017, Devriendt *et al.*, 2014) , Antoniadou *et al.*, 2015)

14.1 Recent Developments

Wireless technologies enable us to implement distributed sensor network and data transmission system in structures more easily. Wu *et al.* (2019) developed an offshore platform stress monitoring system based on a wireless sensor network and a satellite communication system. The wireless sensor network senses the physical parameters of the platform, such as vibration, stress, temperature, displacement, etc. and then forward data to the onshore monitoring host through satellite. Johnson et al. (2018) presented a fatigue assessment strategy through the utilization of wireless hull monitoring system for high-speed aluminium hulls.

Various data-driven approaches for damage detection and diagnosis have been developed and applied to SHM. García and Tcherniak (2019) demonstrated the potential of a data driven SHM methodology for a reasonable damage diagnosis in a large wind turbine blade considering only one accelerometer and one actuation location. The proposed method found combinations of variables that describe major trends and fluctuations and can be used for damage diagnosis. Guo et al. (2018) presented a damage identification method for offshore jacket platforms based on artificial intelligence (AI) neural networks using partially measured modal results. From the case study analysis and checking further calculated results, the proposed method is found to be quite accurate. The prediction errors stay below 8% when the measurement points of the jacket platform are placed near the waterline; however, it's over 16.5% when close to deep water. Li et al. (2019) developed a Principal Components analysis (PCA) based method for damage detection under different random wave excitations. A simulation of a six-legged jacket platform was considered for the dynamic responses for the undamaged and damaged structural condition respectively. The simulated results prove potential of the developed PCA method and the cross-correlation function for damage detection, which can be useful for real-time early warning under changing wave excitations. Vidal Seguí et al. (2019) developed a data driven approach for damage detection in offshore jacket-type wind turbines using only accelerometer information. The proposed approach was validated through an experiment for different types of predefined damages in a small-scale structure - an experimental laboratory tower modelling and an offshore-fixed jacked-type wind turbine. The experimental results demonstrated an overall accuracy of 98.6%, which shows the reliability of the proposed approach. Sen et al. (2019) proposed a semi-supervised learning algorithm for damage detection and a supervised learning algorithm for damage localization for active sensing in pipes. The semi-supervised approach uses undamaged data and a hierarchical clustering scheme for damage detection using low-profile piezo sensors up to damages located up to 90° offset angles from the zenith line of the cylindrical pipe near the actuators. The supervised approach to damage localization is based on a multinomial logistic regression framework. By providing enough training data from a real pipe, the supervised approach accurately classifies the cracks into their originating regions and can be used on complex structures such as pipes. Rezaniaiee Aqdam et al. (2018) proposed a new design of Radial Basis Function (RBF) neural network for damage diagnosis of mooring lines, which is based on Rod theory and Finite Element Method (FEM). In the proposed model, boundary conditions uncertainty is applied using Submatrix Solution Procedure (SSP) and later round-off error is removed using SSP. The experiment results showed that proposed RBF has a better performance compared with conventional one and other well-known methods in the literature. Spanos et al. (2019) presented a comprehensive and critical assessment of the diagnostic performance of five prominent response-only methods based on incipient, 'minor' to 'mild', damages on a lab-scale wind turbine jacket structure under constant boundary conditions. The comprehensive and statistically reliable procedures employed in the study have offered convincing evidence of the statistical time series structural health monitoring (STS-SHM) methods' high diagnostic capabilities. Yang et al. (2018) proposed an SHM for offshore wind turbine jacket structure to monitor vibration, strain, corrosion and hence, to effectively evaluate the structural integrity. Shokrgozar and Asgarian (2018) developed a scaled model of steel

jacket type offshore platform which was newly installed in Persian Gulf to study dynamic system identification using experimental and numerical simulation. The model was tested on a pile supported condition in order to simulate real boundary conditions. The numerical modelling of sample platform was performed using ABAQUS software. The experimental analysis shows that soil-pile-structure interaction significantly decrease the natural frequency of structure. Zhao and Lang (2019) developed a baseline model-based structural health monitoring method and investigated its effectiveness by experimental case studies. The analysis of the field data from an operating wind turbine has demonstrated that the new baseline model-based structural health monitoring technique can distinguish different health conditions of gearbox and generator in wind turbine. It can also be concluded from the field data analysis that vibration and acoustic emission (AE) signals are sensitive to condition changes of the gearbox and generator, respectively. Qiang et al. (2019) developed an improved compressive sensing (CS) algorithm for vibration signal processing by taking advantages of the multi-task Bayesian compressive sensing (MT-BCS) and classification theory for failure detection and identification of a diesel engine. The experimental result indicates a feasible approach to solve the problem of vibration signal transmission and storage in a health monitoring system for a diesel engine.

Assessment of the structural integrity based on fatigue analysis is a key issue in SHM. Yan et al. (2019) developed an SHM system for investigating fatigue characteristics of the stinger structure of pipe-laying ship to increase its safety in the operational conditions. This study suggested a structural health monitoring system of the stinger as it is subjected to extremely complex environmental loads and working loads in deep-sea, which have great influence on its safety. Using the S-lay method, the sea tests were carried out. The test result was compared with the conventional fatigue analysis method and found some significant difference. Ma et al. (2019) conducted long-term stress prediction and fatigue assessment according with stress monitoring data of the 14,000 TEU containers ships and found that the structural elastic vibration may increase the maximum stress by 10-60%. On the other hand, Oka et al. (2019) investigated the wave loads acted on actual ships by using AIS data and wave hindcast data, and they concluded that significant wave height which is related to the vertical bending moment is reduced by 10-20% owing to the seamanship of storm avoidance.

Shape sensing technology based on inverse finite element analysis (iFEM) has been investigated to apply to marine structures. As a part of SHM systems, Kefal et al. (2018) demonstrated that the iFEM and quadrilateral inverse-shell element (iQS4) methodology can be suitably applied to SHM of marine structures having a structural complexity and travelling in oceanographically complex sea conditions. Kefal (2019) also developed a new eight-node curved inverse-shell element iCS8 based on iFEM. The practical modelling capability can allow a relatively sparse placement of sensors, therefore providing an advantage for real-time shape sensing of curvilinear geometries. The high accuracy and practical utility of the iCS8 element is demonstrated for different cylindrical marine structures through examining coarse iCS8 discretization with dense and sparse sensor deployments. Various large-scale marine structures including ship hulls, onshore and offshore structures, submarines etc. can be suitably modelled with a coarser mesh than as what flat surface inverse-elements offer. de Mooij et al. (2019) demonstrated iFEM methodology successfully through the development of tetrahedral and hexahedral inverse-solid elements. iFEM methodology with various types of elements is a promising and smart framework to perform an accurate shape and stress sensing, providing a viable technology for SHM of future marine structures.

14.2 *Digital Twin (DT)*

An idea to model the reliability of offshore structures comprehensively considering all the internal (e.g., deteriorations process, geometric deformations, etc.) and external factors (e.g. presence of personnel, the living products, etc.) affecting the reliability of the system is realised through using the Digital Twins concept. The digital twins of a structure can be defined as its

digital equivalent, which enables for assessing its reliability under different service conditions. The data collected by SHM equipment in real-time are used to make a digital twin of the platforms and evaluate its reliability real-time. The digital twins concept provides with the possibility of real-time surveillance of the system through the combined use of SHM techniques, the internet of things, mathematical modelling, failure history databases and reliability analysis methods. This concept has been first utilised in the aerospace industry for service-life management of airplanes. Several use cases of the digital twins for life-cycle management of different systems have been examined in the work of (Macchi et al., 2018). Examples of such use cases in different industries include (i) Optimised maintenance planning and decision making on the structure subjected to different failure modes (Kampczyk, 2020, Wang et al., 2019, Xiao et al., 2019), (ii) System life-cycle modelling (Kaewunruen and Lian, 2019, Lim et al., 2019), and (iii) System performance optimisation (Zhang et al., 2017, Guerra et al., 2019).

The digital twins are not a new concept, however, the recent advances in the sensor design and the internet of things enhanced the applicability of the concept for solving real-world problems. The offshore industry has already started using the digital twins for operation optimisation, predictive maintenance, anomaly detection and fault isolation purposes (Wanasinghe et al., 2020). Several usages of the digital twin concept for reliability assessment of offshore structures can be realised in the future. For system performance optimisation, one can first build a digital twin of the structure and then study the variations of parameters, to see which ones have the most influence on the reliability of the system. For example, parameters such as collar wall thickness, diameter, member length tolerance of aquaculture sub-system, and anchor placement, line length and soil characteristics of the mooring sub-system of the digital twin can be changed to examine the impact on the reliability of the system. Also, the digital twin serves to check the actual performance against design calculations to help remove conservatism for future designs, thereby improving reliability predictions. In addition, the concept helps with monitoring the stress throughout the structure. This approach would be beneficial both for long-term fatigue and transfer functions if environmental conditions can be monitored using proper monitoring sensors as well. Furthermore, by correlating the monitored stress at a few selected locations with the most critical dynamic response modes, the digital twin can provide a picture of the entire loading distribution throughout the structure, including hot spots. This way, the digital twin concept bridges between monitoring and modelling and eventually allows the use of data analytics and artificial intelligence-based prediction techniques to make real-time predictions of future behaviour and reliability. Examples of the combined use of artificial intelligence-based models and digital twins in offshore industry can be found in the works of (Shirangi et al., 2020), (Tygesen et al., 2019), (Augustyn et al., 2019), and (Kirschbaum et al., 2020). For ship structures, a digital twin concept in which the stress history is calculated at an arbitrary position based on estimated directional wave spectra and response functions is proposed (Chen et al., 2020). They estimated the wave spectra by using actual data (stress/motion) measured in 14,000 TEU large container ships and validated the estimation accuracy as comparing with the ocean wave hindcast database. A ship motion prediction method was validated by using monitoring data of the same container ship (Takami et al., 2021). Other examples implemented in other fields, such as manufacturing industries provided by (Cronrath et al., 2019), (Min et al., 2019) and (Jaensch et al., 2018).

It is worth mentioning robotics and autonomous systems applications for in-service monitoring and similar related issues. Indeed, monitoring equipment and devices now available may provide experimental results which were not available a few years ago. However, effectiveness of these new devices, which were needed and widely used during the pandemic outbreak, has not been verified in depth nor proof of their equivalence to current inspection techniques and state of the art has been analysed in depth. As a matter of fact, for the time being, their introduction in the inspection and maintenance practice is left to the judgment of the attending field surveyor

onboard, without beforehand acceptance criteria and approval. IMO recently discussed the matter at MSC 103 Poggi et al (2020, 2021) attempted to address the issue in the frame of the EU-funded Horizon 2020 ROBINS project (www.robins.project.eu).

15. BENCHMARK STUDY ON FREE-VIBRATION OF A STEEL AND COMPOSITE CANTILEVER BEAM

During the 2nd meeting of the Committee, it has been proposed to carry out a benchmark study aimed at highlighting how much the experimental method may affect the outcomes of an experiment and the effectiveness of the results. Eventually, it was agreed that a rather simple and consolidated test, familiar to all Committee members, shall be carried out by the participants using their own skills, experience and resources. Experimental method is in fact intended not only as the technical specification of measurements but it is also involving all practices so as to encompass a sort of "human factor" assessment within benchmark results.

Test specifications have been agreed among all members. The idea is to provide a clear final goal of the experiment without limiting the test specification itself, thus leaving each participant free to define the test procedure in full detail, to select the instrumentation and other necessary equipment, to elaborate measured data and to present test results as it usually happens when someone is tasked to take measurements either in laboratories or in situ. The goal of the tests is to estimate the first natural frequency of given constrained specimens. It has been eventually agreed to estimate the natural vibration frequencies of small cantilever beams made up of mild steel and of fiberglass sandwich laminate. While the steel material is relatively common and specimens can be easily obtained by each participant, composite specimens were cut from the same sandwich panel by one participant and sent to involved laboratories to avoid introducing in the benchmark the scatter related to material characterization and to fabrication defects and to focus the benchmark to experimental methods only.

Specimens' nominal dimensions were initially defined as follows:

- Mild steel: 550x30x5 mm
- Composite sandwich: 560x30x12 mm

However, it was later decided to leave the steel size somehow free, allowing some flexibility and considering that what is significant for the benchmark is the scatter between nominal and actual size, which is in any case included in the analysis.

Nominal properties considered for materials are shown in Table 6. Composite laminate details are reported in Gaiotti and Rizzo (2012). Basically, sandwich core is a 10 mm thick PVC (75kg/m^3) while skins' stacking sequence includes one biax layer (±45°; 600g/m^2) and one twill layer (0°/90°; 200g/m^2) on each skin.

Table 6: nominal material properties

Steel		**Composite**							
E [N/m^2]	N	E glass [N/m^2]	E epoxy [N/m^2]	ν glass [-]	ν epoxy [-]	G glass [N/m^2]	G epoxy [N/m^2]	E PVC [N/m^2]	ν PVC [-]
2.07E+11	0.29	7.00E+10	3.00E+09	0.25	0.35	3.00E+10	1.50E+09	2.60E+09	0.32

The specimens were constrained such that the cantilever has a nominal free span of 500 mm. No other specifications were provided for the test set up. Table 7 and 8 summarizes the approaches followed by the participants in pursuing the required task. For the sake of shortness only a limited number of photos can be included in this report to describe the tests but, as expected, clamping and impact solutions differed as well as the applied instrumentation and the approaches to face data acquisition and elaboration. Results are reported identifying both,

participant (letter) and specimen (number). E.g., B2 means participant B and specimen no. 2 tested in the B laboratory.

Table 7: summary of test specifications and results - steel specimens

Participant/specimen	Method	Sensor(s)	Set up	Acquisition	Result	Dimension, weight
A1 steel	Hammer excitation	Piezo-resistive accelerometer, 10 mm from end, 2.5 g	Clamped on heavy table	Dewetron, 500 Hz	16.3 Hz	1000x25.2x5.4mm, 1005 grams
A1 steel	Hammer excitation at half length	Piezo-resistive accelerometer, 250 mm from end, 2.5 g	Clamped on heavy table	Dewetron, 500 Hz	16.3 Hz	1000x25.2x5.4 mm, 1005 grams
B1 steel	Hammer excitation at free end	Displacement laser sensor model Acuity AR200-100	Clamped on table	Sensor's software, FFT of acquired time history by Excel	12.45 Hz	550 x 30.25 x 4.5 mm, 538.8 grams
B1 steel	As above	Dantec DIC Q400 System, two 3,1MPix, USB3 cameras	As above	Dantec ISTRA software, v. 4.6.2.383 FFT on point displacement	11.9 Hz	550 x 30.25 x 4.5 mm, 538.8 grams
C1 steel	Manual excitation by hand	Strain gauge, FLAB-3-11 from TML with a 3mm grid in a quarter bridge circuit	Clamped on heavy table	Autolog 3000 from Peekel Instruments, Software: SignaSoft, Frequency 1000 Hz	15.2 Hz	550x30x5 mm, 647.6 grams
C1 steel	Manual excitation by hand	Accelerometer Serie 308B by PCB, Sensitivity 100mV/g, Frequency 1 – 3000Hz, Weight 87mgramm	Clamped on heavy table	Autolog 3000 from Peekel Instruments, Software: SignaSoft, Frequency 1000 Hz	13.2 Hz	550x30x5 mm, 647.6 grams
D1 steel	Manual excitation by hand	Accelerometer (probe mass 57.5 gram)	Clamped on heavy table	VIBXPERT S/N 00321, Sampling frequency: 65.536 kHz	12 Hz	549 x 32 x 4.8 mm, 670.5 grams
E1 steel	Manual excitation by hand	Strain gauge with the gauge length of 10 mm (KYOWA)	Clamped on table	Strain, NI USB 6001, 1 kHz	13.4 Hz	909.5 x 31.7 x 4.25 mm 962.3 grams (incl. strain gauge)
E1 steel	Manual excitation by hand	Laser displacement sensor LK-G85 (sensor head) (Keyence)	Clamped on table	Displacement	13.4 Hz	909.5 x 31.7 x 4.25 mm 962.3 grams (incl. strain gauge)

Table 8: Summary of test specifications and results – composite specimens

A2 composite	Hammer excitation at half length	Piezo-resistive accelerometer, 10 mm from end	Clamped on heavy table	Dewetron, 500 Hz	24.2 Hz	564x30.7x11.8 mm, 66 grams
A2 composite	Hammer excitation at half length	Piezo-resistive accelerometer, 250 mm from end	Clamped on heavy table	Dewetron, 500 Hz	25.6 Hz	564x30.7x11.8 mm, 66 grams
B2 composite	Hammer excitation at free end	Displacement laser sensor model Acuity AR200-100	Clamped on table packed with steel plate	Sensor's software, FFT of acquired time-history a by Excel	25.4 Hz	560 x 30.50 x 11.7 mm, 66 grams
B3 composite	As above	As above	As above	As above	25.8 Hz	560 x 29.20 x 11.7 mm, 64 grams
B3 composite	As above	Dantec DIC Q400 System, two 3,1MPix, USB3 cameras	As above	Dantec ISTRA software, v. 4.6.2.383 FFT on point displacement	26.1Hz	560 x 29.20 x 11.7 mm, 64 grams

C2 composite	Manual excitation by hand	Strain gauge, FLAB-3-11 from TML with a 3mm grid in a quarter bridge art	Clamped on heavy table	Autolog 3000 from Peekel Instruments, Software: SignaSoft, Frequency 1000 Hz	22.8 Hz	550x30x5 mm, 64.4 grams
C2 composite	Manual excitation by hand	Accelerometer Serie 308B by PCB, Sensitivity 100mV/g, Frequency 1 – 3000Hz, Weight 87mgramm	Clamped on heavy table	Autolog 3000 from Peekel Instruments, Software: SignaSoft, Frequency 1000 Hz	11.6 Hz	550x30x5 mm, 64.4 grams
D2 composite	Manual excitation by hand	Accelerometer (probe mass 60.5 gram)	Clamped on heavy table	VIBXPERT S/N 00321. Sampling frequency: 65.536 kHz	11 Hz	565 x 28.5 x 11.5 mm, 62.0 grams
E2 composite	Manual excitation by hand	Strain gauge with the gauge length of 10 mm (KYOWA)	Clamped on table	Strain, NI DAQPad-6259 1 kHz	25.0 Hz	561.5 x 30.6 x 11.9 mm 64.4 gram
E2 composite	Manual excitation by hand	Laser displacement sensor LK-G85 (sensor head) (Keyence)	Clamped on table	Displacement	25.0 Hz	561.5 x 30.6 x 11.9 mm 64.4 gramss, 500 mm
F1 composite	Pull-and-release of beam end	ARAMIS DIC system with cameras (Teledyne Dalsa 12 MP with a resolution of 4096x3072 pixels) recording the motion with 450 fps	Clamped to steel structure on table	ARAMIS software. Displacements processed in Matlab and modal parameters estimated with continuous wavelet transform (CWT) method	25.69 ±1.94 Hz	560x30x12 mm, 75.0 grams incl. glued wooden inserts 60x30x2 mm
F2 composite	Pull-and-release of beam end	ARAMIS DIC system with cameras (Teledyne Dalsa 12 MP with a resolution of 4096x3072 pixels) recording the motion with 450 fps	Clamped to steel structure on table	ARAMIS software. Displacements processed in Matlab and modal parameters estimated with continuous wavelet transform (CWT) method	26.621 ±0.009 Hz	560x30x12 mm, 73.5 grams incl. glued wooden inserts 60x30x2 mm

Most participants used a heavy table to clamp the strips using a clamping device. On top of the strips a few of them placed a steel block or plate, which was firmly clamped to the table. Participant F specifically dealt with the possibility of damaging the sandwich core by gluing wood at specimen end. Participant E measured strain and displacement at the same time with different sensors.

The strips have been excited by an instrumented hammer, a simple hammer or even by manually imposing a certain displacement. Only using an instrumented hammer allows obtaining damping and transfer values, beside natural frequencies. Weight and position of accelerometers showed some influence on the obtained results. Some instrumentation offers embedded data analysis to obtain first natural frequency while in other cases FFT was directly computed using spreadsheet formulae developed on purpose. Figure 27 show some of the experimental set-ups.

Experimental results were assessed using approximated beam theory and FEM method (Eigenvalues analysis) as shown in Table 9. Difference with respect to the average of the experimental estimates is reported. A rule of thumb to estimate cantilever first natural frequency is:

$$\omega = 1.875^2 \cdot \sqrt{\frac{EI}{\rho A L^4}} \quad (1)$$

where EI is the flexural stiffness of the cantilever, ρ its density, A its cross-section area and L its span. FEM calculated values are deviating from a.m. estimates as well as from experimental results.

Results of participant B are given using approximated beam theory and FEM method, considering shell elements and a mesh element size of 5 mm in software ADINA, a 4 mm mesh was built up in FEMAP.

Table 9: analytical and numerical analyses

Material	**Specimen**	**Analysis type**	**Software**	**Estimated frequency**
	A1	**Analytical formula**	**Excel**	**18.0 Hz**
Steel	B1	Beam theory	Excel	14.87 Hz
	B1	FEM	ADINA	14.92Hz
	D1	FEM	FEMAP-NX Nastran	15.98 Hz
Composite	B2	Beam theory	Excel	25.77 Hz
	B2	FEM	ADINA	32.96 Hz
	B3	Beam theory	Excel	25.78 Hz
	B3	FEM	ADINA	33.12 Hz

Measured specimens' dimensions and material input properties used in calculations can be affected by uncertainties. In Table 10, rough uncertainty analysis is proposed. The dimensions may for instance range ±0.1 mm from the measured value, depending mainly on instrumentation accuracy, while material properties scatter is taken in the range of standard material values.

Table 10: Uncertainty analysis

Material	Material reference properties	Material properties variation	
Steel	H-0.1mm L+0.1mm E=2.06E+11 N/m^2 ν=0.27	H+0.1mm L-0.1mm E=2.10E+11 N/m^2 ν =0.30	f range ±0.57 Hz
Composite	H-0.1mm L+0.1mm E_f=6.8E+10 N/m^2 E_m=2.8E+09 N/m^2 ν_f=0.20 ν_m=0.33 G_f=2.8E+10 N/m^2 G_m=1.6E+09 N/m^2	H+0.1mm L-0.1mm E_f=7.2E+10 N/m^2 E_m=3.2E+09N/m^2 ν_f =0.27 ν_m=0.40 G_f=3.2E+10N/m^2 G_m=1.8E+09 N/m^2	f range ±1.46 Hz

This uncertainty can be taken as a minimum measurement uncertainty, especially in the case of the composite, whose characteristics are strongly influenced by the type of fabrication process.

From this relatively simple experimental benchmark performed by 6 parties, it is clear a vast range of choices can be, and is actually made in everyday practice. Understanding the effect of the choices on the end result is essential. For instance, a heavy sensor influences the natural frequency a lot. Also, the chosen instrumentation influences the information one gains from an experiment. Only the first natural frequency was aimed at, by manual excitation, but also damping and higher order modes when using an instrumented hammer could have been obtained enhancing the measurement range but likely also its scatter and uncertainties.

Composite A2

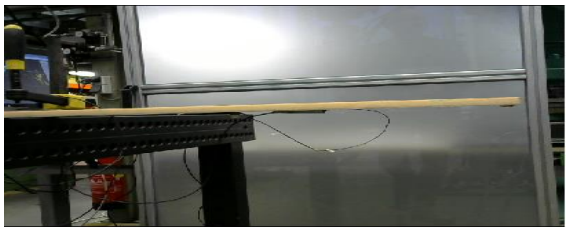

Impact analysis signal

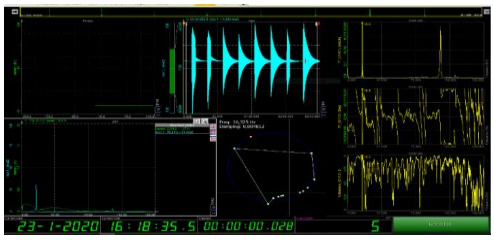

Steel B1

Laser distance measurement signal

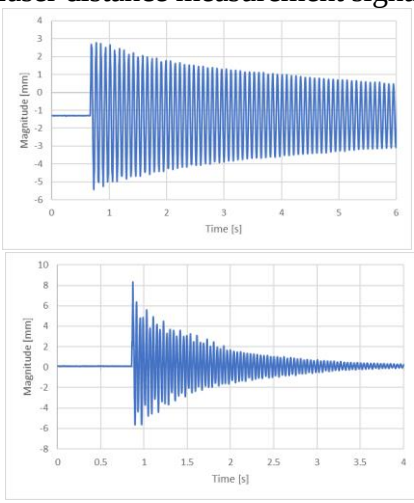

Composite B2

Composite F2 DIC set up

DIC images elaboration

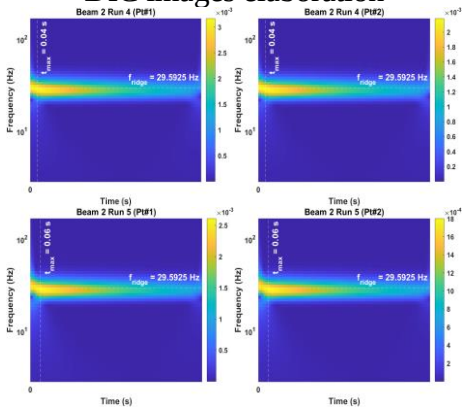

Composite B3 DIC images

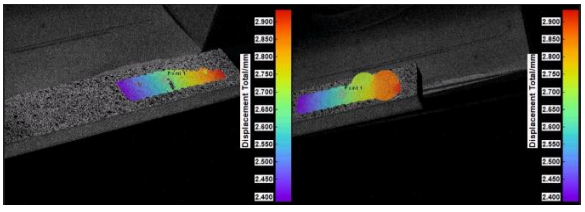

ISTRA software FFT analysis

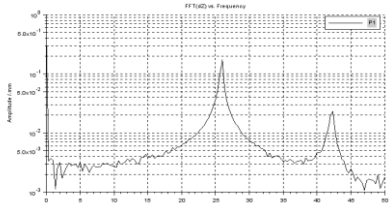

Steel and composite C1 and C3

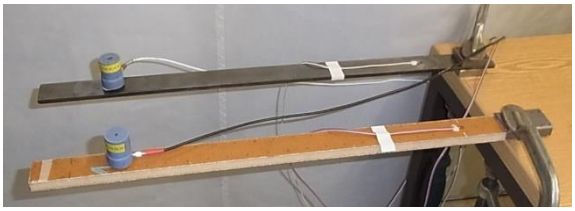

Strain gauge and impact positions

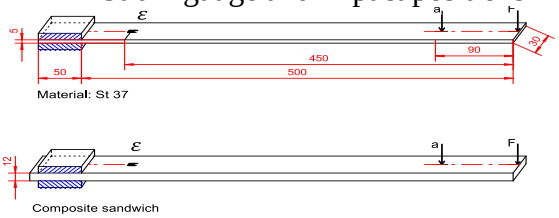

Figure 27: the experimental set-ups

In order to understand the many experiments that are done worldwide, sharing of the results and being transparent on the methodologies of experimentation is very beneficial for making

the most of any experiment. Experimental data should be published as is in digital format and not only as a by-product in a publication as figures are likely limiting the use of it. In general, digitalization should be regarded as the best opportunity to share and exploit experimental data.

16. SUMMARY AND CONCLUSIONS

This report reviews the recent advances of the past years in ships and offshore structural testing area including scaling laws, DIC, hydrodynamic of flexible structures, wave-in-deck, hybrid model testing, corrosion testing, iced load measurements, health monitoring model and digital twin model. The following summary and recommendations are made for future work in the area of innovative experimental methods in ships and offshore industry. It is important to also note that as experimental techniques allow for a greater understanding of the underlying material and structural behaviour, and generate extensive data clouds for processing and evaluation. As a result, we recommend that a future chapter in the next committee report focus on data evaluation and statistical approaches; this can provide an in-depth look of state of the art of processes utilized for evaluating the extensive data captured/utilized during experiments.

In chapter 2, a review of scaling laws is presented in systematic and recent advancements in structural testing related to ships and offshore structures. General scale modelling methods are provided and described the main characteristics of each method such as dimensional analysis, applied to governing equation, energy method, empirical similarity method through the literature review. Recent application of scale models can be found in field of offshore wind turbine structure and ice testing area. These structures are subjected to complex phenomena such as wave loads and drifting forces may also need to be considered in particular applications, ice flows, continuous winter sea ice, and icebergs.

Application DIC in chapter 3, DIC techniques have certainly come into play in many recent experimental evaluations, as the methods allows for elucidating the surface strain behaviour of a component evaluated either in the laboratory and in the field. This chapter has been to give an updated review on applications of DIC techniques in ships and offshore structural tests classifying them by test articles, with a brief insight on commercial instrumentations available on the industry and related to DIC society and a deeper focus on the applied methodologies, providing recent references for those who are interested in this topic. Worth mentioning is that some DIC applications are included in the benchmark study performed by the Committee and reported in section 15.

In chapter 4, A large amount of research has focused on better measuring and predicting the hydrodynamic loads, forming several practical hydrodynamic coefficients databases which have been widely used in VIV prediction tools for flexible structure manufacturing industry. Although these databases make great contributions to the field of VIV research, have not been sufficiently modelled in the coefficient database obtained from rigid cylinder experiments. Recently, the phase angle between cross-flow and in-line response had a strong influence on the hydrodynamic coefficients for both rigid and flexible cylinders. And variations of tension and flow velocity were strongly correlated with time-varying hydrodynamic coefficients, therefore, inputs to the prediction of vessel motion induced VIVs, making the prediction possible. Also, the effects of Re numbers and surface roughness on hydrodynamics of VIV and the effect of wake interference on hydrodynamics of a twin-tube submerged floating tunnel (SFT) can be found for can efficient way and requirement in the literature.

In chapter 5, based on the challenges remaining in the problem of wave-in-deck impact on offshore structures discussed above, there are several research gaps that can be addressed in future. There is still considerable uncertainty about the magnitude and distribution of wave impact loads on structural deck elements near the free-surface. Effects of the columns of the floating platform on the wave-in-deck forces have not been systematically studied. The measurement, estimation and simulation of local pressures due to wave-in-deck impact events on all

types of offshore structures remains challenging. Accurate measurements and prediction of global loads and dynamic response of floating offshore structures due to wave-in-deck impact events is extremely limited. Combined numerical-experimental wave-in-deck investigations on floating offshore structures are not currently available in the open literature.

In chapter 6, this chapter focused on hybrid model testing (HMT) combines physical model test and numerical simulations to solve problems that physical model tests alone cannot conveniently or reliably address. In marine model testing, the challenges like ultra-deep water, multi-phase fluids, parameter traversal and so on cannot be avoided. HMT is regarded as the most promising technique to solve these issues. As of today, HMT is still immature, some advanced applications however have been developed. HMT allows researchers to impose mass-spring-damping parameters in virtual space and can artificially adjust and precisely control these critical parameters. It is a very helpful and exciting idea to solve the involved problems.

In Chapter 7, a brief reviewed of friction test in terms of two main areas exist where friction is of importance: machineries and mechanical connections, and in cargo/ mechanical handling operations. For maritime and offshore applications (e.g. Out-of-Plane Bending) , surface conditions and environmental conditions are important parameters. Small and the smaller specimens may be used for screening the theoretical friction coefficients and find trends. Larger or even real size specimens should be used to confirm the actual behaviour. As per the results of literature, friction tests can be split it eh standard, small size specimen standard tests, and the large size, more representative tests. While the standard tests are well covered by standards and guidelines, the larger set-ups are to be tailor made and require goo understanding of the physics as results require interpretation by the experimenter.

In chapter 8, the measurement, analysis and mitigation of vibrations in ship and offshore structures is rather well established. Nevertheless, measurement and mitigation methods are still being developed. Measurement's techniques may also include laser of video techniques. Mitigation measures include devices that cancel vibrations at a low weight penalty, such as absorbing supports or Tuned Mass Dampers. Numerical developments include methods that use substructuring or modal shapes to reduce the computational cost.

In chapter 9, Material selection for ships and offshore structures exposed to sub-zero temperatures is traditionally based on Charpy and fracture toughness test results of the base materials and its welded connections. In the last years however, fatigue properties have been the focus of a couple of studies due to the acceleration of fatigue crack growth below the so-called fatigue transition temperature, where ductile crack growth is superimposed by cleavage burst. Concluding, fatigue testing at low temperatures demands special attention to the set-up and instrumentation. The testing temperature is normally lower than the application temperature, and liquid nitrogen may be needed to cool down the area of interest to -60 °C. Temperature compensation is required for sensor, either strain gauges or potential drop methods.

In chapter 10, The corrosion process and the interpretation of the effect of corrosion on the structural integrity remains an area of uncertainty. In corrosion testing, a large spread may be observed in measured corrosion rates, as is confirmed by industrial thickness measurement. Including the geometrical effects of corrosion damage in a representative manner in numerical simulations requires the use of probabilistic methods, as a precise description would require model with too many details. Hence, simplifications and generalizations are needed.

In chapter 11, large scale impact experimentation are unique options to verify developments in structures design, analysis and prediction of failure. In turn, this demands good command of the experimentation techniques, and the use of as many sensors as possible to make possible use of the results.

In chapter 12, The chapter present a State-of-the-Art review, to include recent advances and future trends of industry challenge with current standard and out lookout. The wind industry is

concerning with the long time-to-marked for future large turbine blades and are interested in ways to shorten the test time. It is a question at which size and when will it stop to make sense to test these long blades according to current standard. Trends of development of more advanced test methods investigated a dual or multi axis test methods to test blades under more representative loading compared to operational loads and ways to speed up the test and challenge with different SN-curves for different materials. Testing parts of blades captured testing with more complex and realistic loading at forced loading, challenges with boundaries, and using subcomponent testing to validate numerical models.

In chapter 13, Full scale ice load measurements play a significant role in the design of ships and offshore structures in ice covered waters. Full scale measurements of fixed vertical offshore structure are dis-cussed here. Generalizability of the results can be summarised that as pointed out by Kärnä (2009) it is likely that the experimental data recorded on vertical structures is only applicable for the conditions where the data was record-ed. Thus, data recorded for stiff structures might not be applicable for compliant structures. As discussed before, the compliancy might be one source of the observed rate dependency. The collected data is often incomplete: although local and global ice forces can be recorded during ice action, the ice properties (compressive strength, porosity...) might remain unknown. It is because the ice samples cannot be taken during ice action - when ice is moving. Actual local pressure is challenging to measure. It is known that the ice pressure is concentrated in a small area as shown by Joensuu & Riska (1989). They observed in laboratory scale experiments using PVDF-film that the ice pressure is concentrated on narrow, line like high pressure zones. But, the area of the load panels in full scale of often quite big, in the order of 1 m2. Thus, the actual local pressure exerted to structure is significantly higher than the average pressure measured with the big load panels. But there is no method available for more accurate local pressure measurements in full scale. Although field tests are important and can reveal phenomena that cannot be observed in laboratory scale, there are few things to consider when interpreting the results.

In chapter 14, Bridging the relationship between the degradation in the material and the structure is an emerging field of research which requires advanced data fusion, signal processing, AI-based trend detection algorithms and the reliability analysis methods. Data fusion herein refers to combining the data gathered from different SHM sensors by using data fusion algorithms for better damage diagnosis (Eleftheroglou et al., 2018). Other research efforts are recommended for improving the durability of SHM sensors for offshore implementations, inclusion of SHM in the condition monitoring standards and guidelines, addressing big-data issues for developing real-time data collection and analysis frameworks and using the digital twins for real-time reliability assessment.

In the Benchmark study, from this relatively simple experiment performed by 6 parties, it is clear that a vast range of choices can be made to carry out the tests. Understanding the effect of the choices on the end result is essential. For instance, a heavy sensor influences the natural frequency a lot. Also, the chosen instrumentation influences the information to be gained from an experiment. Only the natural frequency, by manual excitation, or also damping and higher order modes when using an instrumented hammer. In order to understand the many experiments that are done worldwide, sharing of the results and being transparent on the methodologies of experimentation is very beneficial for making the most of any experiment. Experimental data should be published as is in digital format and not only as a by-product in a publication as figures limiting the use of it.

ACKNOWLEDGEMENTS

The committee members are thankful for the support of the following contributors to various sections incl. the benchmark study: Francesco Mannacio, Rims Janeliukstis and Sergei Semenov, and Wolfgang Koch.

REFERENCES

Abbas, M. and Shafiee, M. (2018), Structural health monitoring (SHM) and determination of surface defects in large metallic structures using ultrasonic guided waves, Sensors (Switzerland), vol. 18, no. 11.

Abdussamie, N., Amin, W., Ojeda, R., Thomas, G., Drobyshevski, Y. (2014a), Vertical Wave-in-Deck Loading and Pressure Distribution on Fixed Horizontal Decks of Offshore Platforms. Proceedings of the 24th International Offshore and Polar Engineering, Busan, South Korea. International Society of Offshore and Polar Engineers.

Abdussamie, N., Ojeda, R., Amin, W., Thomas, G., Drobyshevski, Y. (2014b), Prediction of Wave-in-Deck Loads on Offshore Structures Using CFD. The 19th Australasian Fluid Mechanics Conference, 2014 Melbourne, Australia. AFMS.

Abdussamie, N., Thomas, G., Amin, W., Ojeda, R. (2014c), Wave-in-Deck Forces on Fixed Horizontal Decks of Offshore Platforms. Proceedings of the ASME 33rd International Conference on Ocean, Offshore and Arctic Engineering, OMAE, San Francisco, CA, USA. American Society of Mechanical Engineers.

Abdussamie, N., Ojeda, R., Drobyshevski, Y., Thomas, G., Amin, W. (2017a), Measurements of global and local effects of wave impact on a fixed platform deck. Proceedings of the Institution of Mechanical Engineers, Part M: Journal of Engineering for the Maritime Environment, 231(1): 212-233. DOI:10.1177/1475090216636410.

Abdussamie, N., Drobyshevski, Y., Ojeda, R., Thomas, G., Amin, W. (2017b), Experimental investigation of wave-in-deck impact events on a TLP model. Ocean Engineering, 142: 541-562.

ABS (2014), Rules for Building and Classing: Floating Production Installation. Houston, USA: American Bureau of Shipping.

ABS (2017), Air Gap Analysis for Semi-Submersibles. Houston, USA.

Aguiar, V. S., Kirkayak, L., Suzuki, K., Ando, H., and Sueoka, H. (2012), Experimental and Numerical Analysis of Container Stack Dynamics Using a Scaled Model Test, Ocean Eng., 39, pp. 24–42.

Ahmed, M. P., Seo, J. K., and Paik, J. K. (2018), Probabilistic approach for collision risk analysis of powered vessel with offshore platforms. Ocean Engineering, 151, pp. 206-221

Alsos, H. S. (2008), Ship Grounding - Analysis of Ductile Fracture, Bottom Damage and Hull Girder Response. PhD, Norwegian University of Science and Technology (NTNU).

API (2007), Recommended Practice for Planning, Designing and Constructing Fixed Offshore Platforms–Working Stress Design, 2A-WSD. American Petroleum Institute.

API (2010), Planning, Designing, and Constructing Tension Leg Platforms: API recommended practice 2T third edition. USA: American Petroleum Institute.

AKVA (2020), Pens and nets. AKWA Group. Retrieved from: https://www.akvagroup.com/pen-based-aquaculture/pens-nets (Accessed 29 March 2020).

Antoniadou, I., Dervilis, N., Papatheou, E., Maguire, A., Worden, K. (2015), Aspects of structural health and condition monitoring of offshore wind turbines. Philosophical Transactions of the Royal Society A: Mathematical, Physical and Engineering Sciences, 373: 20140075.

Aronsen, K. H. (2007), An Experimental Investigation of In-Line and Combined In-Line and Cross-Flow Vortex-Induced Vibrations. PhD Thesis. Department of Marine Technology, NTNU, Trondheim, Norway.

Asl, M. E., Niezrecki, C., Sherwood, J., and Avitabile, P. (2015), Predicting the Vibration Response in Subcomponent Testing of Wind Turbine Blades, Special Topics in Structural Dynamics, Vol. 6, R. Allemang, ed., Springer, Cham, Switzerland.

Asl, M. E., Niezrecki, C., Sherwood, J., and Avitabile, P. (2016), Similitude Analysis of Composite I–Beams with Application to Subcomponent Testing of Wind Turbine Blades, Experimental and Applied Mechanics (Proceedings of the Society for Experimental

Mechanics Series, Vol. 4), C. Sciammarella, J. Considine, and P. Gloeckner, eds., Springer, Cham, Switzerland.

Asl, M. E., Niezrecki, C., Sherwood, J., and Avitabile, P. (2017a), Similitude Analysis of Thin-Walled Composite I–Beams for Subcomponent Testing of Wind Turbine Blades, Wind Eng., 41(5), pp. 297–312.

Asl, M. E., Niezrecki, C., Sherwood, J., and Avitabile, P. (2017b), Vibration Prediction of Thin-Walled Composite I–Beams Using Scaled Models, Thin-Walled Struct., 113, pp. 151–161.

Asl, M. E., Niezrecki, C., Sherwood, J., and Avitabile, P. (2018), Scaled Composites I–Beams for Subcomponent Testing of Wind Turbine Blades: An Experimental Study, Mechanics of Composite and Multi-Functional Materials (Conference Proceedings of the Society for Experimental Mechanics Series, Vol. 6), P. Thakre, R. Singh, and G. Slipher, eds., Springer, Cham, Switzerland.

ASTM 2005. ASTM G133-05, Standard Test Method for Linearly Reciprocating Ball-on-Flat Sliding Wear, ASTM International, West Conshohocken, PA, 2005, www.astm.org

ASTM (2012), Steel chains. The American Society of Testing and Materials ASTM. Retrieved from: https://www.astm.org/Standards/steel-standards.html (Accessed 26 March 2020).

ASTM G99 – 17 (2017), Standard Test Method for Wear Testing with a Pin-on-Disk Apparatus, ASTM International, West Conshohocken, Pennsylvania.

Atkinson, D. and Becker, T. (2020), A 117 Line 2D Digital Image Correlation Code Written in MATLAB, Remote Sens. DOI:10.3390/rs12182906.

Augustyn, D., Tygesen, U. T., Ulriksen, M. D., and Sørensen, J. D. (2019), Data-Driven Design and Operation of Offshore Wind Structures. The 29th International Ocean and Polar Engineering Conference. International Society of Offshore and Polar Engineers.

Baarholm, R. (2009), Experimental and Theoretical Study of Three-Dimensional Effects on Vertical Wave-in-Deck Forces. Proceedings of the ASME 28th International Conference on Ocean, Offshore and Arctic Engineering, OMAE, Honolulu, Hawaii, USA. American Society of Mechanical Engineers.

Bak, C., Zahle, F., Bitsche, B., Kim, T., Yde, A., Henriksen, L. C., Natarajan, A. and Hansen, M. H. (2013), Description of the DTU 10 MW Reference Wind Turbine. DTU Wind Energy Report-I-0092, DTU, Roskilde, Denmark.

Balash, C., Colbourne, B., Bose, N., Raman-Nair, W. (2009), Aquaculture net drag force and added mass. Aquacultural Engineering, 41: 14-21.

Balawi, S., Shahid, O., and Mulla, M. A. (2015), Similitude Scaling laWs-Static and Dynamic Behaviour Beams and Plates, Procedia Eng., 114, pp. 330–337.

Banks, J., Giovannetti, L. M., Soubeyran, X., Wright, A. M., Turnock, S. R., Boyd, S. W. (2015), Assessment of Digital Image Correlation as a method of obtaining deformations of a structure under fluid load, Journal of Fluids and Structures, Vol 58, pages 173-187.

Barone, G. and Frangopol, D. M. (2014), Life-cycle maintenance of deteriorating structures by multi-objective optimization involving reliability, risk, availability, hazard and cost, Struct. Saf., vol. 48, pp. 40–50.

Bayati, I., Belloli, M., Ferrari, D., Fossati, F., and Giberti, H. (2014), Design of a 6-DoF Robotic Platform for Wind Tunnel Tests of Floating Wind Turbines. Energy Procedia, 53:313–323.

Bayati, I., Belloli, M., Bernini, L., and Zasso, A. (2017), Aerodynamic design methodology for wind tunnel tests of wind turbine rotors. Journal of Wind Engineering and Industrial Aerodynamics, 167:217–227.

Belloni V., Ravanelli R., Nascetti A., Di Rita M., Mattei D., Crespi M. (2019), py2DIC: A New Free and Open Source Software for Displacement and Strain Measurements in the Field of Experimental Mechanics, Sensors (Basel), 19(18): 3832. DOI: 10.3390/s19183832 (accessed 5th October 2021).

Bhat, S. S. (1994), Wave slamming on a horizontal plate. MSc thesis, University of British Columbia.

Bienen, B., Gaudin, C., Cassidy, M. J. (2007), Centrifuge tests of shallow footing behaviour on sand under combined vertical torsional loading. International Journal of Physical Modelling in Geotechnics, 7(2): 1-22.

Bienen, B., Cassidy, M. J., Gaudin, C. (2009), Physical modelling of the push-over capacity of a jack-up structure on sand in a geotechnical centrifuge. Canadian Geotechnical Journal, 46(2): 190-207.

Bijleveld, F. W., Hoogeland, M. G., Walters, C. L., and van Bergen, J. W. (2018), A Practical Approach to Ductile Material Failure During Raking Collisions, Paper presented at the The 28th International Ocean and Polar Engineering Conference, Sapporo, Japan, June 2018, ISOPE-I-18-466.

Birknes-Berg, J., and Johannessen, T. (2015), Methods for establishing governing deck impact loads in irregular waves. The ASME 2015 34th Int. Conf. on Ocean, Offshore and Arctic Eng., OMAE2015, St. John's, Newfoundland, Canada. ASME.

Bitner-Gregersen, E. M., and Gramstad, O. (2015), Rogue waves: Impact on ships and offshore structures. DNV.

Blaber, J., Adair, B., and Antoniou, A. (2015), Ncorr: Open-Source 2D Digital Image Correlation Matlab Software. Experimental Mechanics (2015). Retrieved from: http://ncorr.com/index.php/publications/ (accessed on 15 September 2021).

BMT (2020), Demystifying digital twins. BMT. Retrieved from: https://www.bmt.org/insights/demystifying-digital-twins/ (Accessed 29 August 2020).

Boo, S.-H., and Park, J.-B. (2019), Vibration Analysis for Ship Structures Employing the Algebraic Dynamic Condensation Method. The 29th International Ocean and Polar Engineering Conference. Honolulu, Hawaii, USA: International Society of Offshore and Polar Engineers.

Branner, K., Berring, P., and Haselbach, P. U. (2016), Subcomponent testing of trailing edge panels in wind turbine blades. In Proceedings of 17th European Conference on Composite Materials

Branner, K., and Berring, P. (2014), Methods for testing of geometrical down-scaled rotor blades. DTU Wind Energy. DTU Wind Energy E, No. 0069.

Braun, M., Fischer, C., Fricke, W., and Ehlers, S. (2020a), Extension of the strain energy density method for fatigue assessment of welded joints to sub-zero temperatures. Fatigue Fract Eng M. DOI: 10.1111/ffe.13308.

Braun, M., Milaković, A-S, and Ehlers, S. (2020b), Fatigue Assessment of Welded Joints at Sub-Zero Temperatures using the Stress Averaging Approach. International Conference on Ships and Offshore Structures ICSOS; 1 – 4 September; Glasgow, UK.

Braun, M., Milaković, A-S, Ehlers, S., Kahl, A., Willems, T., Seidel, M., and Fischer, C. (2020c), Sub-zero temperature fatigue strength of butt-welded normal and high-strength steel joints for ships and offshore structures in arctic regions. ASME 39th International Conference on Ocean, Offshore and Arctic Engineering; June 28-July 3; Fort Lauderdale, FL, USA.

Braun, M., Milaković, A-S, Renken, F., Fricke, W., and Ehlers, S. (2020d), Application of Local Approaches to the Assessment of Fatigue Test results obtained for Welded Joints at Sub-Zero Temperatures. International Journal of Fatigue. 138. DOI: 10.1016/j.ijfatigue.2020.105672.

Braun, M., Scheffer, R., Fricke, W., and Ehlers, S. (2020e), Fatigue strength of fillet-welded joints at subzero temperatures. Fatigue Fract Eng M. 43(2):403-416. DOI: 10.1111/ffe.13163.

Braun, M. (2021a), Assessment of fatigue strength of welded steel joints at sub-zero temperatures based on the micro-structural support effect hypothesis. Doctoral Thesis. Konstruktion und Festigkeit von Schiffen M-10. Technische Universität Hamburg. DOI: 10.15480/882.3782

Braun, M. (2021b), Statistical analysis of sub-zero temperature effects on fatigue strength of welded joints. Welding in the World, 66(1):159-172. DOI: 10.1007/s40194-021-01207-y.

Braun, M., A. Dörner, K. F. ter Veer, T. Willems, M. Seidel, H. Hendrikse, K. V. Høyland, C. Fischer & S. Ehlers (2022a), Development of Combined Load Spectra for Offshore Structures Subjected to Wind, Wave, and Ice Loading. Energies, 15(2). DOI: 10.3390/en15020559.

Braun, M. and S. Ehlers (2022), Review of methods for the high-cycle fatigue strength assessment of steel structures subjected to sub-zero temperature. Marine Structures, 82. DOI: 10.1016/j.marstruc.2021.103153.

Braun, M., A. Kahl, T. Willems, M. Seidel, C. Fischer & S. Ehlers (2021a), Guidance for Material Selection Based on Static and Dynamic Mechanical Properties at Sub-Zero Temperatures. Journal of Offshore Mechanics and Arctic Engineering, 143: 1-45. DOI: 10.1115/1.4049252.

Braun, M., T. Stange, G. Ziemer, K. F. ter Veer, T. Willems, J. M. Kubiczek, R. U. F. von Bock und Polach & S. Ehlers. (2021b), Einfluss von Minusgraden und variablen Lastamplituden infolge Seegangs- und Eislasten auf den Entwurf von Offshore Windenergieanlagen (Influence of sub-zero temperatures and variable load amplitudes due to sea and ice loads on the design of offshore wind turbines). In Proceedings of 9. Fachtagung Bemessung und Konstruktion, 61-69. Halle, Germany: SLV Halle.

Brett, C., Gunn, D., Dashwood, B., Holyoake, S., and Wilkinson, P. (2018), Development of a technique for inspecting the foundations of offshore wind turbines. Insight-Non-Destructive Testing and Condition Monitoring, 60: 19-27.

Brodersen, M. L., Bjørke, A-S., and Høgsberg, J. B. (2017), Active tuned mass damper for damping of offshore
wind turbine vibrations. Wind Energy, 20(5), 783–796. DOI: 10.1002/we.2063.

Buchner, B., and Bunnik, T. (2007), Extreme wave effects on deepwater floating structures. Offshore Technology Conference, Houston, Texas.

Bullock, G., Crawford, A., Hewson, P., Walkden, M., and Bird, P. (2001), The influence of air and scale on wave impact pressures. Coastal Engineering, 42(4), 291-312.

Byrne, B.W., and Houlsby, G.T. (2001), Observations of footing behaviour on loose carbonate sands. Geotechnique, 51(5): 463-466.

Calle, M. A. G., and Alves, M. (2011), Ship Collision: A Brief Survey, 21st Brazilian Congress of Mechanical Engineering, Natal, Brazil, Oct. 24–28.

Calle, M. A. G., Oshiro, R. E., and Alves, M. (2017), Ship Collision and Grounding: Scaled Experiments and Numerical Analysis, Int. J. Impact Eng., 103, pp. 195–210.

Canestrari, F., Ingrassia, L. P., Ferrotti, G., Lu, X. 2017. State of the art of tribological tests for bituminous binders. Construction and Building Materials, 157: 718-728

Cao, Y. and Tahchiev, G. (2013), A Study on an Active Hybrid Decomposed Mooring System for Model Testing in Ocean Basin for Offshore Platforms. In ASME 2013 32nd International Conference on Ocean, Offshore and Arctic Engineering. American Society of Mechanical Engineers.

Carroll, J. D., Abuzaid, W., Lambros, J., and Sehitoglu, H. (2013), High resolution digital image correlation measurements of strain accumulation in fatigue crack growth. International Journal of Fatigue. 57, 140-150.

Casaburo, A., Petrone, G., Franco, F., and Rosa, S. D. (2019), A review of similitude methods for structural engineering. Applied Mechanics Reviews, 71. 1-32.

Cassidy, M. J., Byrne, B. W., and Randolph, M. F. (2004), A comparison of the combined load behaviour of spudcan and caisson foundations on soft normally consolidated clay. Geotechnique, 54(2): 91-106.

Cassidy, M. J., and Cheong, J. (2005), The behaviour of circular footings on sand subjected to combined vertical-torsion loading. International Journal of Physical Modelling in Geotechnics, 5(4): 1-14.

Cassidy, M. J. (2007), Experimental observations of the combined loading behaviour of circular footings on loose silica sand. Geotechnique, 57(4): 397-401.

Castro, O., Belloni, F., Stolpe, M., Yeniceli, S. C., Berring, P., & Branner, K. (2021). Optimized method for multi-axial fatigue testing of wind turbine blades. Composite Structures, 257, [113358]. https://doi.org/10.1016/j.compstruct.2020.113358

Castro, O., Berring, P., Branner, K., Hvejsel, C. F., Yeniceli, S. C., & Belloni, F. (2021). Bending-moment-based approach to match damage-equivalent strains in fatigue testing. Engineering Structures, 226, [111325]. https://doi.org/10.1016/j.engstruct.2020.111325

Cd-Adapco (2012), User guide - Star-CCM+ Version 7.04. CD-Adapco.

Çengel, Y. A., and Cimbala, J. M. (2006), Fluid Mechanics: Fundamentals and Applications - 1st ed. New York: McGraw-Hill.

Chakrabarti, S. K. (1994), Offshore Structure Modeling. Singapore: World Scientific Publishing Co. Pte. Ltd.

Chatzakos, P., Avdelidis, N., Hrissagis, K., and Gan, T.-H. (2010), Autonomous Infrared (IR) Thermography based inspection of glass reinforced plastic (GRP) wind turbine blades (WTBs). 2010 IEEE Conference on Robotics, Automation and Mechatronics. IEEE, 557-562.

Chen, H. C., Lee, S. K., and Seah, A. K. (2008), Overset grid CFD applications for challenging offshore hydrodynamic problems. ABS Technical Paper.

Chen, X., Okada, T., Kawamura, Y., and Mitsuyuki, T. (2020), Estimation of on-site directional wave spectra using measured hull stresses on 14,000 TEU large container ships. Journal of Marine Science and Technology, 25:690-706. https://doi.org/10.1007/s00773-019-00673-w.

Chen, X., Berring, P., Madsen, S. H., Branner, K., & Semenov, S. (2019). Understanding progressive failure mechanisms of a wind turbine blade trailing edge section through subcomponent tests and nonlinear FE analysis. Composite Structures, 214, 422-438. https://doi.org/10.1016/j.compstruct.2019.02.024

Chen, X., Haselbach, P. U., Branner, K., & Madsen, S. H. (2019). Effects of different material failures and surface contact on structural response of trailing edge sections in composite wind turbine blades. Composite Structures, 226, [111306]. https://doi.org/10.1016/j.compstruct.2019.111306

Cheong, N., and Cassidy, M. J. (2016), Combined loading capacity of spudcan footings on loose sand. International Journal of Physical Modelling in Geotechnics, 16(1): 31-44.

Cho, U., and Wood, K. (1997), Empirical Similitude Method for the Functional Test with Rapid Prototypes, Symposium for Solid Freeform Fabrication, The University of Texas at Austin, Austin, TX.

Cho, U., Dutson, A. J., Wood, K. L., and Crawford, R. H. (2005), An Advanced Method to Correlate Scale Models With Distorted Configurations, ASME J. Mech. Des., 127(1), pp. 78–85.

Chu, Y., Wang, C., Park, J., and Lader, P. (2020), Review of cage and containment tank designs for offshore fish farming. Aquaculture, 519: 734928.

Christoforou, A. P., and Yigit, A. S. (2009), Scaling of Low-Velocity Impact Response in Composite Structures, Compos. Struct., 91(3), pp. 358–365.

Coutinho, C. P., Baptista, A. J., and Dias Rodriges, J. (2018), Modular Approach to Structural Similitude, Int. J. Mech. Sci., 135. 294–312.

Cronrath, C., Aderiani, A. R., and Lennartson, B. (2019), Enhancing digital twins through reinforcement learning. 2019 IEEE 15th International Conference on Automation Science and Engineering (CASE). IEEE, 293-298.

Cuomo, G., Shimosako, K.-i., and Takahashi, S. (2009), Wave-in-deck loads on coastal bridges and the role of air. Coastal Engineering, 56(8), 793-809. DOI: 10.1016/j.coastaleng.2009.01.005.

Cuomo, G., Allsop, W., and Takahashi, S. (2010), Scaling wave impact pressures on vertical walls. Coastal Engineering, 57(6), 604-609. DOI: 10.1016/j.coastaleng.2010.01.004.

Galbraith, D. and Sharp, J. (2007), Recommendations for Design Life Extension Regulations.

Da Silva, L. F. B. A., Yang, Z., Pires, N. M. M., Dong, T., Teien, H.-C., Storebakken, T., and Salbu, B. (2018), Monitoring Aquaculture Water Quality: Design of an Early Warning Sensor with Aliivibrio fischeri and Predictive Models. Sensors (Basel, Switzerland), 18: 2848.

De Mooij, C., Martinez, M., and Benedictus, R. (2019), iFEM benchmark problems for solid elements. Smart Materials and Structures, 28: 065003.

Dean, E. T. R., James, R. G., Schofield, A. N., and Tsukamoto, Y. (1996), Drum centrifuge study of three-leg jackups models on clay. Report CEUD/D-Soils/TR289. University of Cambridge.

Decew, J., Fredriksson, D., Lader, P., Chambers, M., Howell, W., Osienki, M., Celikkol, B., Frank, K., and Høy, E. (2013), Field measurements of cage deformation using acoustic sensors. Aquacultural engineering, 57: 114-125.

Deng, S., Ren, H., Xu, Y., Fu, S., and Gao, Z. (2020a), Experimental study on the drag forces on a twin-tube submerged floating tunnel segment model in current. Applied Ocean Research, 104, 102326.

Deng, S., Ren, H., Xu, Y., Fu, S., and Gao, Z. (2020b), Experimental study of vortex-induced vibration of a twin-tube submerged floating tunnel segment model. Journal of Fluids and Structures, 94, 102908.

Devriendt, C., Magalhães, F., Weijtjens, W., De Sitter, G., Cunha, Á., and Guillaume, P. (2014), Structural health monitoring of offshore wind turbines using automated operational modal analysis. Structural Health Monitoring, 13: 644-659.

Dias, F., and Ghidaglia, J.-M. (2018), Slamming: Recent progress in the evaluation of impact pressures. Annual Review of Fluid Mechanics, 50, 243-273.

DNV (2004), DNV-OS-J101-Design of offshore wind turbine structures. Det Norske Veritas.

DNV (2014), Recommended Practice DNV-RP-C205: Environmental Conditions and Environmental Loads. Høvik, Norway: Det Norske Veritas, DNV.

DNV (2015). Rotor blades for wind turbines. Standard, DNVGL-ST-0376, Edition December 2015.

Doremus, L., Nadot, Y., Henaff, G., Mary, C., and Pierret, S. (2015), Calibration of the potential drop method for monitoring small crack growth from surface anomalies – Crack front marking technique and finite element simulations. International Journal of Fatigue. 70:178-185. DOI: 10.1016/j.ijfatigue.2014.09.003.

Dragt, R. C., Heuvel, W. Van den, Gelink, E. R. M., and Slot, H. M. (2015), Testing of full scale composite journal bearings for offshore underwater applications, 34th International Conference on Ocean, Offshore and Arctic Engineering, St. John's, Newfoundland, Canada.

Du, W. Lei, D. Bai, P. Zhu, F, and Huang, Z. (2019), Dynamic Measurement for Stay-Cable Force Using Digital Image Techniques. Measurements.

Dutson, A. J., Wood, K. L., Beaman, J. J., Crawford, R. H., and Bourell, D. L. (2003), Application of Similitude Techniques to Functional Testing of Rapid Prototypes, Rapid Prototyping J., 9(1), pp. 6–13.

Eberl, C., Thompson, R., Gianola, D., and Bundschuh, S. (2021), Digital Image Correlation and Tracking with Matlab, Retrieved from: http://geoserver.ing.puc.cl/info/docencia/ice1603/DIC/Correlation_Tracking_Guide_2010.htm, (accessed on 5 October 2021).

Eleftheroglou, N., Zarouchas, D., Loutas, T., Alderliesten, R., and Benedictus, R. (2018), Structural health monitoring data fusion for in-situ life prognosis of composite structures. Reliability Engineering & System Safety, 178: 40-54.

Ersdal, G., Hörnlund, E., and Spilde, H. (2011), Experience from Norwegian Programme on Ageing and Life Extension, in Proceedings of the ASME 2011 30th International Conference on Ocean, Offshore and Arctic Engineering, January 2011, pp. 517–522.

Fan, D., Wang, Z., Triantafyllou, M. S., and Karniadakis, G. E. (2019), Mapping the properties of the vortex-induced vibrations of flexible cylinders in uniform oncoming flow. Journal of Fluid Mechanics, 881, 815-858.

Fernandez, I. and Berrocal, C. G. (2019), Mechanical Properties of 30 Year-Old Naturally Corroded Steel Reinforcing Bars, Int. J. Concr. Struct. Mater., vol. 13, no. 1.

Fluent, A. (2009). Ansys Fluent 12.0 user guide. ANSYS Inc.

Fredriksson, D. W., and Beck-Stimpert, J. (2019), Basis-of-Design Technical Guidance for Offshore Aquaculture Installations in the Gulf of Mexico.

Friedrich, N., and Ehlers, S. (2019), Crack Monitoring in Resonance Fatigue Testing of Welded Specimens Using Digital Image Correlation. J. Vis. Exp. (151), e60390, doi:10.3791/60390.

Fu, S., Lie, H., Wu, J., and Baarholm, R. (2017), Hydrodynamic Coefficients of a Flexible Pipe With Staggered Buoyancy Elements and Strakes Under VIV Conditions. ASME 2017, International Conference on Ocean, Offshore and Arctic Engineering (pp. V002T08A044).

Gaiotti, M. and Rizzo, C. M. (2012), Buckling behavior of FRP sandwich panels made by hand layup and vacuum bag infusion procedure, In: Sustainable Maritime Transportation and Exploitation of Sea Resources – Rizzuto & Guedes Soares (eds) Taylor & Francis Group, London, ISBN 978-0-415-62081-9 (IMAM 2011 Congress).

Galbraith, D., and Sharp, J., "Recommendations for Design Life Extension Regulations," 2007.

Gao, B., He, Y., Woo, W. L., Tian, G. Y., Liu, J., and Hu, Y. (2016), Multidimensional tensor-based inductive thermography with multiple physical fields for offshore wind turbine gear inspection. IEEE Transactions on Industrial Electronics, 63: 6305-6315.

Garbatov, Y., Guedes Soares, C., and Wang, G. (2005), Non-linear Time Dependent Corrosion Wastage of Deck Plates of Ballast and Cargo Tanks of Tankers, in international conference on offshore mechanics and arctic engineering, 2005, pp. 67–75.

Garbatov, Y. and Guedes Soares, C. (2010), Maintenance planning for the decks of bulk carriers and tankers, Safety, Reliab. Risk Struct. Infrastructures Eng. Syst., pp. 3517–3524.

Garbatov, Y., Saad-Eldeen, S., Guedes Soares, C., Parunov, J. and Kodvanj, J. (2019), Tensile test analysis of corroded cleaned aged steel specimens, Corros. Eng. Sci. Technol., vol. 54, no. 2, pp. 154–162.

García, D. and Tcherniak, D. (2019), An experimental study on the data-driven structural health monitoring of large wind turbine blades using a single accelerometer and actuator. Mechanical Systems and Signal Processing, 127: 102-119.

Gathimba, N. and Kitane, Y. (2018), Static ductility evaluation of corroded steel plates considering surface roughness characteristics, 2018 Struct. Congr., p. 13.

Gathimba, N., Kitane, Y., Yoshida, T. and Itoh, Y. (2019), Surface roughness characteristics of corroded steel pipe piles exposed to marine environment, Constr. Build. Mater., vol. 203, pp. 267–281.

Gaudin, C., Cassidy, M.J., Bienen, B., and Ilossain, M.S. (2011), Recent contributions of geotechnical centrifuge modeling to the understanding of jack-up spudcan behaviour. Ocean Engineering, 38: 900-914.

Gopalkrishnan, R. (1993), Vortex-induced Forces on Oscillating Bluff Cylinders. PhD thesis. Department of Ocean Engineering, Massachusetts Institute of Technology, Cambridge, MA, USA.

Güemes, A., Fernandez-Lopez, A., Pozo, A. R., and Sierra-Pérez, J. (2020), Structural Health Monitoring for Advanced Composite Structures: A Review. Journal of Composites Science, 4: 13.

Guerra, R. H., Quiza, R., Villalonga, A., Arenas, J., and Castaño, F. (2019), Digital twin-based optimization for ultraprecision motion systems with backlash and friction. IEEE Access, 7: 93462-93472.

Gunn, D., Holyoake, S., Dashwood, B., Wilkinson, P., Brett, C., Wallis, H., Leman, W., and Rees, J. (2019), Ultrasonic testing of laboratory samples representing monopile wind turbine foundations. Insight-Non-Destructive Testing and Condition Monitoring, 61: 187-196.

Guo, J., Wang, G., Ivanov, L., and Perakis, A. N. (2008), Time-varying ultimate strength of aging tanker deck plate considering corrosion effect, Mar. Struct., vol. 21, no. 4, pp. 402–419.

Guo, J., Wu, J., Guo, J., and Jiang, Z. (2018), A Damage Identification Approach for Offshore Jacket Platforms Using Partial Modal Results and Artificial Neural Networks. Applied Sciences, 8: 2173.

Haag, S. (2017), Grounding Damage Estimate Through Acceleration Measurements. Proceedings of the ASME 2017 36th International Conference on Ocean and Arctic Engineering, Trondheim, OMAE.

Harilal, R., and Ramji, M. (2014), Adaptation of Open Source 2D DIC Software Ncorr for Solid Mechanics Applications. 9th International Symposium on Advanced Science and Technology in Experimental Mechanics. Retrieved from http://ncorr.com/index.php/publications/ (accessed on 15 Sep 2021). DOI: 10.13140/2.1.4994.1442.

Hauge, M., Maier, M., Walters, C. L., Østby, E., Kordonets, S. M., Zanfir, C., and Osvoll, H. (2015), Status update of ISO TC67/SC8/WG5: Materials for Arctic Applications. Paper presented at the 25th International Ocean and Polar Engineering Conference.

Hawkes, I. and Mellor, M. (1970), Uniaxial testing in rock mechanics, Engineering Geology, 4, pp. 177–285.

Hellgren, R., Malm, R., Fransson, L., Johansson, F., Nordström, E., and Westberg Wilde, M. (2020), Measurement of ice pressure on a concrete dam with a prototype ice load panel. Cold Regions Science and Technology, 170, 102923. DOI: 10.1016/j.coldregions.2019.102923.

Hennig, J., Scharnke, J., Buchner, B., and Van Den Berg, J. (2011), Extreme Load-Response Mechanisms of a Tension Leg Platform due to Larger Wave Crests: Some Results of the 'CresT'JIP. ASME 2011 30th International Conference on Ocean, Offshore and Arctic Engineering. American Society of Mechanical Engineers, 855-864.

Hosdez, J., Witz, J-F., Martel, C., Limodin, N., Najjar, D., Charkaluk, E., Osmosd, P. and Szmytka, F. (2017), Fatigue Crack Growth Law Identification by Digital Image Correlation and Electrical Potential Method for Ductile Cast Iron. Journal of Engineering Fracture Mechanics.

Hover, F. S., Techet, A. H., and Triantafyllou, M. S. (1998), Forces on oscillating uniform and tapered cylinders in cross flow. Journal of Fluid Mechanics, 363:97–114.

Høyland, K. V., T. Nord, J. Turner, V. Hornnes, E. D. Gedikli, M. Bjerkås, H. Hendrikse, T. Hammer, G. Ziemer, T. Stange, S. Ehlers, M. Braun, T. Willems & C. Fischer. (2021), Fatigue damage from dynamic ice action – The FATICE project. In Proceedings of 26th International Conference on Port and Ocean Engineering under Arctic Conditions. Moscow, Russia.

Hu, Y. Q. (2000), Application of Response Number for Dynamic Plastic Response of Plates Subjected to Impulsive Loading, Int. J. Pressure Vessels Piping, 77(12), pp. 711–714.

Hughes, S., Musial, W. and Stensland, T. (1999), Implementation of two axis servo-hydraulic system for full-scale testing of wind turbine blades. In: Windpower '99, Burlington, Vermont, 20–23 June 1999, pp. 67–76.

iDICs (2021), Retrieved from http://www.idics.org, (accessed on 5 October 2021).

IEC 61400-23 (2014), Wind turbines - Part 23: Full-scale structural testing of rotor blades. Edition 1.0, 2014-04-08, TC/SC 88, IEC, Geneva, Switzerland.

Igwemezie, V., Mehmanparast, A., and Kolios, A. (2018), Materials selection for XL wind turbine support structures: A corrosion-fatigue perspective. Marine Structures, 61: 381-397.

ISO 19906:2010(E) (2010), Petroleum and natural gas industries - Arctic offshore structures. Geneva, Switzerland: ISO.

ISO (2007), Petroleum and natural gas industries-fixed steel offshore structures, International Organization for Standardization. In: Organization, I. S. (ed.) ISO 19902.

ITTC (1999). The Specialist Committee on Deep Water Mooring Final Report and Recommendations to the 22nd ITTC. Technical report.

Iwanowski, B., Lefranc, M., and Wemmenhove, R. (2009), CFD simulation of wave run-up on a semi-submersible and comparison with experiment. The ASME 28th Int. Conf. on Ocean, Offshore and Arctic Eng. ASME.

Iwanowski, B., Vestbostad, T., and Lefranc, M. (2014), Wave-In-Deck Load on a Jacket Platform, CFD Calculations Compared with Experiments. The ASME 33rd Int. Conf. on Ocean, Offshore and Arctic Eng., OMAE, San Francisco, CA, USA. ASME.

Jaensch, F., Csiszar, A., Scheifele, C., and Verl, A. (2018), Digital twins of manufacturing systems as a base for machine learning. 25th International Conference on Mechatronics and Machine Vision in Practice (M2VIP). IEEE, 1-6.

Jiao, J., Ren, H., and Adenya, C. (2015), Experimental and Numerical Analysis of Hull Girder Vibrations and Bow Impact of a Large Ship Sailing in Waves. Shock and Vibration: 1-10.

Joensuu, A. and Riska, K. (1989). Contact between ice and a structure. Report M-88. Espoo, Finland, Helsinki University of Technology, Ship Laboratory, 57p. + App (in Finnish).

Johannessen, T., Haver, S., Bunnik, T., and Buchner, B. (2006), Extreme Wave Effects on Deep Water TLPs Lessons Learned from the Snorre A Model Tests. Proc. Deep Offshore Technology 2006: 28-30.

Johnson, N. R., Lynch, J. P., and Collette, M. D. (2018), Response and fatigue assessment of high speed aluminium hulls using short-term wireless hull monitoring. Structure and Infrastructure Engineering, 14: 634-651.

Jones, E.M.C. and Iadicola, M. A. (2018), A Good Practices Guide for Digital Image Correlation, International Digital Image Correlation Society.

Jones, N. (2012), Structural impact- 2nd ed. Cambridge university press, New York, USA.

Jones, S. J. (1982), The Confined Compressive Strength of Polycrystalline Ice, Journal of Glaciology, 28(98), pp. 171–177.

Jones, S. J. (2007), A review of the strength of iceberg and other freshwater ice and the effect of temperature, Cold Regions Science and Technology, 47(3), pp. 256–262. DOI: 10.1016/j.coldregions.2006.10.002.

Jüngert, A. (2008), Damage Detection in wind turbine blades using two different acoustic techniques. The NDT Database & Journal (NDT).

Kaewunruen, S., and Lian, Q. (2019), Digital twin aided sustainability-based lifecycle management for railway turnout systems. Journal of Cleaner Production, 228: 1537-1551.

Kaiser, M. J., Yu, Y., and Jablonowski, C. J. (2009), Modeling lost production from destroyed platforms in the 2004–2005 Gulf of Mexico hurricane seasons. Energy, 34: 1156-1171.

Kampczyk, A. (2020), Measurement of the Geometric Center of a Turnout for the Safety of Railway Infrastructure Using MMS and Total Station. Sensors, 20: 4467.

Kandasamy, R., Cui, F., Townsend, N., Foo, C. C., Guo, J., Shenoi, A., and Xiong, Y. (2016), A review of vibration control methods for marine offshore structures. Ocean Engineering, 127: 279-297.

Kaplan, P., Murray, J., and Yu, W. (1995), Theoretical analysis of wave impact forces on platform deck structures. Offshore Technology Conference Houston, USA.

Karimi, M. R., Brosset, L., Kaminski, M. L., and Ghidaglia, J. M. (2017). Effects of ullage gas and scale on sloshing loads. European Journal of Mechanics - B/Fluids, 62, 59-85. DOI: 10.1016/j.euromechflu.2016.11.017.

Kärnä, T. (2009). Use of Field Data – a Note of Caution. Karna Research and Consulting, Helsinki, Finland. Report Nro Karna-28-2009

Kasivitamnuay, J., and Singhatanadgid, P. (2005), Application of an Energy Theorem to Derive a Scaling Law for Structural Behaviors, Thammasat. Int. J. Sc. Tech., 10(4), pp. 33–40.

Kasivitamnuay, J., and Singhatanadgid, P. (2017), Scaling Laws for Displacement of Elastic Beam by Energy Method, Int. J. Mech. Sci., 128–129, pp. 361–367.

Kefal, A., Mayang, J. B., Oterkus, E., and Yildiz, M. (2018), Three dimensional shape and stress monitoring of bulk carriers based on iFEM methodology. Ocean Engineering, 147: 256-267.

Kefal, A. (2019), An efficient curved inverse-shell element for shape sensing and structural health monitoring of cylindrical marine structures. Ocean Engineering, 188: 106262.

Khaja, A., and Samad, W. (2020), Hybrid Digital Image Correlation. Journal of Engineering Mechanics, ASCE.

Kim, N. S., Kwak, Y. H., and Chang, S. P. (2004), Pseudodynamic Tests on Small-Scale Steel Models Using the Modified Similitude Law, 13th World Conference of Earthquake Engineering, Vancouver, Canada, Aug. 1–6, Paper No. 3360.

Kim, N. S., Lee, J. H., and Chang, S. P. (2009), Equivalent Multi-Phase Similitude Law for Pseudodynamic Test on Small Scale Reinforced Concrete Models, Eng. Struct., 31(4), pp. 834–846.

Kirschbaum, L., Roman, D., Singh, G., Bruns, J., Robu, V., Flynn, D. (2020), AI-Driven Maintenance Support for Downhole Tools and Electronics Operated in Dynamic Drilling Environments. IEEE Access, 8: 78683-78701.

Kong, V.W. (2012), Jack-up reinstallation near existing footprints. PhD Thesis. The University of Western Australia. 2012.

Kolari, K. (2016). Strain-Rate Softening of Granular Ice in Brittle Regime: Fact or Artifact? In: 23rd IAHR International Symposium on Ice, Ann Arbor, Michigan USA, May 31 to June 3, 2016. pp. 1–8.

Kovárík, O., Haušild, P., Medřický, J., Tomek, L., Siegl, J., Mušálek, R., Curry, N., and Björklund, S. (2016), Fatigue crack growth in bodies with thermally sprayed coating. Journal of Thermal Spray Technology. 25, (1-2), 311-320.

Kubiczek, J., Herrnring, H., Kellner, L., Ehlers, S., and Diewald, R. (2019), Simulation of temperature distribution in ship structures for the determination of temperature- dependent material properties. 12th European LS-DYNA Conference Koblenz, Germany.

Kumar, S., Itoh, Y., Saizuka, K., and Usami T. (1997), Pseudodynamic testing of scaled models J Struct Eng, ASCE, 123 (4), pp. 524-529

Kunes, J. (2012), Similarity and Modeling in Science and Engineering, Springer, Cambridge International Science Publishing Ltd. and Springer, Cambridge, UK.

Laakso, A., Avi, E., and Romanoff, J. (2019), Correction of local deformations in free vibration analysis of ship deck structures by equivalent single layer elements. Ships and Offshore Structures, 14: 135-147.

Lahuerta, F., De Ruiter, M. J., Chavez, L. E. E., Koorn, N., and Smissaert, D. (2017). Assessment of wind turbine blade trailing edge failure with sub-component tests. In Proceedings of 21st International Conference on Composite Materials.

Lee, J. H., and Bernitsas, M. M. (2011), High-damping, high-Reynolds VIV tests for energy harnessing using the VIVACE converter, Ocean Engineering. 38, 1697–1712.

Lee, S.-K., Yu, K., and Huang, S. C. (2014), CFD Study of Air-Gap and Wave Impact Load on Semisubmersible Under Hurricane Conditions. The ASME 33rd Int. Conf. on Ocean, Offshore and Arctic Eng., OMAE, San Francisco, CA, USA. ASME.

Lehmann, E., and Peschmann, J. (2002), Energy Absorption of the Steel Structure of Ships in the Event of Collisions, Mar. Struct., 15(4–5), pp. 429–441.

Li, L., Li, C.-Q., and Mahmoodian, M. (2019), Effect of applied stress on corrosion and mechanical properties of mild steel, J. Mater. Civ. Eng., vol. 31, no. 2.

Li, Y., Zhou, Q., Zhou, L., Zhu, L., and Guo, K. (2019), Flexural wave band gaps and vibration attenuation characteristics in periodic bi-directionally orthogonal stiffened plates. Ocean Engineering, 178: 95-103.

Li, W., Huang, Y., and Tian, Y. (2019), A PCA-Based Damage Detecting Method for Jacket Platform Under Random Wave Excitations. The 29th International Ocean and Polar Engineering Conference. Honolulu, Hawaii, USA: International Society of Offshore and Polar Engineers.

Liao, Y.-T., Lin, J.-H., and Lee, C.-Y. (2018), A tuned vibration absorber constituted of shape memory alloy wires for vibration reduction of platform structures: design and implementation. MATEC Web of Conferences, 185: 00013.

Liao, X., Wang, Y., Wang, Z., Feng, L., and Shi, Y. (2019), Effect of low temperatures on constant amplitude fatigue properties of Q345qD steel butt-welded joints. Engineering Failure Analysis. 105:597-609. DOI: 10.1016/j.engfailanal.2019.07.006

Lim, K. Y. H., Zheng, P., and Chen, C.-H. (2019), A state-of-the-art survey of Digital Twin: techniques, engineering product lifecycle management and business innovation perspectives. Journal of Intelligent Manufacturing: 1-25.

Liu, C., Fu, S., Zhang, M., and Ren, H. (2018), Time-varying hydrodynamics of a flexible riser under multi-frequency vortex-induced vibrations. Journal of Fluids and Structures, 80, 217-244.

Liu, C., Fu, S., Zhang, M., Ren, H., and Xu, Y. (2020), Hydrodynamics of a flexible cylinder under modulated vortex-induced vibrations. Journal of Fluids and Structures, 94, 102913.

Liu, G., Wang, S., Xie, Y., Tian, X., Leng, D., Malekain, R., and Li, Z. (2018), Damage detection of offshore platforms using acoustic emission analysis. Review of Scientific Instruments, 89: 115005.

Luo, Z., Zhu, Y., Wang, Y., and Zhao, X. (2013), Study of the Structure Size Interval of Incomplete Geometrically Similitude Model of the Elastic Thin Plates, J. Meas. Eng., 1(4), pp. 207–218.

Luo, Z., Zhu, Y., Zhao, X., and Wang, D. (2014), Determination Method of Dynamic Distorted Scaling Laws and Applicable Structure Size Intervals of a Rotating Thin-Wall Short Cylindrical Shell, Proc. Inst. Mech. Eng., Part C, 229(5), pp. 806–817.

Ma, C., Oka, M., and Ochi, H. (2019), An investigation of fatigue and long-term stress prediction for container ship based on full scale hull monitoring system. The 14th International Symposium on Practical Design of Ships and Other Floating Structures (PRADS 2019), Yokohama, Japan, Sep. 22-26, T2-A-2.

Macchi, M., Roda, I., Negri, E., and Fumagalli, L. (2018), Exploring the role of digital twin for asset lifecycle management. IFAC-PapersOnLine, 51: 790-795.

Mackowski, A. W., and Williamson, C. H. K. (2011), Developing a cyber-physical fluid dynamics facility for fluid-structure interaction studies, Journal of Fluids and Structures. 27, 748–757.

Maes, K., Iliopoulos, A., Weijtjens, W., Devriendt, C., and Lombaert, G. (2016), Dynamic strain estimation for fatigue assessment of an offshore monopile wind turbine using filtering and modal expansion algorithms. Mechanical Systems and Signal Processing, 76: 592-611.

Malitckii, E., Remes, H., Lehto, P., and Bossuyt, S. (2019), Full-field strain measurements for microstructurally small fatigue crack propagation using digital image correlation method. Journal of Visualized Experiments. (143), e59134.

Martin, H. R. (2011), Development of a Scale Model Wind Turbine for Testing of Offshore Floating Wind Turbine Systems. MS thesis. The University of Maine. USA.

Mazzariol, L. M., and Alves, M. (2013), Experimental Study on Scaling of Circular Tubes Subjected to Dynamic Axial Crushing Using Models of Different Materials, 22nd International Congress of Mechanical Engineering, (COBEM), Ribeir~ao Preto, Brazil, Nov. 3–7, pp. 8065–8074.

Mazzariol, L. M., and Alves, M. (2014), Scaling of the Impact of a Mass on a Plate Using Models of Different Materials, Fourth International Conference on Impact Loading of Lightweight Structures, Cape Town, South Africa, Jan. 12–16, pp. 1275–1289.

Melchers, R. E., Ahammed, M., Jeffrey, R., and Simundic, G. (2010), Statistical characterization of surfaces of corroded steel plates, Mar. Struct., vol. 23, no. 3, pp. 274–287.

Melchers, R. E. (2014), Long-term immersion corrosion of steels in seawaters with elevated nutrient concentration, Corros. Sci., vol. 81, pp. 110–116.

Mellor, M., Cox, G. and Bosworth, H. (1984), Mechanical Properties of Multi-Year Sea Ice. Testing Techniques. U. S. Army Cold Regions Research & Engineering Lab, Hanover, NH, USA: U.S. Army Cold Regions Research and Engineering Laboratory (CRREL). Retrieved from: http://www.dtic.mil/docs/citations/ADA144431.

Menezes, P. L., Nosonovsky, M., Kailas, S. V., Lovell, M. R. 2013. Friction and wear. Tribology for scientists and engineers. Springer.

McKown, S., Cantwell, W. J., and Jones, N. (2008), Investigation of Scaling Effects in Fiber-Metal Laminates, J. Compos. Mater., 42(9), pp. 821–829.

Mieloszyk, M., and Ostachowicz, W. (2017), An application of Structural Health Monitoring system based on FBG sensors to offshore wind turbine support structure model. Marine Structures, 51: 65-86.

Milaković, A-S, Braun, M., Willems, T., Hendrikse, H., Fischer, C., and Ehlers, S. (2019), Methodology for estimating offshore wind turbine fatigue life under combined loads of wind, waves and ice at sub-zero temperatures. International Conference on Ships and Offshore Structures ICSOS 4 - 8 November 2019; Cape Carnival, USA.

Min, Q., Lu, Y., Liu, Z., Su, C., and Wang, B. (2019), Machine learning based digital twin framework for production optimization in petrochemical industry. International Journal of Information Management, 49: 502-519.

Mishnaevsky, L., Branner, K., Petersen, H. N., Beauson, J., McGugan, M. and Sørensen, B. F. (2017), Materials for Wind Turbine Blades: An Overview. Materials, vol 10, no. 11. DOI: 10.3390/ma10111285.

Moan, T. and Ayala-Uraga, E. (2008), Reliability-based assessment of deteriorating ship structures operating in multiple sea loading climates, Reliab. Eng. Syst. Saf., vol. 93, no. 3, pp. 433–446.

Mohajernasab, S. (2021), Investigation into the Effects of Air Entrapment on the Wave-In-Deck Loads on Offshore Structures in Extreme Weather Events, PhD Thesis, Maritime Engineering & Hydrodynamics, Australian Maritime College, University of Tasmania.

Moslet, P. O. (2007), Field testing of uniaxial compression strength of columnar sea ice, Cold Regions Science and Technology, 48(1), pp. 1–14. Retrieved from: http://www.sciencedirect.com/science/article/B6V86-4M7CD92-1/2/71ff3c143261c62cabb6ef4c855d21c6.

Muse, J. A., Kutay, A., and Calise, A. J. (2008), A novel force control traverse for simulating UAV flight in a wind tunnel, AIAA Paper No. 2008–6714.

Myrli, O. E., and Khawaja, H. (2019), Fluid-Structure Interaction (FSI) Modelling of Aquaculture Net Cage.

Nakai, T., Matsushita, H. and Yamamoto, N. (2007), Assessment of corroded conditions of web of hold frames with pitting corrosion.

Neumann, K. M., Vårdal, O. T. and Ehlers, S. (2018), Updatable Spatio-Temporal Probabilistic Corrosion Modeling for Offshore Structures, in ASME 2018 37th International Conference on Ocean, Offshore and Arctic Engineering.

Neumann, K. M. and Ehlers, S. (2019), Power Spectrum for Surface Description of Corroded Ship, in Proceedings of the ASME 2019 38th International Conference on Ocean, Offshore and Arctic Engineering.

Neumann, K. M., Leira, B., Vårdal, O. T., and Ehlers, S. (2019a), Time-variant rule-based reliability of corroded structures by Monte Carlo simulation, COTech.

Neumann, K. M., Ehlers, S., and Vårdal, O. T. (2019c), Tensile tests of corroded steel and prediction of strength, ICSOS.

Newman, J. W. (2016), System and method for ground based inspection of wind turbine blades. Google Patents.

Ngeljaratan, L., and Moustafa, M. (2020), Structural Health Monitoring and Seismic Response Assessment of Bridge Structures Using Target-Tracking Digital Image Correlation. Journal of Engineering Structures.

Nielsen, P. H., Berring, P., Pavese, C., and Branner, K. (2013), Rotor blade full-scale fatigue testing technology and research, DTU Wind Energy E-0041, Department of Wind Energy, Technical University of Denmark.

Ohtsubo, H., Kawamoto, Y., and Kuroiwa, T. (1994), Experimental and Numerical Research on Ship Collision and Grounding of Oil Tankers, Nucl. Eng. Des., 150(2–3), pp. 385–396.

Oka, M., Takami, T., and Ma, C. (2019), Evaluation method for the maximum wave load based on AIS and hindcast wave data. The 14th International Symposium on Practical Design of Ships and Other Floating Structures (PRADS 2019), Yokohama, Japan, Sep. 22-26, W1-D-2.

Olufsen, S. N., Andersen, M. E. and Fagerholt, E. (2020), μDIC: An open-source toolkit for digital image correlation, SoftwareX, 11,2020, 100391, DOI: 10.1016/j.softx.2019.100391 (accessed on 5 October 2021).

Oshiro, R. E., and Alves, M. (2009), Scaling Structures Subject to Impact Loads When Using a Power Law Constitutive Equation, Int. J. Solids Struct., 46(18–19), pp. 3412–3421.

Oshiro, R. E., and Alves, M. (2012), Predicting the Behaviour of Structures Under Impact Loads Using Geometrically Distorted Scaled Models, J. Mech. Phys. Solids, 60(7), pp. 1330–1349.

Oshiro, R. E., Calle, M. A. G., Mazzariol, L. M., and Alves, M. (2011), Experimental Study of Scaled T Cross–Section Beams Subjected to Impact Load, 21st Brazilian Congress of Mechanical Engineering, Natal (RN), Brazil, Oct. 24–28.

Oshiro, R. E., Calle, M. A. G., Mazzariol, L. M., and Alves, M. (2017), Experimental Study of Collision in Scaled Naval Structures, Int. J. Impact Eng., 110, pp. 149–161.

Pacheco, J., Oliveira, G., Magalhães, F., Cunha, Á., and Caetano, E. (2017), Wind turbine vibration based SHM system: influence of the sensors layout and noise. Procedia engineering, 199: 2160-2165.

Paik, J. K. and Kim, D. K. (2012), Advanced method for the development of an empirical model to predict time-dependent corrosion wastage, Corros. Sci., vol. 63, pp. 51–58.

Paik, J. K., Lee, J. M., Hwang, J. S., and Park, Y. II (2003), A Time-Dependent Corrosion Wastage Model for the Structures of Single and Double Hull Tankers and FSOs and FPSOs, Mar. Technol., vol. 40, no. 3, pp. 201–217.

Pansart, S. (2015), A new rotor blade standard for high product quality and flexible certification. Poster, European Wind Energy Association (EWEA), 17 - 20 November 2015, Paris, France.

Poggi, L., Gaggero, T., Gaiotti, M., Ravina, E. and Mario Rizzo, C. (2020), Recent developments in Remote Inspections of Ship Structures, International Journal of Naval Architecture and Ocean Engineering, 12, 881-891; ref. IJNAOE 334, DOI: 10.1016/j.ijnaoe.2020.09.001.

Poggi, L., Gaggero, T., Gaiotti, M., Ravina, E. and Mario Rizzo, C. (2021), Robotic inspection of ships: inherent challenges and assessment of their effectiveness, Ships and Offshore Structures, DOI: 10.1080/17445302.2020.1866378.

Qiang, W., Peilin, Z., Chen, M., Huaiguang, W., and Cheng, W. (2019), Multi-task Bayesian compressive sensing for vibration signals in diesel engine health monitoring. Measurement, 136: 625-635.

Ramu, M., Prabhu Raja, V., and Thyla, P. R. (2010), Development of Structural Similitude and Scaling Laws for Elastic Models, Int. J. Manuf. Eng., 9, pp. 67–69.

Rahbar-Ranji, A. (2012), Ultimate strength of corroded steel plates with irregular surfaces under in-plane compression, Ocean Eng., vol. 54, pp. 261–269.

Ren, B., and Wang, Y. (2004), Numerical simulation of random wave slamming on structures in the splash zone. Ocean engineering, 31: 547-560.

Ren, H., Xu, Y., Zhang, M., Fu, S., Meng, Y., and Huang, C. (2019), Distribution of drag coefficients along a flexible pipe with helical strakes in uniform flow. Ocean Engineering, 184, 216-226.

Ren, H., Zhang, M., Cheng, J., Cao, P., and Wang, Y. (2020), Magnification of hydrodynamic coefficients on a flexible pipe fitted with helical strakes in oscillatory flows. Ocean Engineering, 210, 107543.

Reuters (2016), North Sea storm forces oil platform evacuations, output shutdown. Retrieved from: http://www.reuters.com/article/us-weather-northsea-idUSKBN0UE0OR20151231 (Accessed on 30 June 2020).

Rezaeepazhand, J., and Wisnom, M. R. (2009), Scaled Models for Predicting Buckling of Delaminated Orthotropic Beam-Plates, Compos. Struct., 90(1), pp. 87–91.

Rezaeepazhand, J., and Yazdi, A. A. (2011), Similitude Requirements and Scaling Laws for Flutter Prediction of Angle-Ply Composite Plates, Compos. Part B, 42(1), pp. 51–56.

Rezaniaiee Aqdam, H., Ettefagh, M. M., and Hassannejad, R. (2018), Health monitoring of mooring lines in floating structures using artificial neural networks. Ocean Engineering, 164: 284-297.

Rosemeier, M., Antoniou, A., Chen, X., Lahuerta, F., Berring, P., & Branner, K. (2019). Trailing edge subcomponent testing for wind turbine blades–Part A: Comparison of concepts. Wind Energy, 22(4), 487-498. https://doi.org/10.1002/we.2301

Rudman, M., and Cleary, P. W. (2013), Rogue wave impact on a tension leg platform: The effect of wave incidence angle and mooring line tension. Ocean Engineering, 61: 123-138.

Rupil, J., Roux, S., Hild, F., and Vincent, L. (2011), Fatigue microcrack detection with digital image correlation. The Journal of Strain Analysis for Engineering Design. 46, (6), 492-509.

Sallaba, F., F. Rolof, S. Ehlers, C. L. Walters & M. Braun (2022), Relation between the Fatigue and Fracture Ductile-Brittle Transition in S500 Welded Steel Joints. Metals, 12. DOI: 10.3390/met12030385.

Sauder, T., Chabaud, V., Thys, M., Bachynski, E. E., and Sæther, L. O. (2016), Real-time Hybrid Model Testing of a Braceless Semi-submersible Wind turbine. Part I: The Hybrid Approach. In ASME 2016 35th International Conference on Ocean, Offshore and Arctic Engineering, No OMAE2016-54435.

Sauder, T., Sørensen, A. J., and Larsen, K. (2017), Real-Time Hybrid Model Testing of a Top Tensioned Riser: A Numerical Case Study on Interface Time-Delay and Truncation Ratio. In ASME 2017 36th International Conference on Ocean, Offshore and Arctic Engineering, Trondheim, Norway.

Sauder, T., Marelli, S., Larsen, K., and Sørensen, A. J. (2018), Active truncation of slender marine structures: Influence of the control system on fidelity. Applied Ocean Research, 74:154–169

Sauder, T., Marelli, S., and Sørensen, A. J. (2019), Probabilistic Robust Design of Control Systems for High-Fidelity Cyber-Physical Testing. Automatica, 101:111-119.

Scharnke, J., Vestbostad, T., Wilde, J. D., and Haver, S. K. (2014), Wave-In-Deck Impact Load Measurements on a Fixed Platform Deck. Proceedings of the ASME 33rd International Conference on Ocean, Offshore and Arctic Engineering, OMAE, San Francisco, CA, USA. American Society of Mechanical Engineers.

Scharnke, J., and Hennig, J. (2015), Vertical wave impact loading on a fixed platform deck. Proceedings of the ASME 2015 34th International Conference on Ocean, Offshore and Arctic Engineering, OMAE2015, St. John's, Newfoundland, Canada. American Society of Mechanical Engineers.

Scharnke, J. (2019), Elementary Loading Processes and Scale Effects Involved in Wave-in-Deck Type of Loading: A Summary of the BreaKin JIP. Paper presented at the ASME 2019 38th International Conference on Ocean, Offshore and Arctic Engineering.

Schubel, P., Crossley, R., Boateng, E., and Hutchinson, J. (2013), Review of structural health and cure monitoring techniques for large wind turbine blades. Renewable energy, 51: 113-123.

Schulson, E., Hoxie, S., Nixon, W. 1989. The tensile strength of cracked ice. Philosophical Magazine A, 59: 303-311.

Schulson, E. M., Gies, M. C., Lasonde, G. J. and Nixon, W. A. (2017), The effect of the specimen-platen interface on internal cracking and brittle fracture of ice under compression:

high-speed photography, Journal of Glaciology. International Glaciological Society, 35(121), pp. 378–382.
Schulson, E. M. and Duval, P. (2009), Creep and Fracture of Ice. Cambridge University Press. Retrieved from: https://doi.org/10.1017/CBO9780511581397.
Schwarz, J. (1977), New developments in modeling ice problems, in the 4th international conference on port and ocean engineering under Arctic conditions, (POAC 77), St. John's, pp. 45–61.
Scott, D., and Muir, J. (2000), Offshore cage systems: A practical overview. Option Mediterraneennes-International Centre for Advanced Mediterranean Agronomic Studies: 79-89.
Sen, D., Aghazadeh, A., Mousavi, A., Nagarajaiah, S., Baraniuk, R., and Dabak, A. (2019), Data-driven semi-supervised and supervised learning algorithms for health monitoring of pipes. Mechanical Systems and Signal Processing, 131: 524-537.
Sheng, J. and Xia, J. (2017), Effect of simulated pitting corrosion on the tensile properties of steel, Constr. Build. Mater., vol. 131, pp. 90–100.
Shi, X. H., and Gao, Y. G. (2001), Generalization of Response Number for Dynamic Plastic Response of Shells Subjected to Impulsive Loading, Int. J. Pressure Vessels Piping, 78(6), pp. 453–459.
Shirangi, M. G., Ettehadi, R., Aragall, R., Furlong, E., May, R., Dahl, T., Samnejad, M., and Thompson, C. (2020), Digital twins for drilling fluids: advances and opportunities. IADC/SPE International Drilling Conference and Exhibition, Society of Petroleum Engineers.
Shokrgozar, H. R., and Asgarian, B. (2018), System Identification of Steel Jacket Type Offshore Platforms using Vibration Test. 9th European Workshop on Structural Health Monitoring, Manchester, United Kingdom. NDT.net, 15.
Shokrieh, M. M., and Askari, A. (2013), Similitude Study of Impacted Composite Under Buckling Loading, J. Eng. Mech., 139(10), pp. 1334–1340.
Simitses, G. J., Starnes, J. H., Jr., and Rezaeepazhand, J. (2000), Structural Similitude and Scaling Laws for Plates and Shells: A Review, AIAA Paper No. AIAA-2000-1383.
Sims, N. A., and Key, G. (2011), Fish without footprints. OCEANS'11 MTS/IEEE KONA, IEEE, 1-6.
Singhatanadgid, P., and Na Songkhla, A. (2008), Experimental Investigation into the use of Scaling Laws for Predicting Vibration Responses of Rectangular Thin Plates, J. Sound Vib., 311(1–2), pp. 314–327.
Song, L., Fu, S., Cao, J., Ma, L., Wu, J. (2016), An investigation into the hydrodynamics of a flexible riser undergoing vortex-induced vibration. Journal of Fluids & Structures, 63, 325-350.
Spanos, N. A., Sakellariou, J. S., and Fassois, S. D. (2019), Vibration-response-only statistical time series structural health monitoring methods: A comprehensive assessment via a scale jacket structure. Structural Health Monitoring: 1475921719862487.
Sterrett, S. G. (2006), Models of Machines and Models of Phenomena, Int. Stud. Philos. Sci., 20(1), pp. 69–80.
Sterrett, S. G. (2009), Similarity and Dimensional Analysis, Philosophy of Technology and the Engineering Sciences (Handbook of the Philosophy of Science, Vol. 9), A. Meijers, ed., Elsevier, Amsterdam, The Netherlands, 799–824.
Sterrett, S. G. (2014), The Morals of Model-Making, Stud. Hist. Philos. Sci., 46, pp. 31–45.
Sterrett, S. G. (2015a), Experimentation on Analogue Models, Springer Handbook of Model-Based Science, L. Magnani and T. Bertolotti, eds., Springer International Publishing, Berlin.
Sterrett, S. G. (2015b), Physically Similar Systems: A History of the Concept, Springer Handbook of Model-Based Science, L. Magnani and T. Bertolotti, eds., Springer International Publishing, Berlin.

Streicher, M., Kortenhaus, A., Hughes, S., Hofland, B., Suzuki, T., Altomare, C., Marinov, K. and Cappietti, L. (2019), Non-Repeatability, Scale-and Model Effects in Laboratory Measurement of Impact Loads Induced by an Overtopped Bore on a Dike Mounted Wall. Paper presented at the ASME 2019 38th International Conference on Ocean, Offshore and Arctic Engineering.

Sun, X., Kong, H., Wang, H., and Zhang, Z. (2018), Evaluation of corrosion characteristics and corrosion effects on the mechanical properties of reinforcing steel bars based on three-dimensional scanning, Corros. Sci., vol. 142, pp. 284–294.

Suominen, M. T. O., von Bock und Polach, R. U. F. and Haase, A. (2019), The effect of sample dimensions on the compressive strength of model-scale ice, in Proceedings of the International Conference on Port and Ocean Engineering under Arctic Conditions, POAC.

Tabri, K., Maattanen, J., and Ranta, J. (2008), Model-Scale Experiments of Symmetric Ship Collisions, J. Mar. Technol., 13(1), pp. 71–84.

Takami, T., Nielsen, U.D., and Jensen, J.J. (2021), Real-time deterministic prediction of wave-induced ship responses based on short-time measurements. Ocean Engineering, 221: https://doi.org/10.1016/j.oceaneng.2020.108503.

Tan, Q. M. (2011), Dimensional Analysis with Case Studies in Mechanics, Springer-Verlag, Berlin.

Taylor, R. N. (1995), Geotechnical Centrifuge Technology. Taylor & Francis Group,19-33.

Teh, K. L., and Leung, C. F. (2010), Centrifuge model study of spudcan penetration in sand overlying clay. Geotechnique, 60(11): 825-842.

Thompson, D., Beasley, D. J., True, D. G., Lin, S. T., Briaud, J.-L., Seelig, W. N., and Jung, B. (2012), Handbook for marine geotechnical engineering. Naval Facilities Engineering Command Port Hueneme Ca Engineering Service Center.

Tian, Z., Lai, Q., Li, W., Li, Z., He, W., and Liu, G. (2018), Experimental Study on the Vibration Characteristics of Ship Propulsion Forced by the Hull Deformations. The 28th International Ocean and Polar Engineering Conference. Sapporo, Japan: International Society of Offshore and Polar Engineers.

Tian, Z., Shao, Y., Zhou, L., and Xie, Y. (2019), An Experimental Research on the Vibration of a Ship Propulsion Model Excited by Dynamic Excitations. The 29th International Ocean and Polar Engineering Conference. Honolulu, Hawaii, USA: International Society of Offshore and Polar Engineers.

Torkamani, S., Jafari, A. A., and Navazi, H. M. (2008), Scaled Down Models for Free Vibration Analysis of Orthogonally Stiffened Cylindrical Shells Using Similitude Theory, 26th International Congress of the Aeronautical Sciences (ICAS), Anchorage, AL, Sept. 14–19, pp. 3458–3469.

Torkamani, S., Jafari, A. A., Navazi, H. M., and Bagheri, M. (2009), Structural Similitude in Free Vibration of Orthogonally Stiffened Cylindrical Shells, Thin-Walled Struct., 47(11), pp. 1316–1330.

Tsukamoto, Y. (1994), Drum centrifuge tests of three-leg jack-ups on sand. PhD thesis. University of Cambridge.

Tygesen, U., Worden, K., Rogers, T., Manson, G., and Cross, E. (2019), State-of-the-art and future directions for predictive modelling of offshore structure dynamics using machine learning. Dynamics of Civil Structures, Volume 2. Springer.

Tziavos, N. I., Hemida, H., Dirar, S., Papaelias, M., Metje, N., and Baniotopoulos, C. (2020), Structural health monitoring of grouted connections for offshore wind turbines by means of acoustic emission: An experimental study. Renewable Energy, 147: 130-140.

Ungbhakorn, V., and Singhatanadgid, P. (2009), A Scaling Law for Vibration Response of Laminated Curved Shallow Shells by Energy Approach, Mech. Adv. Mater. Struct., 16(5), pp. 333–344.

Vassalos, D. (1998), Physical Modelling and Similitude of Marine Structures, Ocean Eng., 26(2), pp. 111–1232.

Vidal Seguí, Y., Rubias, J. L., and Pozo Montero, F. (2019), Wind turbine health monitoring based on accelerometer data. In: A. BENJEDDOU, N. M. A. J. F. D. U. (ed.) IX ECCOMAS Thematic Conference on Smart Structures and Materials SMART 2019.

Vlahos, G., Cassidy, M.J., and Martin, C.M. (2008), Experimental investigation of the system behaviour of a model three-legged jack-up on clay. Applied Ocean Research, 30(4): 323-337.

Vlahos, G. (2004), Physical and numerical modelling of a three-legged jack-up structure on clay soil. PhD thesis. The University of Western Australia.

von Bock und Polach, R., Ehlers, S. and Kujala, P. (2013), Model-scale ice — Part A: Experiments, Cold Regions Science and Technology, 94, pp. 74–81. DOI: 10.1016/j.coldregions.2013.07.001.

von Bock und Polach, R. U. F. (2015), Numerical analysis of the bending strength of model-scale ice, Cold Regions Science and Technology, 118. DOI: 10.1016/j.coldregions.2015.06.003.

von Bock und Polach, R. U. F., Ettema, R., Gralher, S., Kellner, L., Stender, M. (2019a), The non-linear behavior of aqueous model ice in downward flexure, Cold Regions Science and Technology. Elsevier. doi: 10.1016/J.COLDREGIONS.2019.05.001.

von Bock und Polach R. U. F., Klein, M., Kubiczek, J., Kellner, L., Braun, M., Herrnring, H. (2019b), State of the Art and Knowledge Gaps on Modelling Structures in Cold Regions. ASME 2019 38th International Conference on Ocean, Offshore and Arctic Engineering June 9–14; Glasgow, Scotland.

Vredeveldt, A.W., and L.J. Wevers. (1992), Full-scale ship collision tests. in Proceedings, First Conference on Marine Safety and Environment Ship Production. Delft, June 1-5. Delft: Delft University Press. 743-769.

Vu, N. A., Castel, A. and François, R. (2009), Effect of stress corrosion cracking on stress–strain response of steel wires used in prestressed concrete beams, Corros. Sci., vol. 51, pp. 1453–1459.

Walters, C. L., Alvaro, A., and Maljaars, J. (2016), The effect of low temperatures on the fatigue crack growth of S460 structural steel. International Journal of Fatigue, 82, 110-118.

Wanasinghe, T. R., Wroblewski, L., Petersen, B., Gosine, R. G., James, L. A., De Silva, O., Mann, G. K., and Warrian, P. J. (2020), Digital Twin for the Oil and Gas Industry: Overview, Research Trends, Opportunities, and Challenges. IEEE Access.

Wang, J., Ye, L., Gao, R. X., Li, C., and Zhang, L. (2019), Digital Twin for rotating machinery fault diagnosis in smart manufacturing. International Journal of Production Research, 57: 3920-3934.

Wang, Y., Xu, S., Wang, H. and Li, A. (2017), Predicting the residual strength and deformability of corroded steel plate based on the corrosion morphology, Constr. Build. Mater., vol. 152, pp. 777–793.

Wave Dragon (2020). A WEC and aquaculture MPOP. Retrieved from: http://www.wavedragon.net/ (Accessed 16 Jun 2020).

WSA (2012). Steel solutions in the green economy. World Steel Association. Retrieved from: https://www.worldsteel.org/en/dam/jcr:41f65ea2-7447-4489-8ba7-9c87e3975aab/Steel+solutions+in+the+green+economy:+Wind+turbines.pdf (Accessed 30 July 2020).

Wu, G., Jang, H., Kim, J. W., Ma, W., Wu, M.-C., and O'sullivan, J. (2014), Benchmark of CFD Modeling of TLP Free Motion in Extreme Wave Event. ASME 2014 33rd International Conference on Ocean, Offshore and Arctic Engineering. American Society of Mechanical Engineers, V002T08A086-V002T08A086.

Wu, J., Lie, H., Larsen, C. M., Liapis, S., and Baarholm, R. (2016), Vortex-induced vibration of a flexible cylinder: Interaction of the in-line and cross-flow responses. Journal of Fluids and Structures, 63, 238-258.

Wu, J., Lie, H., Fu, S. X., Baarholm, R., and Constantinides, Y. (2017), VIV Responses of Riser with Buoyancy Elements: Forced Motion Test and Numerical Prediction. ASME 2017, International Conference on Ocean, Offshore and Arctic Engineering (pp.V002T08A013).

Wu, R. Zhang, D. Yu, Q. Jiang, Y. and Arola, D. (2019), Health Monitoring of wind Turbine Blades in Operation Using Three-Dimensional Digital Image Correlation, Mechanical Systems and Signal Processing.

Wu, Y., Chen, D., Xia, Z., and Yang, S. (2019), Development of Offshore Platform Stress Monitoring System based on Internet of Things Technology. E3S Web Conf., 136.

Wu, J., Yin, D., Lie, H., Riemer-Sørensen, S., Sævik, S., Triantafyllou, M. 2020. Improved VIV response prediction using adaptive parameters and data clustering. Journal of Marine Science and Engineering, 8: 127.

Xiao, L., Xia, T., Pan, E., and Zhang, X. (2019), Long-term predictive opportunistic replacement optimisation for a small multi-component system using partial condition monitoring data to date. International Journal of Production Research: 1-18.

Xu, Z., Yang, F., Guan, Z. W., and Cantwell, W. J. (2016), An Experimental and Numerical Study on Scaling Effects in the Low Velocity Impact Response of CFRP Laminates, Compos. Struct., 154, pp. 69–78.

Xu, S. and Wang, Y. (2015), Estimating the effects of corrosion pits on the fatigue life of steel plate based on the 3D profile, Int. J. Fatigue, vol. 72, pp. 27–41.

Xu, S., Wang, H., Li, A., Wang, Y., and Su, L. (2016), Effects of corrosion on surface characterization and mechanical properties of butt-welded joints, J. Constr. Steel Res., vol. 126, pp. 50–62.

Yamamoto, M., Hirosawa, N., Yoshida, K., Kato, C. and Hada, T. (1992), Characterization of Surface Texture of Corroded Steel Plates Exposed in Marine Environment, Zairyo-to-Kankyo, vol. 41, pp. 803–808.

Yan, H., Wei, D., Wang, X.-B., Chen, Y.-X., and Meng, X.-W. (2019), Research of structural health monitoring system for stinger of large deep water pipe-laying ship. Ocean Engineering, 171: 361-376.

Yang, F. J., Hassan, M. Z., Cantwell, W. J., and Jones, N. (2013), Scaling Effects in the Low Velocity Impact Response of Sandwich Structures, Compos. Struct., 99, pp. 97–104.

Yang, S., Chung, C., Wu, H., Chang, Y., Wu, Y., Lyu, J., Chen, S., and Lee, Y. (2018), Structural Health Monitoring of Offshore Jacket Structure. International Conference on Renewable Energy and Power Engineering (REPE), 24-26 Nov. 2018. pp. 39-42.

Yang, X., Utne, I. B., and Holmen, I. M. (2020), Methodology for hazard identification in aquaculture operations (MHIAO). Safety Science, 121: 430-450.

Yazdi, A. A. (2013), Prediction Flutter Boundaries of Laminated Cylindrical Shells Using Scaling Laws, J. Aerosp. Eng., 27(1).

Yazdi, A. A., and Rezaeepazhand, J. (2013), Applicability of Small-Scale Models in Prediction Flutter Pressure of Delaminated Composite Beam-Plates, Int. J. Damage Mech., 22(4), pp. 590–601.

Yin, D., Lie, H., and Baarholm, R. J. (2018a), Prototype Reynolds Number Vortex-Induced Vibration Tests on a Full-Scale Rigid Riser. Journal of Offshore Mechanics and Arctic Engineering, 140(1), 011702.

Yin, D., Passano, E., and Larsen, C. M. (2018b), Improved In-Line Vortex-Induced Vibrations Prediction for Combined In-Line and Cross-Flow Vortex-Induced Vibrations Responses. Journal of Offshore Mechanics and Arctic Engineering, 140(3), 031802.

Yucel, A., Arpaci, A., Degirmenci, S., and Tuzdengi, T. (2020), A new foundation design approach as a vibration reducer for marine gensets. Ships and Offshore Structures, 15: 89-98.

Zai, B. A., Sami, S., Khan, M. A., Ahmad, F., and Park, M. K. (2015), Prediction of Vibration Characteristics in Beam Structure Using Sub-Scale Modeling with Experimental Validation, Chin. J. Mech. Eng., 28(5), pp. 928–933.

Zhang, M., Fu, S., Song, L., Wu, J., Lie, H., and Ren, H. (2018), Hydrodynamics of Flexible Pipe With Staggered Buoyancy Elements Undergoing Vortex-Induced Vibrations. ASME 2017, International Conference on Ocean, Offshore and Arctic Engineering (pp.V002T08A030).

Zhang, M., Fu, S., Liu, C., Ren, H., and Xu, Y. (2021), Experimental investigation on vortex-induced force of a steel catenary riser under in-plane vessel motion. Marine Structures, 78(8), 102882.

Zhang, Y. (2018), Investigation of spudcan-footprint interaction in clay with a novel implementation of a three-dimensional large deformation finite element method. PhD thesis. The University of Western Australia.

Zhang, Y., Bienen, B., and Cassidy, M. J. (2013), Development of a combined VHM loading apparatus for a geotechnical drum centrifuge. International Journal of Physical Modelling in Geotechnics, 13(1): 13-30.

Zhang, H., Liu, Q., Chen, X., Zhang, D., and Leng, J. (2017), A digital twin-based approach for designing and multi-objective optimization of hollow glass production line. IEEE Access, 5: 26901-26911.

Zhao, W., Feng, G., Liu, W., and Ren, H. (2020a), Research on Fatigue Properties of Typical Welded Joints of DH36 Steel at −60 °C. Applied Sciences. 10(11). DOI: 10.3390/app10113742.

Zhao, W., Feng, G., Zhang, M., Ren, H, and Sinsabvarodom, C. (2020b), Effect of low temperature on fatigue crack propagation rates of DH36 steel and its butt weld. Ocean Engineering. 196. DOI: 10.1016/j.oceaneng.2019.106803.

Zhao, X., and Lang, Z. (2019), Baseline model based structural health monitoring method under varying environment. Renewable Energy, 138: 1166-1175.

Zhu, Y., Luo, Z., Zhao, X., and Han, Q. (2014), Determination Method of the Structure Size Intervals of Dynamically Similar Models for Predicting Vibration Characteristics of the Coated Thin Plates, Proc. Inst. Mech. Eng., Part C, 229(1), pp. 59–68.

Zhu, Y., Wang, Y., Luo, Z., Han, Q., and Wang, D. (2017), Similitude Design for the Vibration Problems of Plates and Shells: A Review, Front. Mech. Eng., 12(2), pp. 253–264.

Ziegler, L., Cosack, N., Kolios, A., and Muskulus, M. (2019), Structural monitoring for lifetime extension of offshore wind monopiles: Verification of strain-based load extrapolation algorithm. Marine Structures, 66: 154-163.

Zohuri, B. (2012), Dimensional Analysis and Self-Similarity Methods for Engineers and Scientists, Springer International Publishing, Cham, Switzerland.

Zohuri, B. (2017), Dimensional Analysis Beyond the Pi Theorem, Springer International Publishing, Cham, Switzerland.

Zou, D., Lv, F., Ta, N., and Rao, Z. (2020), Study on bearing force of marine propeller induced by longitudinal vibration of propulsion-shafting. Ships and Offshore Structures, 15: 162-173.

Zufelt, J. E. and Ettema, R. (1996), Model Ice Properties, CRREL Report 96-1, U.S. Army Corps of Engineers, Cold Regions Research and Engineering Laboratory (CRREL).